REPORT DOCUMENTATION PAGE

Form Approved OMB No. 0704-0188

1. REPORT DATE *(DD-MM-YYYY)*	2. REPORT TYPE	3. DATES COVERED *(From – To)*
22-11-2004	Final Report	23 February 2001 - 23-Feb-04

4. TITLE AND SUBTITLE

Novel, Solvent Free, Single Ion Conductive Polymer Electrolytes (Warsaw-2001)

5a. CONTRACT NUMBER
F61775-01-WE019

5b. GRANT NUMBER

5c. PROGRAM ELEMENT NUMBER

6. AUTHOR(S)

Professor Zbigniew Florjanczyk

5d. PROJECT NUMBER

5d. TASK NUMBER

5e. WORK UNIT NUMBER

7. PERFORMING ORGANIZATION NAME(S) AND ADDRESS(ES)

Warsaw University of Technology
ul. Noakowskiego 3
Warsaw PL-00 664
Poland

8. PERFORMING ORGANIZATION REPORT NUMBER

N/A

9. SPONSORING/MONITORING AGENCY NAME(S) AND ADDRESS(ES)

EOARD
PSC 802 BOX 14
FPO 09499-0014

10. SPONSOR/MONITOR'S ACRONYM(S)

11. SPONSOR/MONITOR'S REPORT NUMBER(S)
SPC 01-4019

12. DISTRIBUTION/AVAILABILITY STATEMENT

Approved for public release; distribution is unlimited.

13. SUPPLEMENTARY NOTES

14. ABSTRACT

This report results from a contract tasking Warsaw University of Technology as follows: The main task of this project is to design and characterize novel types of lithium conducting polymer electrolytes. This task will be pursued by the combined efforts of three academic groups having world-wide recognized experience in polymer electrolyte science, namely, the Group of Professors Wladyslaw Wieczorek and Florjanczyks of the Warsaw University of Technology in Poland, the Group of Professor Emanuel Peled at the University of Tel Aviv, Israel and the Group of Professor Bruno Scrosati at the University 'La Sapienza' of Rome, Italy. Broadly, the Polish Group will be involved in the synthesis of the new polymer electrolytes; the Italian Group will act as the coordinator of the Project, in their basic electrochemical characterization; and the Group in Israel in the fabrication and test of laboratory cell prototypes.

The work plan to be carried out at the Faculty of Chemistry of Warsaw Technical University will involve the following items: 1) Synthesis of polymer in salt system by in-situ polymerization or co-polymerization of acrylate (methacrylate) monomers in the presence of plasticizing salt; and 2) Optimization of the electrolyte conductivity as a function of the polymer matrix composition and the concentration of the added salt.

15. SUBJECT TERMS
EOARD, Power, Electrochemistry, Batteries

16. SECURITY CLASSIFICATION OF:			17. LIMITATION OF ABSTRACT	18, NUMBER OF PAGES	19a. NAME OF RESPONSIBLE PERSON
a. REPORT	b. ABSTRACT	c. THIS PAGE			WAYNE A. DONALDSON
UNCLAS	UNCLAS	UNCLAS	UL		19b. TELEPHONE NUMBER *(Include area code)* +44 (0)20 7514 4299

From: **Zbigniew Florjańczyk**
Warsaw University of Technology, Faculty of Chemistry
00-664 Warszawa, ul. Noakowskiego 3, Poland
Tel.: (+4822) 660-7303; fax: (+4822) 660-7279;
e-mail: nolang@ch.pw.edu.pl; evala@ch.pw.edu.pl

Date: **October 18, 2004**

To: **Wayne Donaldson**
Department of the Air Force
European Office of Aerospace Research and Development
223/231 Old Marylebone Rd
London, NW1 5TH, England
e-mail: wayne.donaldson@london.af.mil

Subject: **Final Report concerning the project "Novel, solvent free, single ion conductive polymer electrolytes (Warsaw-2001)" (Contract F61775-01-WE019; contractor: Professor Zbigniew Florjańczyk)**

Copy to: **Lawrence G. Scanlon**
Wright Laboratory, Wright – Patterson AFB
Dayton, Ohio 45433-7251
e-mail: lawrence.scanlon@wpafb.af.mil

Bruno Scrosati (bruno.scrosati@uniroma1.it)
Department of Chemistry, University of Rome "La Sapienza"
Piazza Aldo Moro 5, 00185 Rome, Italy

Emanuel Peled (peled@post.tau.ac.il)
Diana Golodnitsky (golod@post.tau.ac.il)
School of Chemistry, Tel Aviv University
Tel Aviv, 69978 Israel

The contractor, Professor Zbigniew Florjańczyk, hereby declares that, to the best of his knowledge and belief, the technical data delivered herewith under Contract No. F61775-01-WE019 is complete, accurate, and complies with all requirements of the contract.

October 18, 2004 ....Zbigniew Florjańczyk.....

Disclosures of all subject inventions as defined in FAR 52.227-13, have been reported in accordance with this clause.

October 19, 2004 .....

Professor Gabriel Rokicki
Vice-Dean of Faculty of Chemistry,
Warsaw University of Technology

POLITECHNIKA WARSZAWSKA
WYDZIAŁ CHEMICZNY
ul. Noakowskiego 3, 00-664 Warszawa
tel. 660-7507, tel/fax 628-27-41

Content:

I. INTRODUCTION

Our work concerned studies on the synthesis of new polymer electrolytes for application in lithium and lithium-ion batteries, characterized by limited participation of anions in the transport of electrical charge. Studies were carried out in the following directions:

- The first one involved the synthesis and characterization of new polymer-in-salt electrolytes showing high salt concentrations. These studies cover the determination of the conducting properties of electrolytes as a function of salt concentration, kind of lithium salt anion and chemical structure of the polymer matrix. Acrylonitrile and butyl acrylate copolymers of various compositions, well soluble in acetonitrile, which is easily removable during the membrane preparation, were used as polymer matrixes. Poly(butyl acrylate) and poly(methyl methacrylate) were additionally applied for the analysis of the effect of the polymer matrix on the electrolyte conductivity. $LiAlCl_4$, $LiClO_4$, $LiCF_3SO_3$, LiI, $LiN(CF_3SO_2)_2$ and $LiBF_4$ were used as lithium salts. To become better acquainted with the nature of conduction in such systems, lithium cations transference numbers t_+ of several selected samples were determined in the Tel Aviv research group of Professors Emanuel Peled and Diana Golodnitsky, as well as thermal (DSC) and FTIR characteristics were performed. These studies are described in chapter II.1.

  Similar studies were carried out for the polymer-in-salt system using polyacrylamide as the polymer matrix. The effect of the type of lithium salt and its concentration on the conductivity and microstructure of the studied electrolytes have been analyzed. Impedance spectroscopy, infra- red spectroscopy, DSC and MALDI-ToF techniques have been applied. (Chapter II.2.)
- The second one concerned the synthesis of new lithium salts based on carboxylic and phosphoric lithium salt complexes with Lewis acids of various strength. The purpose of anion complexation is to increase the negative charge delocalization by distributing it over a greater number of atoms. The application of lithium salts containing superweak anions also may have decreased the coulombic interaction between the lithium ion and the anion in the aprotic solvents, owing to large anionic size and delocalization of the anionic charge. (Chapter III.)
- The third one concerns the synthesis and characterization of anion-trapping supramolecular additives. Calix[4]arene R-urea derivatives (where R = phenyl, *t*-butyl, *p*-nitrophenyl) were applied as anion receptors. The effect of the type of anion receptor, its concentration and the concentration of the dopant salt on the conductivity and microstructure of composite polyether-lithium electrolytes have been studied. (Chapter IV.)

II. POLYMER IN SALT ELECTROLYTES

II. 1. Polymer-in-Salt Electrolytes Based on Acrylonitrile / Butyl Acrylate Copolymers and Lithium Salts

II.1.1. Abstract

Solid polymeric electrolytes for battery purposes in the form of composites of lithium salts (LiI, $LiN(CF_3SO_2)_2$, $LiClO_4$, $LiAlCl_4$, $LiCF_3SO_3$ and $LiBF_4$) and acrylic polymeric matrices [poly(acrylonitrile-*co*-butyl acrylate), poly(methyl methacrylate) and poly(butyl acrylate)] by film casting from acetonitrile have been obtained. The ionic conductivity (σ) as a function of temperature was studied by the impedance spectroscopy method. These systems show the highest σ values of the order of $10^{-4} - 10^{-7}$ S·cm^{-1} at high salt concentration (above 50 wt. %), characteristic of polymer-in-salt electrolytes. The ionic conductivity and mechanical properties of composites depend on the chemical structure of the polymer matrix, the anion and the salt concentration. The glass transition temperature (T_g) was determined from DSC studies. The introduction of a salt causes, in a majority of composites studied, a considerable decrease in the

T_g values indicating its strong plasticizing effect. DSC studies show a multiphase character of the composites, in which, with the exception of the amorphous system with $LiN(CF_3SO_2)_2$, phases of the plasticized matrix, complexes of the salt with the matrix of varying stoichiometry and often the separating salt are observed. The logarithm of the decoupling index ($\log R_\tau$) of the order of 3 – 5 as well as the shift in the IR spectrum of the groups present in the polymer (C≡N and C=O) by about 20 – 30 cm^{-1} indicate a weak interaction of the salt with the matrix. The ion transference numbers (0.5 – 0.8) determined by the electrochemical method indicate an increased participation of cations in the electrical charge conduction and different conduction mechanism in relation to that of classical electrolytes based on complexes with polyethers.

II.1.2. Introduction

There is great interest in the development of high-performance sources of energy for applications such as mobile telephones, laptops and also electric vehicles and engine/battery hybrid vehicles. Among these energy sources, great attention is devoted to studies on lithium and lithium-ion cells. The application in lithium batteries of polymer electrolytes in the place of liquid ones avoids the problems of electrolyte leakage from devices and also enables the design of devices with large surfaces and any shape. The large share of anions in the electric charge transfer is an important problem both in solid and liquid systems. During the operation of a cell, agglomeration of anions around the anode takes place with the formation of a charged layer. This lowers the cation transport from the anode to the electrolyte, which is revealed in a decrease in the power of the cell. The cation transference numbers are often not larger than 0.5,[1,2] and the average t_+ value is ca. 0.3, both for solid and gel electrolytes.[3] A cation transference number of 1.0 is obtained for polyelectrolytes, in which the anions are covalently bonded with the polymer matrix. However, because of the strong interaction of ions, the conductivity of solid polyelectrolytes is low. An increase in the degree of dissociation is achieved by the addition of a highly polar solvent, such as DMSO or DMA, but this is connected with strong passivation of the electrodes.[4]

A method has been proposed of obtaining electrolytes with high anion immobilization which involves the use of high salt concentrations (exceeding 50 wt. %). This type of electrolyte, called polymer-in-salt solid electrolyte (PISE), was first described by Angell et al..[5,6] In most often until now studied solid polymer electrolytes, the polymer is the main component and the lithium salt is introduced in an amount from several to ten or so mol % and therefore they can be called salt-in-polymer systems. In the systems of high salt content the polymer induces mechanical stability of the conducting composite and suppresses the salt crystallization due to the interaction with the lithium cations. Many papers appeared since then on PISEs, reporting mainly systems based on polyacrylonitrile (PAN) and its copolymers.[7–11] These systems combine the excellent mechanical properties characteristic of polymeric electrolytes with features of fast-ion-conducting glasses. It is assumed, on the basis of conductivity measurements of the polyacrylonitrile (PAN) – $LiCFSO_3$ system in the glass transition temperature region that long-range ion transport is not connected with the segmental relaxation of the polymer chain, since no rapid decrease in ionic conduction below T_g was observed.[7,8] Thus, there is a considerable difference in behavior between these systems and the classical “salt-in-polymer” systems. In the latter case ion transport is due to motions of the matrix and at temperatures below the glass transition temperature, when the relaxation disappears, the conductivity is minimal. It is assumed that in “polymer-in-salt” electrolytes the effective ion transport is connected with a high degree of ionic aggregation. At an appropriately high salt concentration, aggregates of varying degrees of association, $Li^+_mX^-_n$, form internal clusters, the charge of which is transported mainly by cations. FT-Raman spectroscopic studies carried out for $LiCF_3SO_3$ confirm the high degree of aggregation of the ionic salt and the absence of “free” anions.[9] This suggests that the anions are involved in extensive ionic aggregation, due to which they are much less mobile than the cations.

A conduction mechanism based on a dynamic percolation model with a "smeared" percolation threshold is postulated for these electrolytes.[10] According to the studies of Bushkova et al. carried out for systems with $LiClO_4$, the formation of an ionic structure favoring fast transport of lithium ions is dependent on the salt concentration and on the absence of traces of low-molecular-weight additives, e.g. solvent.[11] When a critical cluster concentration has been achieved, all separate single clusters come into contact with each other, forming an infinite cluster. According to these authors the presence of a solvent disturbs this structure, causing a remarkable decrease in the conductivity and cation transference number values.

PAN is most often used as a polymer additive in "polymer-in-salt" systems and, as appears from the comparison of this matrix with polyvinylpyrrolidone and poly(N,N-dimethylacrylamide), PAN affords better results.[12] The data of FT-Raman spectral measurements presented for $LiCF_3SO_3$ and $LiN(CF_3SO_2)_2$ in a system with PAN,[9,13] and also studies carried out for systems comprising polyacrylamide[14] show the occurrence of a distinct interaction of cations with the matrix. The interaction of the salt with the matrix is revealed also by the decrease in the glass transition temperatures of the electrolytes.

In this paper we have investigated the conductivity behavior in a number of PISEs as a function of salt concentration, type of lithium salt anion and chemical structure of the polymeric matrix. Since PAN is soluble in a small number of aprotic solvents, such as DMSO and DMF, which could never be completely removed, the electrolytes involving PAN were obtained by hot pressing at 150 °C and under high pressure. In this paper we propose the application of acrylonitrile (AN) and butyl acrylate (BuA) copolymers [poly(AN-*co*-BuA)] as the matrix. These copolymers are soluble in acetonitrile, a volatile solvent easily removable from the solvent-cast films.

In an attempt to understand the nature of conduction in salt-rich electrolytes, we investigated the thermal (DSC) and FTIR characteristics of the systems studied. An additional goal of this investigation was to find whether lithium ions are more mobile in PISE than in classic electrolytes of low salt concentrations, by measuring the cation transference number by means of the electrochemical method.[15,16]

II.1.3. Experimental Section

II.1.3.1. Synthesis of the polymeric matrix

Poly(AN-*co*-BuA)s (both monomers, AN and BuA, from Aldrich, commercial grade) were obtained by radical polymerization in the presence of azo-bis-isobutyronitrile as initiator. The reactions were carried out in a solvent (acetonitrile) at 70 °C for 5 h. The polymers were isolated with methanol, washed several times and dried under dynamic vacuum for 72 h. The reaction yield was over 95%. The reactions were carried out with varying compositions of the monomer feed. The copolymer composition was determined by elemental analysis, on the basis of the percentage content of C, H and N. Poly(methyl methacrylate) (PMMA) and poly(butyl acrylate) (PBuA) were obtained and purified by the same technique using benzoyl peroxide as initiator.

II.1.3.2. Characteristics of poly(AN-co-BuA)

The molecular weights of the copolymers were determined by gel permeation chromatography in THF with polystyrene as a standard (GPC LabAlliance). The values of M_w, M_n and degree of polydispersity (D) are presented in Table II.1.1. On the basis of DSC studies, the phase transitions of the copolymers studied were determined (Table II.1.1).

As noted, the glass transition temperatures of the matrices vary over a broad temperature range, from 15 °C at an equimolar composition, to 56 °C at a molar ratio of AN monomeric units (m.u.) to BuA m.u. equal 5 (83 mol %). The copolymer comprising 50 mol % of AN m.u. is amorphous, while the other copolymers contain a crystalline fraction (ΔH of the order of several J/g) of melting point close to the glass transition temperature. In the second heating cycle

crystallinity disappears, and therefore T_g was determined from the second heating cycle. All the copolymers of the AN m. u. content up to 83 mol % are soluble in acetonitrile.

Table II.1.1. Characteristics of poly(AN-*co*-BuA)s

AN content in copolymer, mol %	M_n kDa	M_w kDa	Polydispersity D	T_g [a] °C	T_m [b] °C
50	36	80	2.2	15.3	-
67	65	109	1.7	42.1	49
75	25	46	1.8	52.1	52
83	6	7	1.2	55.6	57

[a] T_g determined from the second heating cycle
[b] T_m determined from the first heating cycle

II.1.3.3. Preparation of polymer electrolytes

The electrolytes were obtained by the casting technique from a polymer and salt solution in acetonitrile. In the case of PBuA a mixture of acetonitrile and chloroform was used. All operations connected with the obtaining of electrolytes and performing of measurements were carried out in the atmosphere of dried argon. The solvent was removed under dynamic vacuum in two steps, first, for 50 hours at a vacuum of 20 Torr, and then for 140 hours at 10^{-3} Torr at room temperature. In the FTIR spectrum the signals assigned to acetonitrile completely disappeared after about the first 70 h of such drying. The solvents were dried and distilled in an argon atmosphere prior to use. The following lithium salts were used: LiI, $LiN(CF_3SO_2)_2$, $LiClO_4$, $LiAlCl_4$, $LiCF_3SO_3$ and $LiBF_4$ (Aldrich, reagent grades). The salts were dried at 120 °C at a vacuum of 10^{-4} Torr for 24 h. The salt concentration varied from 10 to 80 mol % with respect to AN m. u. in the copolymer. In the case of PMMA and PBuA, the molar ratio salt : MMA m.u. or BuA m.u., respectively, was 1.2. The properties of the electrolyte obtained depend on the lithium salt. When the salt was used at a molar ratio salt : AN m.u. (in the copolymer) equal 1.2, flexible membranes with very good adhesion to the electrodes were obtained only for LiI, $LiN(CF_3SO_2)_2$ and their mixtures. With $LiClO_4$, $LiAlCl_4$, $LiCF_3SO_3$ and $LiBF_4$, the electrolytes were glassy and brittle.

II.1.3.4. Experimental techniques

Impedance spectroscopy. Ionic conductivity was determined by the complex-impedance method. The samples were introduced to a specially designed measuring cell in a dry-box in the atmosphere of argon in which the moisture level was below 10 ppm. The samples were sandwiched between stainless-steel blocking electrodes and placed in a temperature-controlled oven. The impedance measurements were carried out on a Solartron-Schlumberger 1255 impedance analyzer over the frequency range from 1 Hz to 1 MHz.

Transference number (t_+) measurement. The t_+ of cations was determined by the polarization–variable current method described in the literature [1,2].[15,16] According to this method, a constant polarization voltage of 10 mV was applied to the system and the resulting polarization current was monitored until it achieved its constant value, I_{ss}. The impedance spectra were recorded before and after constant current polarization. The transference number was calculated according to the equation:

$$t_+ = \frac{I_{SS}(\Delta V - I_0 R_0)}{I_0(\Delta V - I_{SS} R_{SS})}$$

where:
I_0 and I_{ss} – initial and steady state current
R_0 and R_{ss} – initial and steady state resistance of the solid state interface calculated from the impedance plot before and after polarization

For the system with the imide salt at above 65 °C, and from the system with LiI at near room temperature, we succeeded in separating bulk conductivity, grain-boundary conductivity and the Li/polymer electrolyte interfacial resistance from the Nyquist plot data.

DSC studies. DSC experiments were performed on a Perkin-Elmer Pyris 1 scanning calorimeter equipped with a low-temperature measuring head and liquid-nitrogen-cooled heating element. The samples were placed in hermetically closed aluminum vessels. The measurement was carried out in the −100 – +200 °C temperature range in two heating cycles, after cooling to −150 °C. The heating rate was 20 °/min, and in some cases, when the glass transition was hard to determine, the rate was increased to 40 °/min.

FTIR spectroscopy. Infrared spectra were recorded on a Bio-Rad 165 FTIR spectrophotometer with the samples in KBr pellets or thin membranes deposited on NaCl plates.

II.1.4. Results and Discussion

FTIR and DSC characteristics of electrolytes containing high lithium salt concentrations and acrylic polymeric matrices

Table II.1.2. Phase transitions and absorption bands ν_{CN} in IR spectra of electrolytes comprising poly(AN-*co*-BuA)[a], PMMA or PBuA and various lithium salts

Matrix	Salt[b]	Glass transition temperature T_g /°C	$T_{g\ matrix} - T_{g\ electrolyte}$ /°C	Melting point T_m / °C	$\nu_{C\equiv N}$[c] / $\nu_{C=O}$[d] in FTIR / cm^{-1}
Poly(AN-*co*-BuA 2:1)	---	42-44 (I; II)[e]	---	49-50 (I; II)	2242
	$LiN(CF_3SO_2)_2$	–22.5 (I; II)	64.5	--- (I; II)	2236; **2252**
	LiI	10 (I)	32 (I)	69 (I)	2244, **2264**
		–6.5 (II)	48.5 (II)	--- (II)	
	$LiCF_3SO_3$	56 (I)	–14 (I)	145	**2246**, 2270
		45 (II)	–3 (II)	~140 (trace)	
	$LiAlCl_4$	54 (I)	–12 (I)	98; 105 (I)	**2248**, 2260
		49 (II)	–7 (II)	98.5; 103.5 (II)	(trace)
	$LiClO_4$	–8.5 (I)	50.5 (I)	70; 91 (I)	2242, **2268**
		–27 (II)	69 (II)	65; 95 (II)	
	$LiBF_4$	27 (I)	15 (I)	110 (I)	2242, 2260
		20 (II)	22 (II)	93 (II)	
PMMA	---	105	---	>300	**1735**
	$LiN(CF_3SO_2)_2$	no data	---	---	**1712**
	LiI	50 (I)	55 (I)	---	**1714**
		48 (II)	57 (II)		
PBuA	---	–55	---	---	**1735**
	$LiN(CF_3SO_2)_2$	–72 (I)	17 (I)	---	**1712**
		–73.5 (II)	18.5 (II)		
	LiI	–92 (I)	37 (I)	---	**1718**
		–95 (II)	40 (II)		

[a] poly(AN-*co*-BuA) comprising 67 mol % of AN monomeric units

[b] salt : AN monomeric units (m.u.) in the copolymer molar ratio = 1.2 or salt : MMA m.u. (salt : BuA m.u.) molar ratio for PMMA (PBuA) = 1.2

[c] for poly(AN-*co*-BuA)

[d] for PMMA and PBuA

[e] I and II – first and second heating cycle, respectively

In order to compare the effect of lithium salts on the properties of electrolytes involving various polymeric matrices of clearly differing glassy transformation temperatures, poly(AN-*co*-BuA) (T_g = 43 °C), PMMA (T_g = 105 °C) and PBuA (T_g = –55 °C) were used. The results of

DSC and FTIR studies of electrolytes comprising various lithium salts at the molar ratio of the salt to AN m.u. in the copolymer (or of the salt to MMA m.u. or BuA m.u. in PMMA or PBuA, respectively) of 1.2 are shown in Table II.1.2.

As is seen, the salt acts like a plasticizing agent on the system, causing in a majority of systems a decrease in the glass transition temperature. This effect depends on the salt anion; it is the clearest for $LiN(CF_3SO_2)_2$, in the case of which the system is amorphous, and T_g decreases to about –22 °C for poly(AN-*co*-BuA), about –40 °C for PMMA and –73.5 °C for PBuA. In the case of $LiCF_3SO_3$ separation of the salt and polymer is observed. The transformation at 56°C (I^{st} heating cycle) and the relaxation peaks at 62 and 45 °C (II^{nd} heating cycle) in our opinion correspond to T_g of poly(AN-*co*-BuA) forming a separate phase. This temperature is slightly shifted with respect to T_g of the "pure" copolymer. This fact can be explained by the polydispersity of molecular weights and distribution of the m.u. sequences in the copolymer. A better solubility of the salt can be assigned in such a system to the copolymer phase richer in BuA m.u., and hence the domains of the "free" matrix are enriched in AN m.u. or to interactions of large ionic agglomerates of the salt with the matrix that limit the segmental motion of the polymer chains causing stiffening of the system and increase in T_g. The effect of melting at about 140 °C may result from the complex formed between the salt ionic agglomerates and polymeric matrix. The electrolyte has a milky coloring, which may indicate the occurrence of the polymer and salt microdomains. Such a structure may result from the similar solubility of components in acetonitrile, and thus during solvent removal no clear separation of the phases occurs. It seems that a similar situation takes place in the case of $LiAlCl_4$, where we also observe a slight increase in T_g. For this system, considerable heat effects, however, are observed connected probably with the melting of the crystalline phase of positive ionic associates with the polymeric matrix, of varying stoichiometry (T_m = 98 and 103 °C). The electrolytes have a milky coloring and are rigid, which may also result from the presence of microdomains of the polymer, complexes and also undissolved salt. For $LiClO_4$ the occurrence of melting peaks of complexes at 70 and 91 °C are also observed. This system, despite the low glass transition temperature (T_g = –8.5 °C in the first heating cycle and –26.5 °C in the second one) is rigid due to the high share of the crystalline phase. For LiI, over the whole concentration range studied from 11 to 70 wt. %, the plasticizing effect of the salt is clearly observed; T_g decreases from 42 °C for the pristine poly(AN-*co*-BuA) matrix, to –6.5 °C for the system of the molar ratio salt : AN m.u. in the copolymer of 1.2 (57.9 wt. %) and to –42°C at a two-fold molar excess of the salt (69.6 wt. %). The dependence of T_g on concentration is presented in Figure II.1.1. and Table II.1.3. Furthermore, the DSC studies show that the electrolytes comprising nearly 60 wt. % of LiI contain a crystalline phase with a melting point of about 70 °C. At higher salt concentrations a second crystalline phase appears at 80 °C with a decrease in T_g. These are probably phases of the crystalline complexes of the polymer matrix and positive ions of various degrees of association $[Li_nI_m]^+$.

The plasticizing effect of the lithium salts was observed earlier for PISE containing PAN or its copolymers.[7,9,11,17] Our observations, in accordance with literature reports, show that contrary to classical salt-in-polymer systems based on polyether matrices, in composites containing acrylic matrices [poly(AN-*co*-BuA), PMMA, PBuA] no stiffening of chains due to physical crosslinking occurs, even at low salt concentrations, only an increase in their flexibility. The interaction of the salt with the polymer polar groups such as C≡N or C=O is considerably weaker than that in polyethers and depends on the anion and on the salt concentration. The salt compensates the dipol-dipol interactions between the polymer chains, due to which they achieve greater mobility and the system becomes more flexible. This effect is clearer with an increase in the salt share. Such a situation occurs for salts like $LiN(CF_3SO_2)_2$ or LiI, well dissolving in a given polymeric matrix, and for their complexes with the polymer. In the case of limited

solubility the system becomes heterogeneous and a crystalline phase of the salt or/and its complex with the matrix appears.

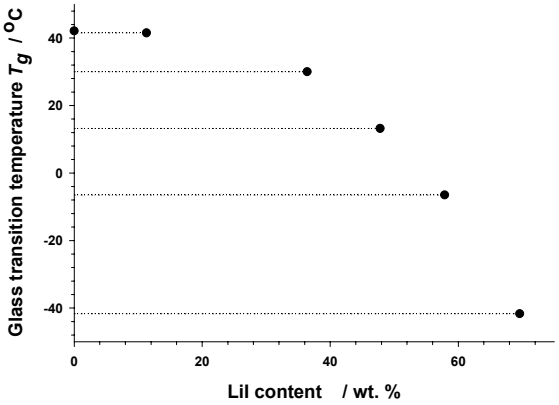

Figure II.1.1. Glass transition temperature T_g of electrolytes comprising poly(AN-co-BuA 2:1) and LiI depending on the salt concentration.

The mode of interaction of the salt with the polymeric matrix can be observed by the changes in the vibration frequencies of polar groups bonds present in the matrix and capable of forming complexes with the salt ions. Examples of the complexation of C≡N groups with lithium salts are known. The formation of these complexes results in an increase in the vibrations frequency of the C≡N bond observed in Raman and IR spectra.[8,9,11,13] As a result of complexing, a new band at about 2270 cm^{-1} attributed to the groups engaged in complexes with positive salt ions appears, besides the band of the "free" C≡N group at 2244 cm^{-1}. Tables II.1.2 and II.1.3 show the bands observed in IR in the C≡N and C=O groups vibration ranges.

Table II.1.3. Phase transitions and absorption bands ν_{CN} in IR spectra of electrolytes comprising poly(AN-*co*-BuA)[a] and LiI

LiI concentration wt. %	Li/CN molar ratio	T_g[b] °C	T_m °C	ν_{CN} cm^{-1}
11.3	0.1	41.5	----	2242
36.4	0.5	30.0	----	2242; 2264
47.8	0.8	13.2	----	2244; **2264**
57.9	1.2	10	69 (I)[c]	2244; **2264**
		-6.5	---- (II)[c]	
69.6	2.0	-41.7	69; 82 (I) 67; 80 (II)	2248 (trace); **2272**

[a] poly(AN-*co*-BuA) comprises 67 mol % of AN monomeric units
[b] glass transition temperature was determined from the second heating cycle
[c] I, II – first and second heating cycle, respectively

It can be noted that in the case of $LiCF_3SO_3$ and $LiAlCl_4$ the interaction of the salt with the matrix is weak and uncomplexed C≡N groups dominate in the system. In the case of $LiAlCl_4$ this interaction is weaker and a weak band at 2260 cm^{-1} is observed. Similarly, the share of bands derived from complexed C=O groups in the copolymer is small (these data are not shown in the table). In the pristine copolymer $\nu_{C=O}$ appears at 1732 cm^{-1}. The salt causes broadening and splitting of this band with a shift towards lower wavelengths. Salts well plasticizing the copolymer, $LiN(CF_3SO_2)_2$, and also LiI, interact stronger with the matrix, which is exhibited by the greater intensity of the complexed groups bands. For LiI (Table II.1.3), at a two-fold molar excess of the salt, a band derived from complexed C≡N groups is present almost alone in the FTIR spectrum, and in the C=O group region well splitted bands appear at 1700, 1710 and 1720

cm^{-1}. For electrolytes involving $LiN(CF_3SO_2)_2$, LiI and for PMMA and PBuA matrices bands of complexed carbonyl groups are mainly present. This may result from the better solubility of these salts in polymers containing exclusively ester substituents.

Table II.1.4. Phase transitions and absorption bands ν_{CN} in IR spectra of electrolytes comprising poly(AN-*co*-BuA)[a] and mixtures of lithium salts with $LiN(CF_3SO_2)_2$

Salt[b] + $LiN(CF_3SO_2)_2$	T_g[c] / °C	T_m / °C	ν_{CN} /cm^{-1}
$LiN(CF_3SO_2)_2$	-22.5	---	2236; **2252**
$LiClO_4$	-23.4	79	**2244**; 2260
LiI	-21.4; 4	71.5	**2272**
$LiAlCl_4$	-22.5	---	**2248**; 2260

[a] poly(AN-*co*-BuA) containing 67 mol % of AN monomeric units
[b] total salt : AN monomeric units (m.u.) in the copolymer molar ratio = 1.2; molar ratio of salts = 1 : 1
[c] glass transition temperature determined from the second heating cycle

Table II.1.4 shows the temperatures of phase transitions for electrolytes comprising equimolar mixtures of the imide salt with other lithium salts at the Li : CN groups molar ratio of 1.2. The T_g values of these systems decrease to −22 - −23 °C, characteristic of electrolytes with $LiN(CF_3SO_2)_2$. We also see changes in the melting points, the system with $LiAlCl_4$ becomes amorphous, and in that with $LiClO_4$ one of the crystalline phases of higher melting point disappears. The plasticizing effect of the imide salt is clearly revealed in these systems. Electrolytes comprising a mixture of salts, LiI and $LiN(CF_3SO_2)_2$, behave differently from the other systems. In the FTIR spectrum the ν_{CN} band derived from the uncomplexed group is not present and a much shifted signal at 2272 cm^{-1} occurs. In DSC these electrolytes show two glass transition temperatures characteristic of systems with neat LiI and $LiN(CF_3SO_2)_2$ salts (Table II.1.4).

The results presented show the occurrence of weak interactions of the lithium salts with polar C≡N and C=O groups in the studied acrylic matrices, which result in a considerable decrease in the glass transition temperatures, and in some cases by the appearance of crystalline phases. These interactions are visible in the form of new absorption bands in the IR, shifted by about 20-30 cm^{-1}. The magnitude of these effects depends on the lithium salt and its concentration, which is probably connected with the solubility in the matrix of the salt and its complexes with the polymer.

Conductivity of electrolytes comprising various lithium salts

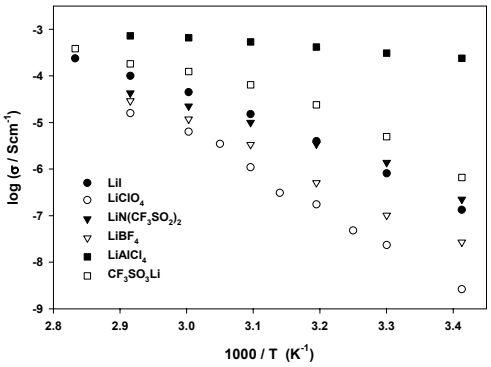

Figure II.1.2. Ionic conductivity of electrolytes based on poly(AN-co-BuA 2 :1) with different lithium salts (molar ratio of salt : AN m. u. in the copolymer = 1.2).

Figure II.1.2 shows the conductivity as a function of temperature for electrolytes comprising poly(AN-*co*-BuA) (2:1) and various lithium salts (LiI, $LiN(CF_3SO_2)_2$, $LiClO_4$, $LiAlCl_4$, $LiCF_3SO_3$ and $LiBF_4$) at the salt : AN m.u. molar ratio of 1.2. As can be seen, the salt anion

clearly affects the electrolyte conductivity. The highest conductivity, of the order of 10^{-4} S·cm^{-1}, is shown by the system with $LiAlCl_4$, with a slight effect of temperature on its value. The electrolytes involving this salt have a milky coloring and are rigid. The DSC and FTIR studies show a multiphase structure of this system and very weak interaction with the polymer matrix (Table II.1.2). High conductivity stands for a favorable structure for fast ionic transport. Similar properties are shown by electrolytes involving $LiCF_3SO_3$, but the interaction with the matrix is stronger and in the FTIR spectrum a band at 2270 cm^{-1} besides the $\nu_{C\equiv N}$ band of the uncomplexed matrix at 2246 cm^{-1} is present. The conductivity of this system was lower, but the highest from among the other salts studied. The lowest conductivity, especially in the temperature range close to ambient temperature, was shown by the electrolyte with $LiClO_4$. In this system, similarly as with $LiAlCl_4$, crystalline phases of high fusion heat ($\Delta H \approx 50$ J/g) are present, providing the composite with stiffness and rigidity, despite that T_g is lower than ambient temperature. It does not show, however, a milky coloring and strongly shifts the absorption bands of C≡N and C=O groups in FTIR, which may indicate good mixing of the salt and polymer. Transparent and flexible membranes were obtained for systems comprising $LiN(CF_3SO_2)_2$ and LiI, at the same molar concentration of the salt. The conductivity of these membranes is similar, with values of the order of 10^{-7} S·cm^{-1} at 20 °C and 10^{-5} S·cm^{-1} at 60 °C. The fact that in subsequent heating and cooling cycles the conductivity values are repeated, also for LiI after heating up to above its T_m value, is a characteristic fact for these systems. The temperature dependence of conductivity for these systems is well described by the VTF equation.

$$\sigma(T) = \sigma_o T^{-0.5} \exp[-B / (T - T_o)]$$

In this equation, σ_o is the pre-exponent conductivity, B is the pseudoactivation energy for conduction and T_o is the ideal glass transition temperature. The parameters of the equation obtained from optimization are presented in Table II.1.5. This table shows also the logarithm values of conductivity of electrolytes at T_g (log σ_{Tg}) and the corresponding decoupling index (log R_τ). The R_τ parameter is defined as the ratio of the structural relaxation time (τ_s) to the conductivity relaxation time (τ_o) and describes to what extent the mobility of ions is connected with the segmental relaxation of the polymer chains.[18] For highly conducting glasses the log decoupling index value is high, of about 12.[19]

Table II.1.5. VTF parameters and logarithm of decoupling indexes (log R_τ) of electrolytes comprising poly(AN-*co*-BuA) and $LiN(CF_3SO_2)_2$ or LiI [a]

Salt [b]	σ_o S·cm^{-1}	B K	T_o K	T_g [c] K	log σ_{Tg}	log R_τ
$LiN(CF_3SO_2)_2$	5.18	1810	182	250	–11.1	3.3
LiI	4.93	799	195	266	–9.9	4.4

[a] VTF parameters and log R_τ were determined from conductivity results from the second heating cycle
[a] salt : AN monomeric units (m.u.) in the copolymer molar ratio = 1.2
[b] determined from DSC

Log R_τ was calculated on the basis of the approximate relaxation:[20]

$$\log R_\tau \approx 14.3 + \log \sigma_{Tg}$$

The log R_τ value of the system with $LiN(CF_3SO_2)_2$ is 3.3 and of that with LiI is higher and equal to 4.4. The log R_τ values of the order of 3 - 5 are achieved for electrolytes of high $LiClO_4$ concentrations, for which it is assumed that the lithium cation motion is highly decoupled from the structural relaxation.[21] If the T_g value of the system with $LiAlCl_4$ is assumed as 49 °C, then the log R_τ value for this system would be 11. For the pristine $LiAlCl_4$ salt the determined R_τ

value is 9.3.[22] Thus, it can be preliminarily assumed that the conductivity of the systems studies depends on the degree of interaction of the salt with the matrix, and the stronger are these interactions, the less mobile are the ions in the conduction process. Good conduction is possible at appropriate organization of the salt, complexes of various stoichiometry and polymer microphases, and these depend on the anion and polymer as well as on the salt concentration. The results of studies carried out for systems containing mixtures of salts confirm such a conception. Figure II.1.3 shows changes in conductivity as a function of temperature of electrolytes comprising poly(AN-*co*-BuA 2:1) and equimolar mixtures of $LiN(CF_3SO_2)_2$ with LiI, $LiClO_4$ or $LiAlCl_4$.

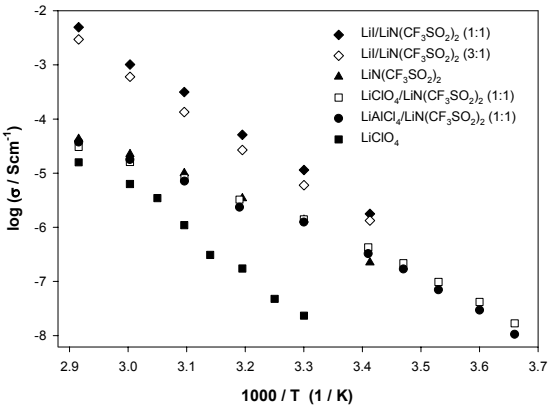

Figure II.1.3. Ionic conductivity of electrolytes based on poly(AN-co-BuA 2:1) and mixtures of lithium salts with $LiN(CF_3SO_2)_2$ (molar ratio of salt : AN m. u. in the copolymer = 1.2).

As can be noted, the use of various lithium salts together with the imide salt causes that the electrolytes achieve conductivity values similar to those of the system with the imide salt alone. A clear increase in conductivity can be noted for the electrolytes containing $LiN(CF_3SO_2)_2$ and $LiClO_4$ over that for the perchlorate alone, especially in the range of lower temperatures. For mixtures with $LiAlCl_4$ a decrease in conductivity is seen, the system becomes more flexible, the solubility of the salt and its interaction with the matrix increases, and thus the fine phase structure responsible for the high conductivity is destroyed. Systems with $LiN(CF_3SO_2)_2$/LiI show conductivity values larger than those for singular systems and the composition of this mixture in the concentration ranges studied does not affect significantly the conductivity of the system. In DSC traces these electrolytes show two glass transition temperatures close to the T_g values of systems with neat LiI and $LiN(CF_3SO_2)_2$ salts (Table II.1.4). Thus, the addition of the imide salt causes changes in the mode of interaction of ions with the matrix and of the microstructure of composites, which affects their conducting properties.

Effect of the salt concentration on the conductivity of PISEs

The dependence of ionic conductivity on salt concentrations was determined for LiI and $LiN(CF_3SO_2)_2$ with poly(AN-co-BuA 2:1) as the polymeric matrix.

The conductivity isotherms at 30 and 70 °C presented in Figures II.1.4 and II.1.5 show that, with an increase in the salt concentration a gradual increase in conductivity occurs, until reaching a maximum value, and a further increase in concentration causes a slight drop in conductivity, after which it increases again. For LiI the maximum occurs at the salt concentration of 53 wt. %, which corresponds to the equimolar ratio of the salt to the CN groups of the matrix.

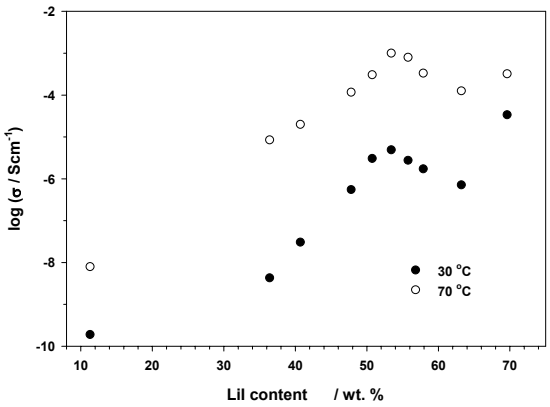

Figure II.1.4. Conductivity isotherms determined at (●) 30 and (o) 70 °C for electrolytes comprising poly(AN-co-BuA 2:1) and LiI depending on the salt concentration.

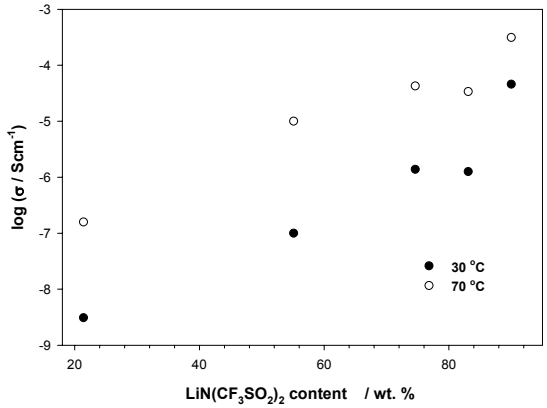

Figure II.1.5. Conductivity isotherms determined at (●) 30 and (o) 70 °C for electrolytes comprising poly(AN-co-BuA 2:1) and $LiN(CF_3SO_2)_2$ depending on the salt concentration.

The DSC traces, at the Li to CN groups molar ratio of 1.2, show the presence of a crystalline phase of the complex of T_m = 69 °C, the share of which increases with an increase in the salt concentration, and at a two-fold molar excess of the salt a second phase of the complex of $T_m \approx 80$ °C is present, probably with the participation of larger ionic agglomerates, and also the phase of the recrystallizing salt is also possible. At the same time, an increase in intensity of absorption bands of complexed C≡N and C=O groups is seen in infrared spectra, which indicates a nearly complete engagement of the matrix polar groups in the interaction with positive salt ions. An increase in conductivity with increasing concentration results probably from the gradual increase in the charge carriers concentration. The decreasing distances between the ion agglomerates and possibility of their aggregation into clusters changes the conduction mechanism to one involving increasing decoupling from the matrix. The decrease in conductivity after reaching a maximum and then again an increase in it is hard to explain. In this concentration range changes in the ion agglomerates structure probably take place and the conduction mechanism changes to a one similar to that of conduction in glasses. A similar relationship occurs for $LiN(CF_3SO_2)_2$ with a maximum at 75 wt. % of the salt, which corresponds to the molar ratio of the salt to CN groups of the matrix equal to 1.2. At the salt concentration above equimolar the system becomes heterogeneous and crystalline islands are visible on the electrolyte surface in SEM images. In the DSC studies of this sample, no melting effect is observed up to 200 °C. It can therefore be suggested that crystallization of the salt takes place on the surface of the film (T_m = 234 °C). SEM images of the electrolyte containing poly(AN-*co*-BuA) and 75 wt. % of $LiN(CF_3SO_2)_2$ (obtained by casting from solution) are shown

in Figure II.1.6. The system with the imide at a very high salt concentration of over 90 wt. % has the form of a very viscous metastable liquid of high conductivity, which after a certain time is transformed into a high-melting-point solid (Figure 5).

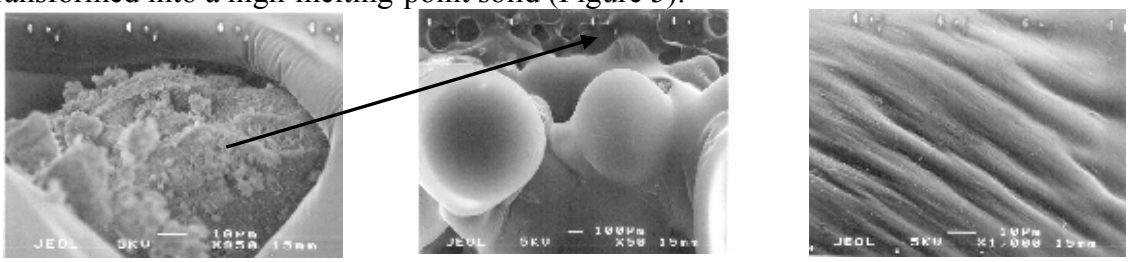

Figure II.1.6. SEM images of the polymer electrolyte based on poly(AN-co-BuA 2:1) and 74.6 wt. % of $LiN(CF_3SO_2)_2$.

Effect of the chemical structure of the polymeric matrix on the PISE conductivity

For these studies, the systems chosen were poly(AN-co-BuA 2 : 1) (T_g = 42 °C) and polymers of drastically different glass transition temperatures such as PMMA (T_g = 105 °C) and PBuA (T_g = –55 °C). The conductivity behavior of systems comprising $LiN(CF_3SO_2)_2$ and LiI is shown in Figure II.1.7.

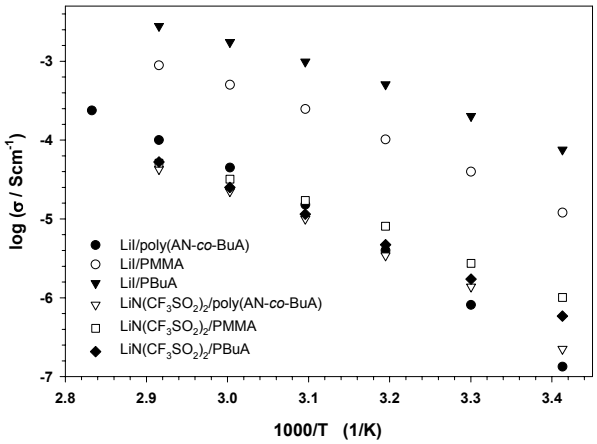

Figure II.1.7. Conductivity of electrolytes comprising 58 wt. % of LiI, 75 wt. % of $LiN(CF_3SO_2)_2$ and various polymeric matrixes.

The use of PMMA, or PBuA, as the matrix together with LiI gives a distinct increase in conductivity with respect to that of poly(AN-*co*-BuA) over the whole temperature range. The highest conductivity is achieved by systems of PBuA with LiI. Lithium iodide strongly plasticizes these matrices decreasing T_g by 40 – 60 °C (Table II.1.2). The effect of different polymeric matrices on the conductivity of electrolytes containing $LiN(CF_3SO_2)_2$ is not as pronounced as for those containing LiI. A possible explanation for these differences might lie in the differing degree of dissociation of the salts in the polymers. The imide salt mixes equally well with poly(AN-*co*-BuA), as well as with PMMA and PBuA, whereas LiI dissolves much better in polymers containing ester groups and, as will be noted, a longer aliphatic substituent in this group is favored.

Transference number (t_+) for PISE: poly(AN-co-BuA) with $LiN(CF_3SO_2)_2$ or LiI

Table II.1.6 shows the results of measurements of the cation transference number for the electrolyte containing poly(AN-*co*-BuA 2:1) and lithium salts $LiN(CF_3SO_2)_2$ or LiI, at the salt to AN m.u. molar ratio of 1.2. These electrolytes were selected as optimal ones from the point of view of their conducting and mechanical properties (they form flexible membranes). For the

system with $LiN(CF_3SO_2)_2$, from the measurement carried out at 65 °C the value 0.67 was obtained and at 85 °C that of 0.48. Similarly high values were obtained for the system with LiI (Table II.1.6). In the low-concentrated LiI-PEO polymer electrolytes the transference number is 0.3-0.35,[23] and for $LiN(CF_3SO_2)_2$ 0.1-0.5, depending on the temperature.[24] Thus, it can be noted that in relation to classical systems, electrolytes of high salt concentrations are a great progress from the anion immobilization point of view. It seems that by appropriate selection of the salt concentration and of the matrix it is possible to obtain systems of a dominating share of cations in the electric charge transport. Furthermore, the electrochemical measurements in the system of lithium electrodes indicates a high chemical stability of the electrolytes in relation to lithium electrodes. For example, R_{sei} of electrolytes with $LiN(CF_3SO_2)_2$ at 70 °C varies from 280 to 300 $\Omega \cdot cm^2$ over a period of 320 hours.

Table II.1.6. Transference number (t_+) for polymer in salt electrolytes based on poly(AN-co-BuA 2:1) and $LiN(CF_3SO_2)_2$ or LiI[a]

Salt	Temperature / °C	t_+
$LiN(CF_3SO_2)_2$	65	0.67
	85	0.48
LiI	70	0.54-0.76

[a] molar ratio of salt : AN monomeric units in the copolymer = 1.2

II.1.5. Conclusions

The mechanical properties of electrolytes and ability to conduct an electrical charge are determined by the complex interplay of several factors, such as: salt concentration, chemical structure of the polymer matrix and that of the lithium salt anion.

The application of poly(AN-*co*-BuA) instead of PAN in the synthesis of polymeric electrolytes combines the possibility of introducing AN m.u. to the polymeric matrix with the solubility of these systems in a volatile aprotic solvent, such as acetonitrile. The T_g of the matrix can be controlled in a simple way over a broad temperature range (15 – 56 °C), by appropriate selection of the monomer feed composition. For certain lithium salts, e.g. LiI, acrylic polymers such as PMMA or PBuA are favorable matrices.

The introduction of classical, commercially available salts at a suitable proportion to the polymer permits to achieve highly conducting systems. At high concentrations the salt occurs in the form of aggregates, which interact with the matrix. This was observed in the FTIR spectra as the appearance of a new absorption band of the C≡N and C=O groups. DSC studies show the presence of crystalline phases in a majority of systems, which are probably crystalline complexes of varied stoichiometry of the salt ions and the polymer. The formation of complexes causes a decrease in the glass transition temperature of the system, resulting from the equalization of polar interactions between the polymer chains. This decrease in T_g increases with an increase in the salt concentration. The plasticizing effect depends on the salt anion.

The determined t_+ values indicate an increased participation of cations in the electric charge transport in relation to classic polymer electrolytes.

References

1. Gorecki, W.; Jeannin, M.; Belorizky, E.; Roux, C.; Armand, M. *J. Phys.: Condens. Matter*. **1995**, *7*, 6823.
2. Bruce, P. G.; Haregrave, M. T.; Vincent, C. A. *Solid State Ionics* **1992**, *53-56*, 1087.
3. Tarascon, J. M.; Armand, M. *Nature* **2001**, *414*, 359.
4. Florjańczyk, Z.; Bzducha, W.; Dygas, J. R.; Misztal-Faraj, B.; Krok, F. *Solid State Ionics* **1999**, *119*, 251.
5. Angell, C. A.; Liu, C.; Sanchez, E. *Nature* **1993**, *362*, 137.

6. Fan, J.; Angell, C. A. *Electrochim. Acta* **1995**, *40*, 2397.
7. Forsyth, M.; Sun, J.; MacFarlane, D. R. *Solid State Ionics* **1998**, *112*, 161.
8. Ferry, A.; Edman, L.; Forsyth, M; MacFarlane, D. R.; Sun, J. *J. Appl. Phys.* **1999**, *86*, 2346.
9. Ferry, A.; Edman, L.; Forsyth, M; MacFarlane, D. R.; Sun, J. *Electrochim. Acta* **2000**, *45*, 1237.
10. Forsyth, M.; Sun, J. Z.; MacFarlane, D. R.; Hill, J. A. *J. Polym. Sci., Part B: Polym. Phys.* **2000**, *38*, 341.
11. Bushkova, O. V.; Zhukovsky, V. M.; Lirova, B. I.; Kruglyashov, A. L. *Solid State Ionics* **1999**, *119*, 217.
12. Forsyth, M.; Jiazeng, S.; MacFarlane, D. R. *Electrochim. Acta* **2000**, *45*, 1249.
13. Wang, Zh.; Gao, W.; Chen, L.; Mo, Y.; Huang, X. *Solid State Ionics* **2002**, *154-155*, 51.
14. Zalewska, A.; Pruszczyk, I.; Sułek, E.; Wieczorek, W. *Solid State Ionics* **2003**, *157*, 233.
15. Evans, J.; Vincent, C. A.; Bruce, P. G.; Doyle, M.; Newman, J. *J. Electrochem. Soc*. **1995**, *142*, 3465.
16. Appetecchi, G. B.; Dautzenberg, G.; Scrosati, B. *J. Electrochem. Soc*. **1996**, *143*, 6.
17. Watanabe, M.; Kanba, M.; Nagaoka, K.; Shinohara, I. *J. Polym. Sci., Polym. Phys. Ed.* **1983**, 21, 939.
18. Angell, C. A. *Solid State Ionics* **1986**, *18-19*, 72.
19. Gray, F. M. *Polymer Electrolytes*, The Royal Society of Chemistry, Cambridge, 1997.
20. Angell, C.A. *Annu. Rev. Phys. Chem*. **1992**, *43*, 693.
21. Xu, W.; Wang, L-M.; Angell, C.A. *Electrochim. Acta* **2003**, *48*, 2037.
22. Videa, M.; Angell, C. A. *J. Phys. Chem. B* **1999**, *103*, 4185.
23. Strauss, E.; Golodnitsky, D.; Ardel, G.; Peled, E. *Electrochimica Acta* **1998**, *43*, 1315.
24. Doeff, M. M.; Edman, L.; Sloop, S. E.; Kerr, J.; De Jonghe, L. C. *J. Pow. Sources* **2000**, *89*, 227.

II.2. Polyacrylamide and Poly(acrylonitrile-*co*-Butyl Acrylate) Based Polymer-in-Salt Electrolytes

II.2.1. Introduction

The interest in novel energy storage and conversion devices arises from the predictable increase in energy consumption by human beings in the next century. Therefore, due to limited resources of fossil fuels as well as environmental needs of cleaner and renewable energy sources, there is a search for alternative, possibly renewable energy sources such as sun, wind or geothermal energy together with studies on novel chemical energy conversion and storage devices mainly lithium or lithium ion batteries and fuel cells [1].

Our work within this part of the project dealt with these novel ideas in the field of lithium or lithium-ion batteries based on polymeric solid electrolytes. The solid systems offer several advantages compared to the liquid partners such as: simple design, natural seal, resistance to shocks and vibrations, increased resistance to pressure and temperature variations, broad stability range of electrolyte, possibility of miniaturization. Most of these features can be realized in the systems comprising solid polymeric electrolytes e.g. complexes of electron donor polymers with inorganic salts or acids [2].

Desirable properties of polymeric electrolytes for application in lithium or (and) lithium-ion batteries are as follows: chemical and mechanical stabilities over a wide temperature range, wide electrochemical stability window, low activation energy for ionic conduction, cationic transport numbers close to unity, good electrode-electrolyte characteristics, ease of sample preparation and handling. Most of these properties are satisfied by polyethers (which are the most extensively studied polymeric matrixes) but still there is a number of problems which has to be solved before reaching the commercialization step [3]. The main ones are as follows:

- low cationic transport numbers (close to 0.1) of most of thepolymeric electrolytes studied
- difficulties in evaluation of cationic transport numbers
- formation of highly resistive layers at the anode – electrolyte interface
- high degree of crystallinity of PEO based electrolytes
- ambient temperature conductivity not high enough for application in batteries

An effective approach to achieve polymer electrolytes having single cation conductivity in a solvent-free configuration, is that directed to the synthesis of the so-called polymer in salt systems, in which a large amount of salt is mixed with a small fraction of polymer to induce mechanical integrity of the final membrane [4,5]. It is well known that some pristine lithium salts of low T_g values exhibit ambient temperature conductivity in the range of 10^{-2}-10^{-3} S/cm, i.e. values which are suitable for battery applications. However, the addition of the polymer component usually results in a considerable decay in conductivity [6]. In previous studies, polyacrylonitrile poly(1-vinyl pyrrolidone), and poly(N,N-dimethyl acrylamide) were mostly used as polymer matrixes [6-8]. The highest ambient temperature conductivity exceeding 10^{-6} S/cm was reported for polyacrylonitrile based electrolytes in which lithium triflate was used as a dopant [8].

In our opinion this unfavorable effect, of reduction in conductivity upon the addition of polymer, can be suppressed by a proper choice of the functionality of the polymer chain. To confirm this expectation we have prepared and characterized novel polymer in salt electrolytes based on polyacrylamide (PAAM) or acrylonitrile (AN) – butyl acrylate (BuA) copolymers. The basic idea is to carry out the synthesis by *in situ* polymerization in the presence of the selected lithium salt. The effect of the type of lithium salt and its concentration on conductivity and microstructure of the electrolytes studied is analyzed. To this end impedance spectroscopy, infra-red spectroscopy, DSC and MALDI-ToF techniques have been used.

II.2.2. Experimental

II.2.2.1. Samples Preparation

Polyacrylamide based systems

In the first stage, studies on the synthesis of various polymer in salt electrolytes via *in situ* polymerization of acrylamide (AAM) (Aldrich, reagent grade) in the presence of a lithium salt were undertaken. The following lithium salts were used in these studies: $LiClO_4$, $LiCF_3SO_3$, $LiAlCl_4$ and $LiN(CF_3SO_2)_2$ (all Aldrich, reagent grades). The salt to monomer molar ration varied from 2:1 to 1:2. Two different polymerization procedures have been applied. The first one was the free radical polymerization performed in the molten monomer in the presence of the added salt. In the first step acrylamide was melt at 85 °C. After melting completion, the lithium salt was added stepwise at 85 °C until complete dissolution of the salt in the molten monomer occurred. This was followed by the addition of benzoyl peroxide (Aldrich, reagent grade) (polymerization initiator) while still keeping the constant reaction temperature. The exothermic polymerization immediately followed the addition of the initiator. The key factor for the successful synthesis was to keep the reaction temperature relatively close to 85 °C during the entire procedure. Overheating caused uncontrolled polymerization with visible precipitation of the added salt. After polymerization completion the obtained electrolytes were cooled down to ambient temperature. The polymerization yield was checked by DSC studies of the melting heat of the unreacted monomer in comparison with the heat of melting of the pure acrylamide. The results are included in Table II.2.1.

Table II.2.1. Polymerization yield calculated on the basis of DSC experiments

a) polymerization carried out in melt

Salt	AAM : salt molar ratio	Polymerization yield (%)
$LiAlCl_4$	1 : 0.5	> 95
	1 : 1	> 95
	1 : 1.5	93
	1 : 2	72
$LiN(CF_3SO_2)_2$	1 : 0.5	> 95
	1 : 0.75	> 95
	1 : 1	> 95
	1 : 1.5	> 95

b) polymerization carried out in an acetonitrile solution

Salt	AAM : salt molar ratio	Polymerization yield (%)
$LiAlCl_4$	1 : 1	> 95
$LiClO_4$	1 : 1	> 95

The second procedure involves the free radical polymerization of acrylamide performed in the solution of lithium salt in acetonitrile (Aldrich, spectroscopy grade). The type of salt and samples composition were the same as in the above described “molten” synthetic route. Acrylamide was dissolved in acetonitrile followed by the addition of benzoyl peroxide. The monomer concentration was roughly equal to 5 mass %. The polymerization was carried out at 50 °C. Due to the exothermic nature of the reaction precautions have been undertaken not to overheat the reaction mixtures. The polymerization yield calculated in the same manner as for the “molten” type synthesis is included in Table II.2.1. FT-IR studies performed for the synthesized electrolytes do not show traces of acetonitrile.

Acrylonitrile - butyl acrylate copolymers

The AN and BuA copolymers were obtained in the radical copolymerization of acetonitrile using azo-bis-isobutyronitrile (AIBN) as initiator, at 60 °C. The polymer obtained was dissolved in acetonitrile, and then precipitated with methanol, washed and dried under vacuum. The yield after 5 h of reaction was 95-98%. The macroscopic composition of the copolymer was determined on the basis of elemental analysis, which is approximately equal to the monomer feed composition. The thus obtained polymeric matrix was doped with lithium salts by mixing in acetonitrile the solutions of the polymer and salt, and membranes of the electrolyte were obtained by evaporating off the solvent under dynamic vacuum.

II.2.2.2. Experimental Techniques

Impedance Spectroscopy

Ionic conductivity was determined using the complex impedance method over the temperature range from -30°C to 90°C. The samples were sandwiched between stainless steel blocking electrodes and placed in a temperature controlled oven. The impedance measurements were carried out on a computer-interfaced Solartron-Schlumberger 1255 impedance analyzer over the frequency range from 1 Hz to 1 MHz. The reproducibility of the impedance spectroscopy results was checked by multiple experiments performed at room temperature. The results obtained for samples of the same composition do not differ by more than 10%.

FT-IR spectroscopy

Infrared spectra were recorded on a computer interfaced Perkin-Elmer 2000 FT-IR system with a wavenumber resolution of 1 cm^{-1}. Samples were sandwiched between two NaCl plates and placed in the FT-IR temperature-controlled cell. FT-IR studies were performed at 25°C.

DSC Studies

DSC experiments were performed on a Perkin-Elmer Pyris 1 scanning calorimeter equipped with a low-temperature measuring head and liquid-nitrogen-cooled heating element. Samples in aluminum pans were stabilized by slow cooling to −150°C and then heated at 20°C/min to 150°C. An empty aluminum pan was used as a reference. The estimated error in the determination of the glass transition temperature (T_g) is ±2°C.

MALDI-ToF Studies

The structure of “polymer in salt” electrolytes has been analyzed using Matrix Assisted Laser Desorption and Ionization Time of Flight (MALDI-ToF) technique (Kratos Kompact 4 mass spectrometer equipped with a 337 nm nitrogen laser with a 3 ns pulse duration). The measurements were carried out in the linear mode of the instrument at an acceleration voltage of +20 kV. For each sample, spectra were averaged over 200 laser shots. The samples were dissolved in THF (5 mg/cm^3) and mixed with a solution of the MALDI-ToF matrix (in a majority of cases, 2,5-dihydroxybenzoic acid, 0.2 M in THF). The laser power was moderated in the range of 120-130 units, characteristic of this apparatus, in order to avoid distortion of the mass spectrum.

II.2.3. Results

The synthesized electrolytes were subjected to conductivity experiments as a function of sample composition and temperature. Figure II.2.1 presents conductivity curves shown as a function of inverse temperature for samples prepared by the “molten” procedure. The results for electrolytes doped with various lithium salts with the polymer to salt molar ratio equal 1:1 are shown. Two groups of electrolytes can easily be distinguished. The low conducting systems based on $LiClO_4$ or $LiCF_3SO_3$ doped electrolytes and the highly conducting ones utilizing $LiAlCl_4$ or $LiN(CF_3SO_2)_2$. For the first group, ambient temperature conductivities are in the

range of 10^{-8}-10^{-9} S/cm. For the second group the ambient temperature conductivities are equal to ~10^{-5} S/cm (sample doped with $LiAlCl_4$) and ~10^{-4} S/cm (sample doped with $LiN(CF_3SO_2)_2$.

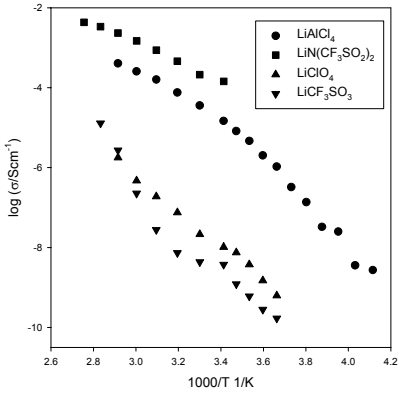

Figure II.2.1. Changes of ionic conductivity as a function of inverse temperature for polyacrylamide - lithium salts electrolytes (polymer to salt ratio =1:1). Samples polymerized in melt.

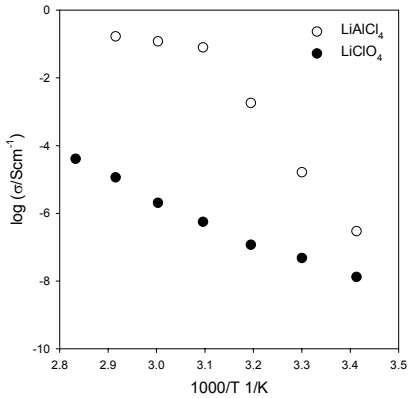

Figure II.2.2. Changes in ionic conductivity as a function of inverse temperature for poly(acrylamide) - lithium salt electrolytes (1:1). Samples polymerized in acetonitrile solutions.

Figure II.2.2 shows the changes in the conductivity as a function of inverse temperature for electrolytes synthesized in acetonitrile solution. Similarly to the results presented in Figure II.2.1, much higher conductivities are measured for $LiAlCl_4$ containing electrolytes for which the value of 10^{-3} S/cm at 40 °C was measured. The characteristic knee point on the conductivity versus reciprocal temperature curve obtained for this electrolyte corresponds to its glass transition temperature.

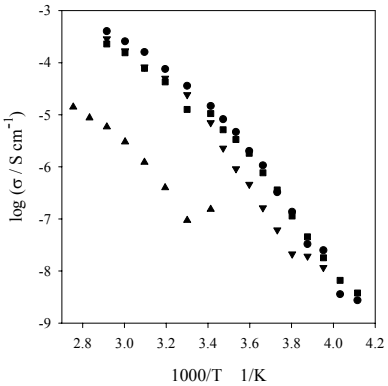

Figure II.2.3. Changes in ionic conductivity as a function of inverse temperature for poly(acrylamide) – $LiAlCl_4$ electrolytes (samples polymerized in melt with various polymer : salt molar ratios: ● - 1:2; ■ - 1:1.5; ▼ - 1:0.5; ▲ - 1:1).

Figure II.2.3 presents conductivity versus inverse temperature curves for electrolytes doped with a various amount of $LiAlCl_4$ (samples polymerized in melt). For all salt concentrations used conductivity increases with temperature from ~10^{-9}-10^{-8} S/cm at –30°C up to 10^{-4}-10^{-3} S/cm at ~100°C. Ambient temperature conductivities for all the electrolytes for which salt to polymer molar ratio is higher than 1 exceed 10^{-5} S/cm. Over almost the entire temperature range the conductivity increases with an increase in the salt concentration. An abrupt increase can be noticed for salt to polymer ratios from 0.5 to 1. For higher salt concentrations conductivity levels off.

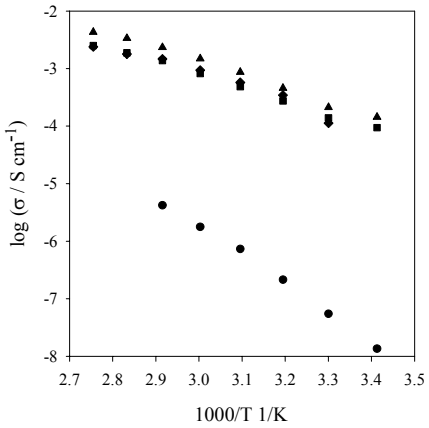

Figure II.2.4. Changes in ionic conductivity as a function of inverse temperature for polyacrylamide – $LiN(CF_3SO_2)_2$ electrolytes (samples polymerized in melt with various polymer : salt molar ratios: ● - 1:0.5; ■ - 1:0.75; ▲ - 1:1; ◊ - 1.1.5).

In Figure II.2.4 changes in the conductivity as a function of reciprocal temperature and $LiN(CF_3SO_2)_2$ concentration are depicted (samples polymerized in melt). The trends observed are similar to those shown in Figure II.2.3 for $LiAlCl_4$ doped electrolytes. However, the conductivities measured for $LiN(CF_3SO_2)_2$ doped electrolytes are higher, exceeding 10^{-4} S/cm at ambient temperatures. For these electrolytes conductivity increases with an increase in the salt concentration and levels off for salt to polymer molar ratios higher than 0.75. It is interesting to note that in these systems the conductivity for samples of the salt to polymer ratio equal to 2 is slightly lower than for electrolytes with lower salt concentration.

All samples studied were subjected to DSC experiments. The only phase transition observed was the glass transition temperature (T_g). DSC data are included in Table II.2.2. The T_g values measured for plasticizing salts ($LiAlCl_4$, $LiN(CF_3SO_2)_2$) are presented together with DSC data for non-plasticizing salt ($LiClO_4$, $LiCF_3SO_3$) based electrolytes. As expected for plasticized systems a decrease in the T_g value is observed with an increase in the plasticizing salt concentration, whereas the addition of non-plasticizing salts induces an increase in the T_g value.

For most of the electrolytes studied the Angell's decoupling index (R_τ) [9] (see equation under Table II.2.2) has been calculated based on the determination of electrolyte conductivity at T_g. The R_τ values varied from 4.5 to 8 for $LiClO_4$ and $LiCF_3SO_3$ doped electrolytes and between 8.4 and 9.1 for $LiAlCl_4$ doped electrolytes. The latter values are close to R_τ of the pure salt (9.6), which according to the Angell's assumption is the evidence of predominantly cationic conductivity.

The structure of "polymer in salt" electrolytes has been analyzed using the Maldi-ToF technique. The possibility of the formation of various types of complexes has been confirmed. The data showing the fraction of the dominant complex phases for electrolytes studied are included in Table II.2.3. For all types of electrolytes the majority complex has an 8:1 polymer to salt ratio. Due to the peak splitting this complex is probably a mixture of a few complexes in which a different degree of the salt association is observed. Molecular weight distribution found

from the Maldi-ToF experiments confirms the oligomeric character of the polymer in salt electrolytes studied. The highest molecular weight found in these experiments was equal to 3×10^3 g/mol.

Table II.2.2. T_g and R_τ values for polyacrylamide based "polymer in salt" electrolytes. Samples polymerized in melt.

Salt	AAM : Salt molar ratio	T_g (°C)	R_τ
$LiClO_4$	1 : 0.5	6	4.7
	1 : 1	36	7.2
	1 : 1.5	40	6.0
	1 : 2	53	7.6
$LiCF_3SO_3$	1 : 0.5	19	5.6
	1 : 1	35	6.4
	1 : 2	70	7.9
$LiN(CF_3SO_2)_2$	1 : 0.75	–69	-
	1 : 1	–72	-
	1 : 1.5	–76	-
	1 : 2	–79	-
$LiAlCl_4$	1 : 0.5	49	8.4
	1 : 1	20	9.1
	1 : 1.5	3	8.6

$log\ R_\tau^* = 14.3 + log\ \sigma_{Tg}$ [9]

Table II.2.3. Samples composition of polyacrylamide – lithium salt electrolytes based on MALDI–ToF studies; (AAM : salt molar ratio = 1:1)

Salt	Majority compounds average composition	Molar percentage of the majority compounds in the sample
$LiClO_4$	$(AAM)_6$	28
	$(AAM)_8$	57
	$(AAM)_9$	14
$LiCF_3SO_3$	$(AAM)_5$	29
	$(AAM)_8$	60
	$(AAM)_{12}$	8.5
$LiN(CF_3SO_2)_2$	$(AAM)_8$	39
	$(AAM)_{10}$	29
	$(AAM)_{12}$	16
	$(AAM)_{15}$	10
$LiAlCl_4$	$(AAM)_4$	16
	$(AAM)_8$	41
	$(AAM)_{11}$	25
	$(AAM)_{15}$	12

The possibility of the formation of polymer–salt complexes has been confirmed by FTIR experiments. In Figure II.2.5 spectra of acrylamide monomer, polyacrylamide, and polyacrylamide based "polymer in salt" electrolytes are presented. The intensity of the peak at ~1615 cm^{-1} characteristic of the monomer decreases upon polymerization with a subsequent increase in the intensity of the peak at ~1670 cm^{-1}. For the "polymer in salt" electrolyte the peak

at 1615 cm^{-1} disappeared and a new peak at ~1630 cm^{-1} is observed. This peak was assigned by us to the formation of the polymer-salt complex.

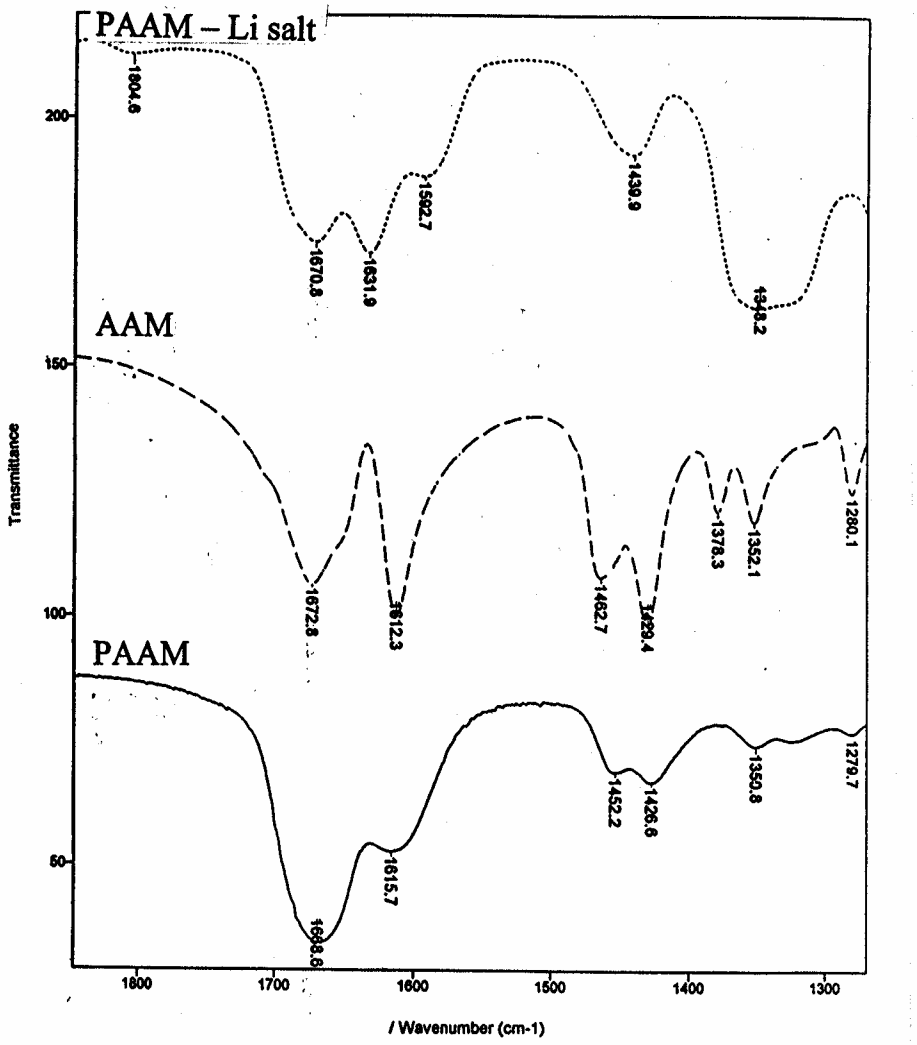

Figure II.2.5. FT-IR spectra of acrylamide (AAM), polyacrylamide (PAAM) and polyacrylamide based "polymer in salt" electrolytes (PAAM : $LiN(CF_3SO_2)_2$ mole ratio = 1:1).

Polymer matrixes characterization:

The next stage of the work was devoted to the synthesis and characterization of acrylonitrile-butyl acrylate copolymers as matrixes for "polymer in salt" electrolytes. The main goal was to achieve an internal plasticizing effect by copolymerization of brittle acrylonitrile with softer butyl acrylate co-monomer. Such a procedure should lead to softening of the polymer matrix and thus decreasing its final T_g and facilitate the preparation of polymeric electrolytes in the form of membranes.

The possibility of affecting the properties of the polymer matrix by changing the copolymer composition has been studied. The changes of glass transition temperature and tendency to copolymer crystallization depending on its composition has been observed on the basis of DSC studies. Monomers, the homopolymers of which considerably differed in glass transition temperature, i.e. BuA (T_g = –55 °C) and AN (T_g = 105 °C), were chosen for the syntheses.

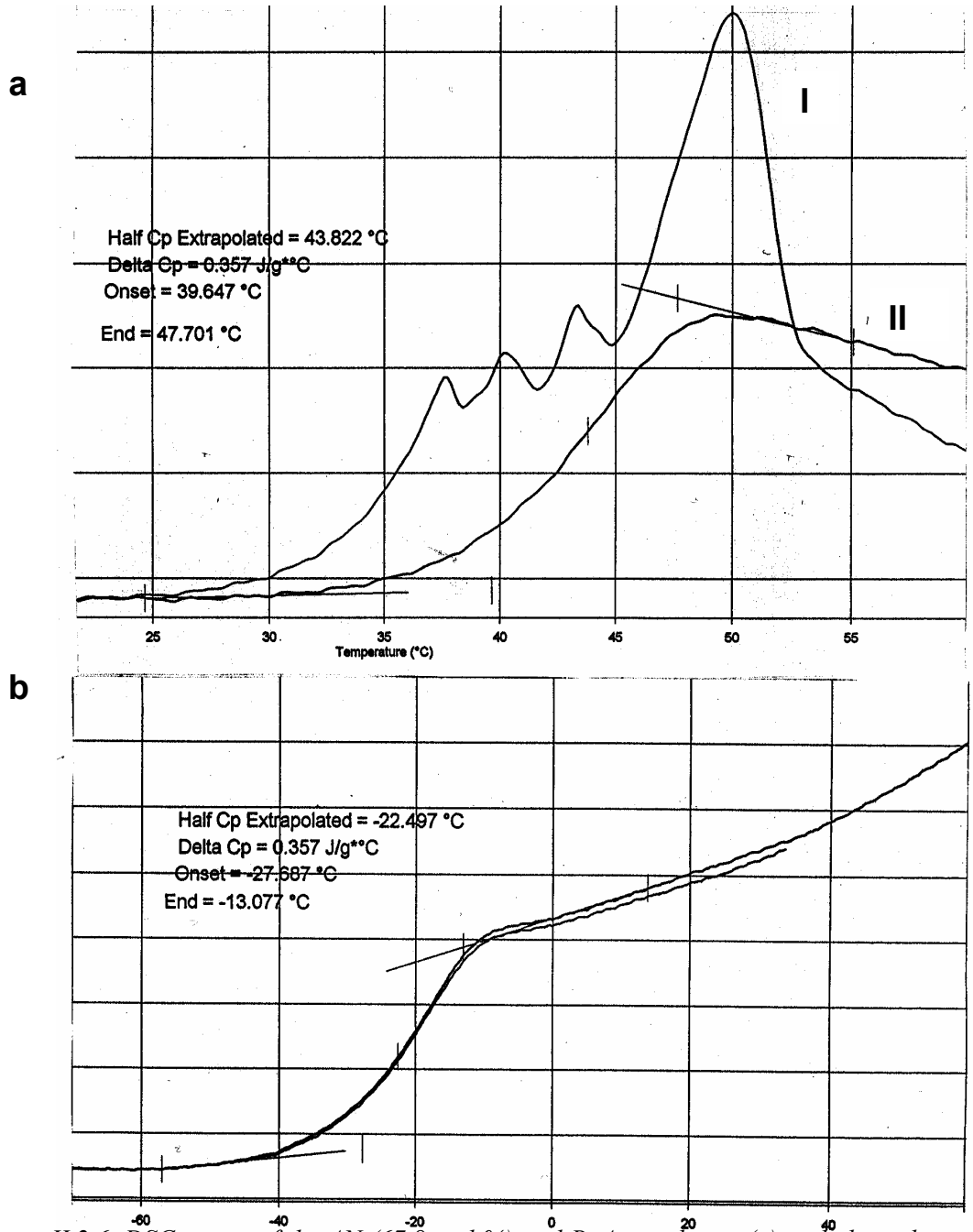

Figure II.2.6. DSC traces of the AN (67.8 mol %) and BuA copolymer (a) and electrolyte comprising 72 wt. % of $LiN(CF_3SO_2)_2$ (b).

The presence of butyl acrylate monomeric units, acting as an internal plasticizer, considerably influences the flexibility of copolymers, causing a decrease in the glass transition temperature, from 105 °C (some sources report 125 °C) for polyacrylonitrile to 15 °C for the copolymer containing 50 mol % of AN monomeric units. The disturbance of the polymer chain structure limits also the ability to crystallization. Melting signals of slight Cp at ca. 50 °C are observed on the DSC traces.

Polymeric electrolytes were obtained using as a matrix a copolymer containing 67.8 mol % of AN monomeric units and doped with one of the following three salts: $LiClO_4$, $LiAlCl_4$ or

$LiN(CF_3SO_2)_2$, or an equimolar mixture of $LiN(CF_3SO_2)_2$ with $LiClO_4$ or $LiAlCl_4$. The salt:AN monomeric units mole ratio was 1.2. The effect of salt addition on the electrolyte membrane properties was observed from DSC studies. The salt applied in an over equimolar amount plasticizes the copolymer and this effect varies depending on the type of salt. The glass transition temperature for membranes with $LiClO_4$ is −8.5 °C, and for the imide salt −22.5 °C. Exemplary DSC traces of the AN (67.8 mol %) and BuA copolymer (a) and electrolyte comprising 72 wt. % of $LiN(CF_3SO_2)_2$ (b) are presented in Fig. II.2.6 The electrolytes comprising mixtures of salts with $LiN(CF_3SO_2)_2$ transfer to the glassy state at a similar temperature (–22 - –24 °C) as the imide salt. Systems comprising $LiN(CF_3SO_2)_2$ are completely amorphous.

Table II.2.4. DSC studies of the acrylonitrile (AN) and butyl acrylate (BuA) copolymers used for studies.

AN monomeric units content in copolymer, mol. %	Salt	T_g °C	T_m °C
100 [a]	-	105	320
74	-	52.1	52
68	-	43.8	50
66	-	42.1	50
50	-	15.3	
0 [b]	-	–55.0	
68	$LiN(CF_3SO_2)_2$	–22.5	
68	$LiClO_4$	–8.5	70, 91
68	$LiClO_4$ / $LiN(CF_3SO_2)_2$	–23.8	
68	$LiAlCl_4$ / $LiN(CF_3SO_2)_2$	–22.5	

[a] polyacrylonitrile; [b] poly(butyl acrylate)

Impedance characterization:

The electrolytes characterized by DSC studies (Table II.2.4) were subjected to impedance spectroscopy measurements. For the measurements, the samples were pressed between two stainless-steel electrodes and placed in an evacuated impedance cell. Due to the poor electrode-electrolyte contact samples were preheated up to ~80 °C and impedance measurements were performed during the cooling cycle, which immediately followed the preheating procedure.

Changes of the ionic conductivity versus reciprocal temperature are shown in Figure II.2.7. The highest values of ionic conductivity of the order of 10^{-4} S·cm^{-1} (over the 0 to 60 °C temperature range) were obtained for the electrolyte with $LiAlCl_4$. Somewhat lower conductivity values were achieved for the system with $LiN(CF_3SO_2)_2$. Electrolytes doped with $LiClO_4$ conduct much weaker and the ionic conductivity values of the order of 10^{-4} S·cm^{-4} are reached only at elevated temperature (70 °C).

Electrolytes doped with $LiN(CF_3SO_2)_2$ (over a broad salt concentration range – up to 2 moles per mole of AN monomeric units in the copolymer) are flexible, homogeneous and amorphous membranes of good adhesion to electrode materials, whereas the mechanical properties of membranes involving $LiAlCl_4$, as well as those with $LiClO_4$ only permit their use in the form of a powder of waxy form. In order to provide them with membrane-forming abilities, mixtures of $LiN(CF_3SO_2)_2$ with $LiClO_4$ or $LiAlCl_4$ were applied. This only slightly improved the mechanical properties of the membranes obtained. No increase in conductivity in relation to systems with one type of salt was observed. An improvement of conducting properties is expected by increasing the concentration of each salt to the level as for systems with one salt.

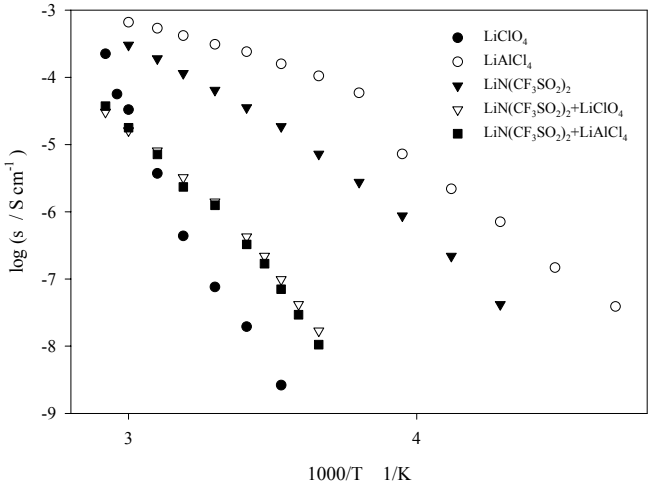

Figure II.2.7. Changes in ionic conductivity as a function of inverse temperature for electrolytes composed of butyl acrylate and acrylonitrile copolymer doped with various salts.

II.2.4. Discussion

The present studies show that by proper choice of the polymer matrix, type of the dopant salt and its concentration, high ambient temperature conductivities, which upon the values of R_τ seem to be due to the dominant cationic transport, can be achieved. Poly(acrylamide) seems to be a very effective matrix in the formation of polymer salt complexes as observed by FT-IR and MALDI-ToF studies. This observation is in agreement with earlier studies on poly(acrylamide) composite systems [10,11] and H_3PO_4 doped poly(acrylamide) based electrolytes [12,13]. As can be deduced from the MALDI-ToF studies, most of the ionic dopant is not complexed by the polymer matrix and is present in the form of associates. Therefore, there is a possibility of transport of ions dissociated due to the complexation with poly(acrylamide) via uncomplexed salt associates. This possibility was previously suggested by Vincent and co-workers for standard polymeric electrolytes [14]. High values of the decoupling index observed for $LiAlCl_4$ doped electrolytes and the conductivities not much lower than for pure $LiAlCl_4$ suggest predominantly a cationic transport in our polymer in salt electrolytes. The plasticizing effect of $LiAlCl_4$ and $LiN(CF_3SO_2)_2$ is confirmed by the lowering of the T_g values of electrolytes with an increase in the salt concentration. However, for high salt concentrations the precipitation of salt during the synthesis is observed and homogeneity of the electrolytes is more difficult to achieve. Moreover, the polymerization yield for these systems is lower than for other electrolytes (see data in Table II.2.1).

From the analysis of the results of these studies the following conclusions can be drawn:

1. none of the systems studied so far satisfied all the requirements necessary for application in lithium or/and lithium ion batteries.
2. for all the systems studied the interfacial electrolyte – lithium electrode resistance is too high.
3. systems of the powder or wax-like form, e.g. those doped with $LiAlCl_4$, exhibit sufficient ionic conductivity for application in batteries. However, their mechanical properties are poor and interfacial resistance is large.
4. membrane-like electrolytes satisfy the mechanical requirements, but despite their too high interfacial resistance, also their ambient temperature ionic conductivity is too low for practical applications.

II.2.5. References

1. S. Kartha and P. Grimes , *Physics Today* 47 (1994) 54.
2. In "Applications of Electroactive Polymers"; B. Scrosati Ed. Chapman and Hall, London, 1993.
3. P.G. Bruce, Solid State Electrochemistry, Cambridge University Press, Cambridge, 1995, Chapters 5 and 6.
4. C.A. Angell, C. Liu, E. Sanchez, *Nature* 362 (1993) 137.
5. M.G. McLin, C.A. Angell, *Solid State Ionics* 53-56 (1992) 1027.
6. A. Ferry, L. Edman, M. Forsyth, D.R. MacFarlane, J. Sun, *Electrochim. Acta* 45 (2000) 1237.
7. M. Forsyth, D.R. MacFarlane , A.J. Hill, *Electrochim. Acta* 45 (2000) 1243.
8. M. Forsyth, J. Sun, D.R. MacFarlane, *Electrochimica Acta* 45 (2000) 1249.
9. S. Zhang, Z. Chang, K. Xu, C.A. Angell, *Electrochim. Acta* 45 (2000) 1229.
10. W. Wieczorek, K. Such, Z. Florjańczyk, J.R. Stevens, *J. Phys. Chem*. 98 (1994) 6840.
11. W. Wieczorek, A. Zalewska, D. Raducha, Z. Florjańczyk, J.R. Stevens, A. Ferry, P. Jacobsson, *Macromolecules* 29 (1996) 143.
12. J.C. Lassegues in Proton Conductors; Solids, Membranes and Gel –Materials and Devices; P. Colomban Ed. Cambridge University Press, Cambridge 1992; Chapter 20.
13. W. Wieczorek, Z. Florjańczyk, J.R. Stevens, *Electrochim. Acta* 40 (1995) 2327.
14. J. Shi and C.A. Vincent, *Solid State Ionics* 60 (1993) 9.

III. NEW LITHIUM SALTS

III.1. Synthesis and Characterization of Lithium Diphenylphosphate Complexes with Triethylene Aluminum and Their Application as Conducting Salts

III.1.1. Abstract

The synthesis and characterization of a new complex salt of lithium diphenylphosphate and triethylaluminum for application in secondary lithium batteries are presented. The obtained salt was applied as a component of a polymer-in-salt electrolyte using 79 wt. % of the salt, and an acrylonitrile – butyl acrylate copolymer was the polymer component of the electrolyte. On the basis of impedance spectroscopy studies very low ionic conductivity values on the order of 10^{-10}-10^{-9} S·cm^{-1} were obtained, which shows small mobility of the lithium cation in the system. The preliminary results of applying BF_3 in the complexation of lithium diphenylphosphate show more effective separation of the lithium cation and increase in the electrolyte ionic conductivity by over two orders of magnitude.

III.1.2. Introduction

Polymer electrolytes receive great attention of research centers due to their potential application in energy sources, such as lithium and lithium-ion batteries [1–3]. Polymer separators in cells provide high operating safety and assure flexibility and low weight of devices. Complexes of polyethers with lithium salts, for which it is assumed that the lithium ions transport is connected with the segmental motion of the polymer matrix, are the best studied electrolytes. The salt anions do not undergo coordination via the basic centers in the polymer matrix and thus their transport proceeds much easier. The lithium ion transference numbers are low; for polyether electrolytes they usually range from 0.1 to 0.3 [4, 5]. The accumulation of anions in the near-electrode region is the reason for the formation of polarization layers, unfavorable from the cell operation point of view. Completely immobilized anions occur in polyelectrolytes by chemical bonding with the matrix. However, due to the low degree of dissociation, such salts show a too low ionic conductivity for practical applications. Many works concern the obtaining of a considerably high anion immobilization and high ionic conductivity in polymer electrolytes. It has been shown that the introduction to the system with poly(ethylene oxide) of a nanoceramic additive, such as e.g. Al_2O_3 or TiO_2 permits to achieve an increase in ionic conductivity and the lithium ion transference number [6–11]. The inorganic filler prevents crystallization of the polymer and promotes specific interaction between the surface groups and polymer chain and ionic species. The problem which appears in composite systems is connected with the uniform distribution of the filler in the polymer matrix and prevention of agglomeration. Another idea of the synthesis of electrolytes of high lithium cation transference numbers consists in the introduction to the system of compounds acting as anion traps. Boron organic derivatives are usually such compounds. As a result of the interaction of the receptor's acidic fragment with the anion, its considerable immobilization is obtained and due to the cation separation an increase in mobility of the positive charge carriers takes place. McBreen et al. reported that by the addition of borate compounds, especially those containing strong electron withdrawing fluorine substituents, it is possible to achieve an increase in the ionic conductivity of weakly dissociating salts in aprotic electrolyte solutions [12-14]. The anion receptors can be introduced to an electrolyte in the form of a low molecular weight compound [12–15] or they can constitute functional groups in the polymer matrix [16–22]. Fujinami et al. reported that by incorporating anion trapping groups into the polymer host it is possible to achieve cation transference numbers much greater than 0.5 [16, 17]. The use of hard Lewis acids such as $AlCl_3$ or NbF_3 for the complexation of anions, which can greatly enhance the degree of ion dissociation and consequently the ionic conductivity of an electrolyte, is also known [23–26]. The complexation

of the salt anions provides an effect of increase in the negative charge delocalization by distributing it over a greater number of atoms. The application of lithium salts comprising super weak anions may have also decreased the coulombic interaction between the lithium ion and the anion in the aprotic solvents, owing to large anion size and delocalization of the anion charge. These are most often salts containing anions or macroanions [17, 27–29].

In this part of the report we describe the preparation and characterization of a new type of lithium salt obtained from the complexation of lithium diphenylphosphate by means of triethylaluminum ($AlEt_3$). Thus, we expect to obtain an anion of large charge delocalization and weak interaction with the lithium cation. Moreover, such a salt due to the presence of an active carbon-aluminum bond may be an agent preventing the lithium electrode against various acidic or basic impurities, moisture and also oxygen, with which it undergoes a chemical reaction. The obtained salt was applied as a component of a polymer-in-salt type electrolyte. These systems, first described by Angell et al. [30, 31], combine the excellent mechanical properties characteristic of polymeric electrolytes with features of fast-ion-conducting glasses. We suggest the use of an acrylonitrile and butyl acrylate copolymer [poly(AN-*co*-BuA)], which, in contrast to polyacrylonitrile (PAN), most often used in this type of electrolytes, dissolves well in acetonitrile.

III.1.3. Experimental

III.1.3.1. Experimental techniques

^{1}H, ^{13}C, ^{31}P and ^{27}Al NMR

The NMR spectra were recorded on a Varian Mercury 400 MHz spectrometer at room temperature using DMSO-d_6 or $CDCl_3$ as solvent.

FTIR spectroscopy

Infrared spectra were recorded on a Bio-Rad 165 FTIR spectrophotometer with the samples in KBr pellets or thin membranes deposited on NaCl plates.

Impedance spectroscopy

Ionic conductivity was determined by the complex-impedance method. The samples were sandwiched between stainless-steel blocking electrodes and placed in a temperature-controlled oven. The impedance measurements were carried out on a Solartron-Schlumberger 1255 impedance analyzer over the frequency range from 1 Hz to 1 MHz.

III.1.3.2. Preparation of the salt complexes

The synthesis of the complexes was carried out in two stages:

Ist stage: reaction of diphenylphosphoric acid with n-butyllithium

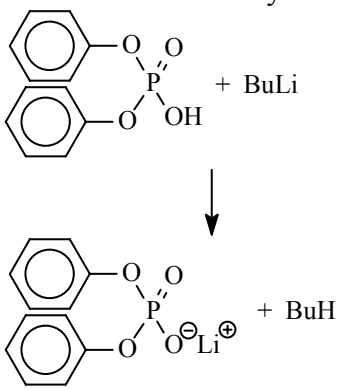

The reaction of diphenylphosphoric acid with n-butyllithium (BuLi) was carried out in the atmosphere of argon applying a slight excess (1.2 mol) of BuLi. In the first step the acid was dissolved in toluene and then, through a funnel, the BuLi solution in hexane was dropped in. The reaction product precipitated in the form of a white solid. The precipitate was isolated by filtration. It was then washed with toluene and dried under reduced pressure.

The lithium diphenylphosphate (LiDPhP) obtained is an amorphous, melting with difficulty (m.p. > 250 °C) solid, well soluble in DMSO.

IInd stage: reaction with $AlEt_3$:

Toluene was added to the thus isolated lithium salt, and then triethylaluminum was introduced to the suspension in the form of a 25% solution in toluene. Ethane evolved during the reaction and the complex formed dissolved in toluene. The solvent was removed under reduced pressure and a viscous, transparent product was obtained.

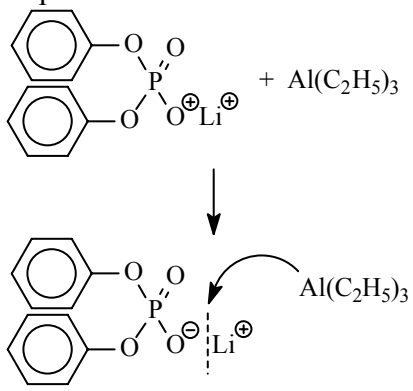

III.1.3.3. Synthesis of the polymeric matrix

Poly(AN-*co*-BuA)s (both monomers, AN and BuA, from Aldrich, commercial grade) were obtained by radical polymerization in the presence of azo-bis-isobutyronitrile as initiator. The reactions were carried out in a solvent (acetonitrile) at 70°C for 5 hours. The polymers were isolated by casting with methanol, washed several times and dried under dynamic vacuum for 72 hours. The reaction yield was over 95%. The reactions were carried out at 2:1 AN to BuA mole compositions of the monomer feed. The T_g value of the copolymer determined on the basis of DSC studies from the second heating cycle was equal to 42.1°C.

III.1.3.4. Preparation of polymer electrolytes

The electrolytes were obtained by the casting technique from a polymer and salt solution in acetonitrile. The solvent was removed under dynamic vacuum in two steps. First, for 50 hours at a vacuum of 20 Torr, and then for 140 hours at 10^{-3} Torr. The solvents were dried and distilled in an argon atmosphere prior to use.

III.1.4. Results and Discussion

III.1.4.1. Characteristics of the LiDPhP complex with triethylaluminum

^{13}C and ^{31}P NMR analysis

The ^{31}P spectrum of LiDPhP in DMSO-d_6 shows the presence of one signal at −8.0 ppm. The same signal of phosphorus present in the salt complexed with triethylaluminum appears at the chemical shift value as in uncomplexed LiDPhP, at −7.9 ppm. This means that the phosphorus atom is not susceptible to the complexation reaction.

Figs III.1.1 and III.1.2 present ^{13}C NMR spectra of LiDPhP and its complex with $AlEt_3$. Also in the case of the carbon resonance no changes are observed in the chemical shifts upon the reaction with $AlEt_3$. This analysis shows that the complexation reactions only slightly affect the chemical shifts of carbon and phosphorus in the LiDPhP molecule.

^{1}H NMR analysis

In Fig. III.1.3 is presented the ^{1}H NMR spectrum of the LiDPhP complex with triethylaluminum, obtained in the reaction of an equimolar amount of reactants. The ratio of the phenyl groups proton signals to that of $AlEt_3$ ethyl groups shows that about 60 mol % of LiDPhP underwent complexation. At the same time, no differences in the proton signals of the phenyl groups in the complex (Figure III.1.3) in relation to those of the uncomplexed salt were observed

(Figure III.1.4). This indicates that these groups are not involved in the formation of the complex.

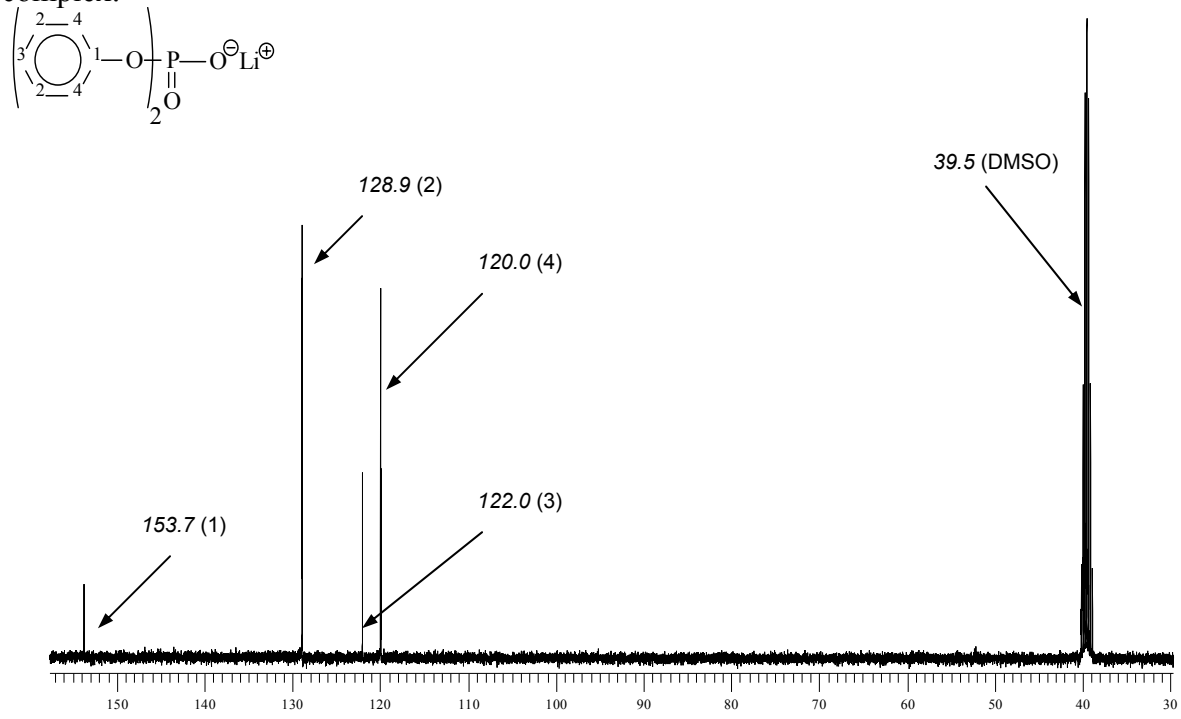

Figure III.1.1. ^{13}C NMR spectrum of LiDPhP (DMSO-d_6)

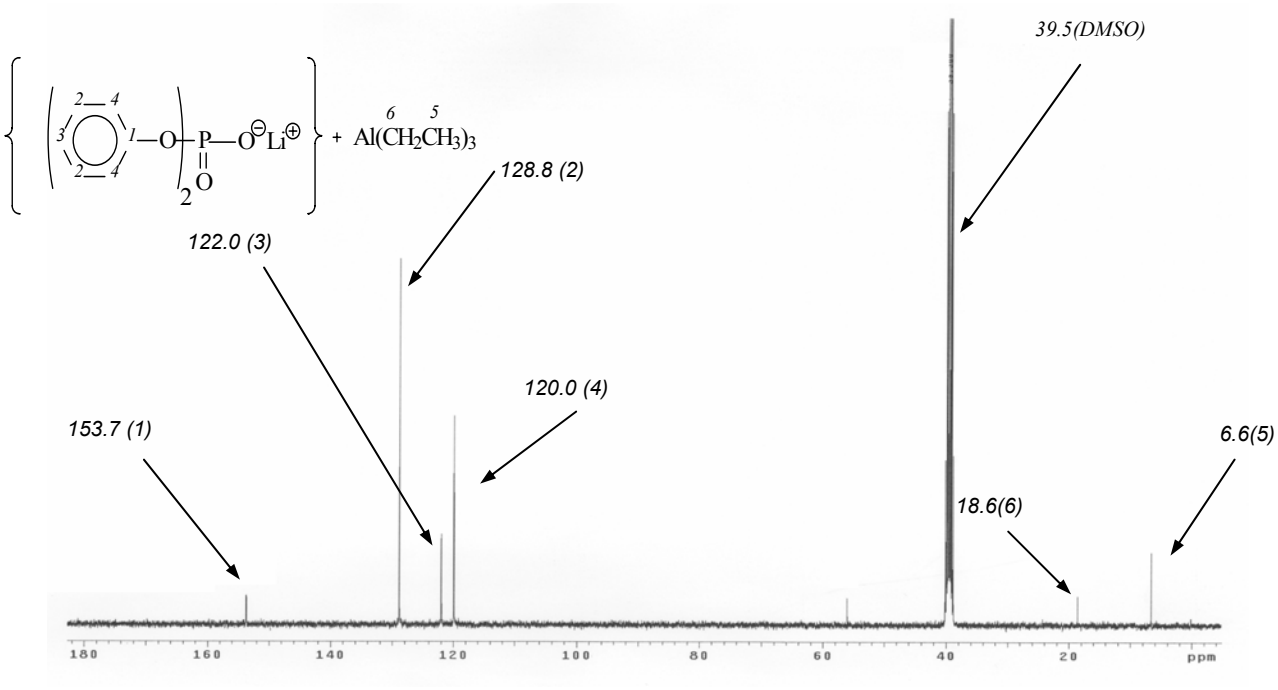

Figure III.1.2. ^{13}C NMR spectrum of LiDPhP complexed with $Al(C_2H_5)_3$ (DMSO-d_6)

In the NMR spectrum of the complexation product using a large (six-fold) molar excess of Lewis acid (Figure III.1.5) the ratio of signals originating from ethyl groups protons to that of phenyl ones indicates that about 4 molecules of the acid falls per 1 LiDPhP molecule. Within the region of phenyl groups protons new signals appear (shifted with respect to the same signals in

the spectrum of the LiDPhP salt) indicating the participation of Ar–O–P groups in the formation of complexes under the conditions of an excess of the Lewis acid.

In the spectrum, the signals of $-OCH_2$ groups derived from the products of the triethylaluminum oxidation reaction are also present.

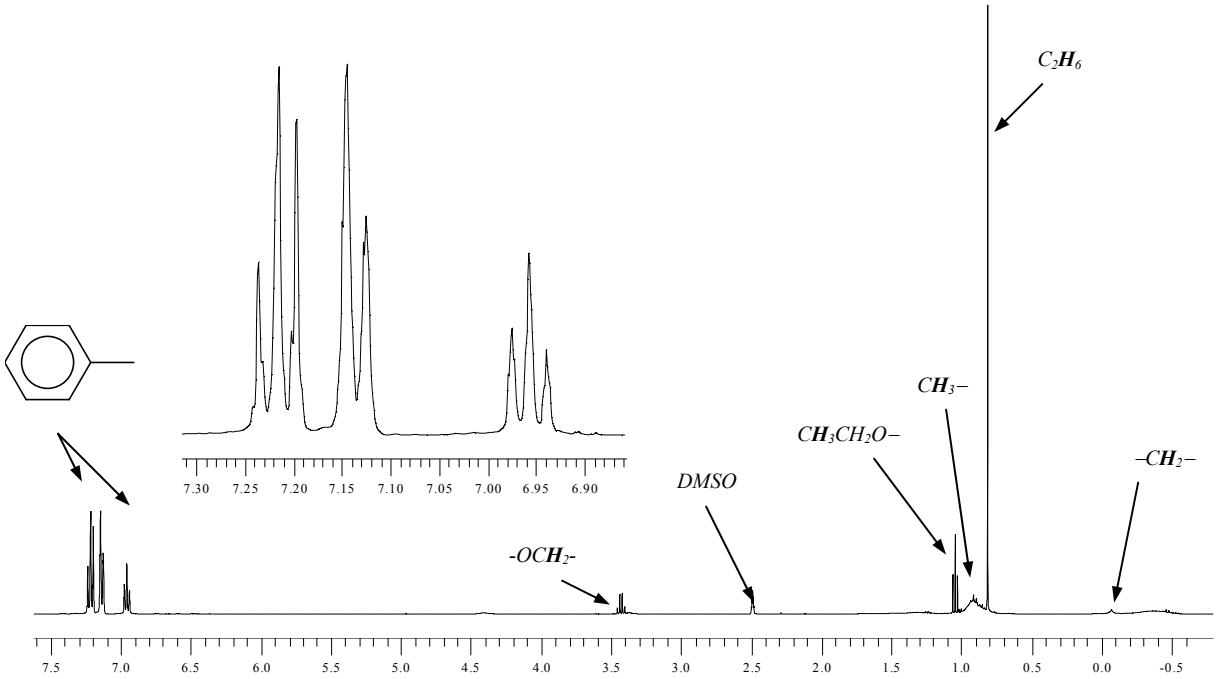

Figure III.1.3. ^1H NMR spectrum of LiDPhP and $Al(C_2H_5)_3$ (equimolar ratio of Lewis acid to LiDPhP) (DMSO-d_6).

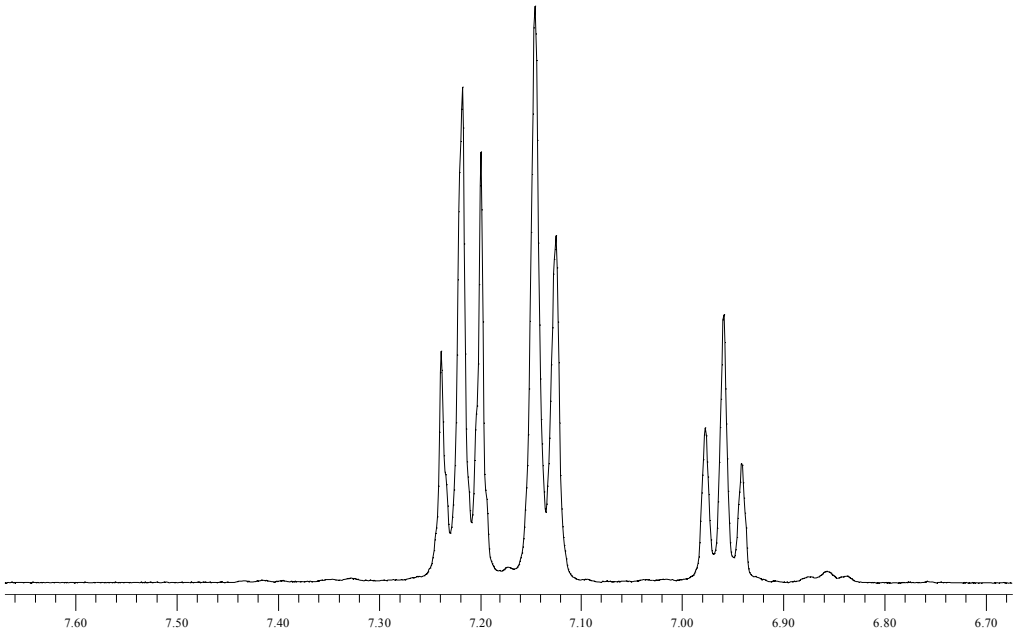

Figure III.1.4. ^1H NMR spectrum of LiDPhP (DMSO-d_6).

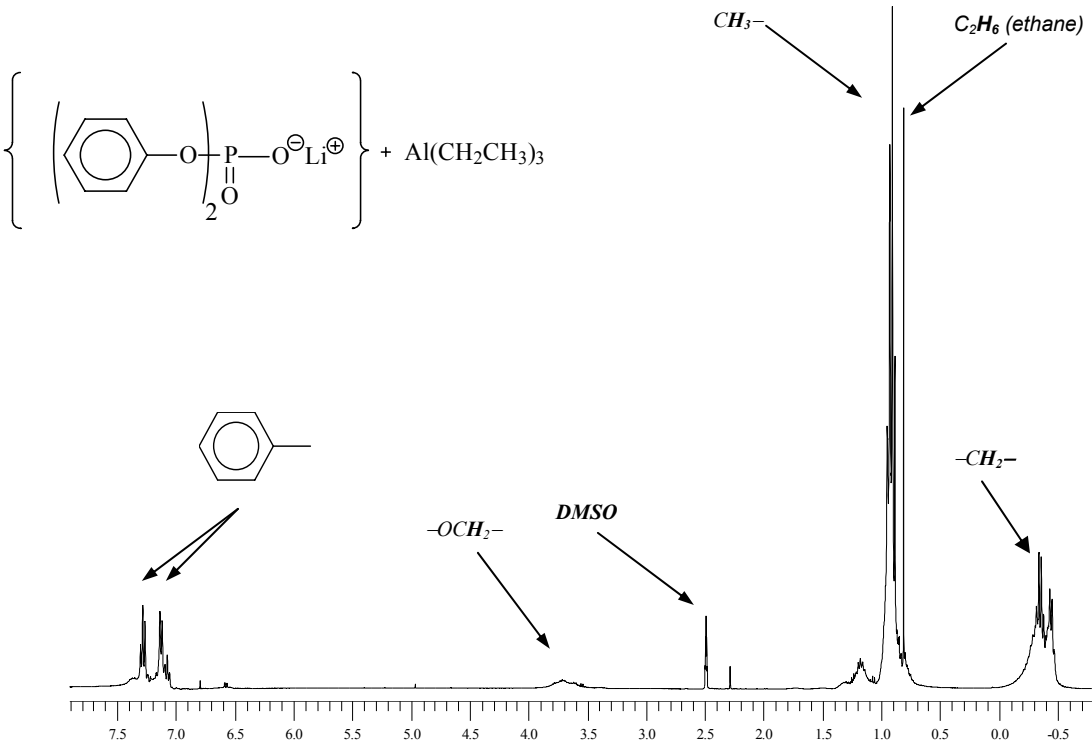

Figure III.1.5. ^{1}H NMR spectrum of the LiDPhP complex with $Al(C_2H_5)_3$ (6-fold excess of the Lewis acid with respect to LiDPhP) (DMSO-d_6).

^{27}Al NMR analysis

The spectral analysis of the obtained LiDPhP complex with $AlEt_3$ showed that the aluminum atom in this compound occurs in a five-coordinative form (Figure III.1.6). The signal present at 159.0 ppm is assigned to the $(C_2H_5)_4Al^-$ anion formed under these conditions.

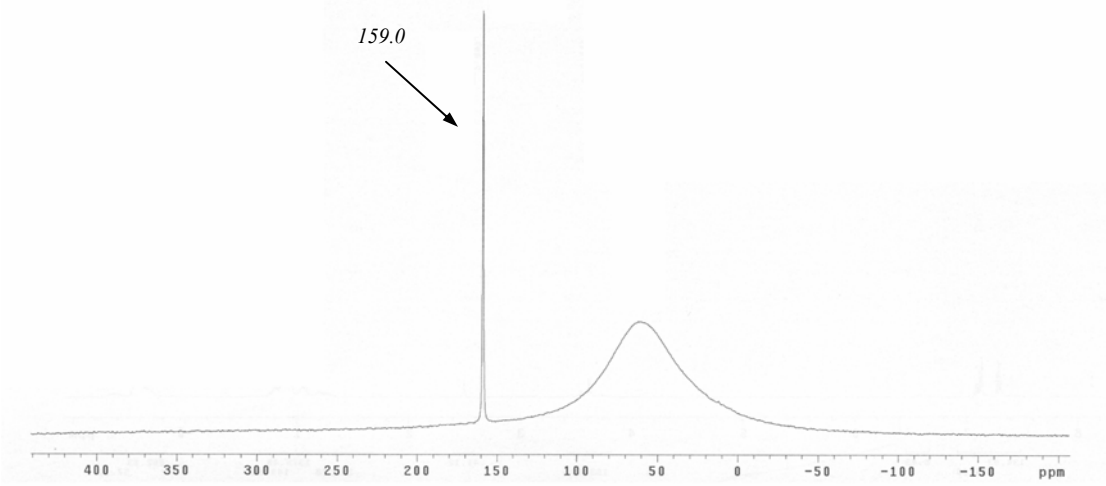

Figure III.1.6. ^{27}Al NMR spectrum of the LiDPhP complex with $Al(C_2H_5)_3$ (DMSO-d_6).

FTIR analysis

The FTIR spectra recorded for diphenylphosphoric acid and its lithium salt are presented in Figures III.1.7 and III.1.8. Changes in the absorption bands wavelength characteristic of P–O bonds in the acid, after reaction with butyllithium and complexation with triethylaluminum were observed (Figure III.1.9).

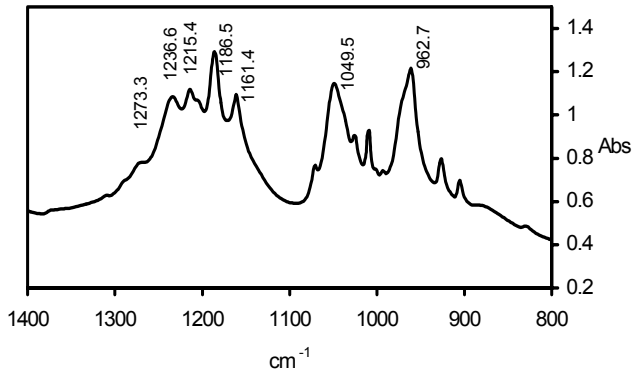

Figure III.1.7. FTIR spectrum of diphenylphosphoric acid.

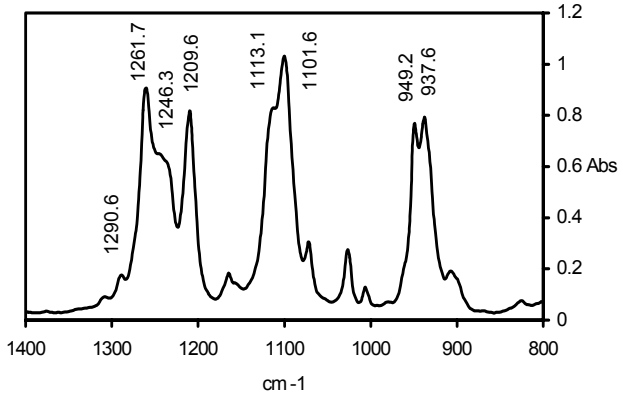

Figure III.1.8. FTIR spectrum of LiDPhP.

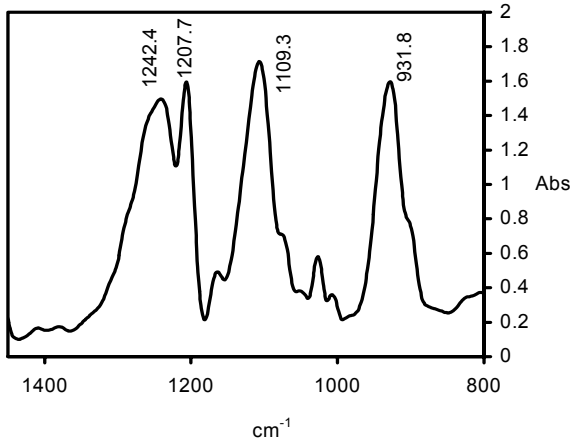

Figure III.1.9. FTIR spectrum of the LiDPhP complex with $Al(C_2H_5)_3$.

In the spectrum of diphenylphosphoric acid, the bands of vibrations of ester bonds P–O(Ar) (Ar = C_6H_5) at 963, 1161 and 1187 cm^{-1}, bands of that of the ester P=O bond at 1273 cm^{-1}, as well as two types of bands characteristic of the phosphate group, resulting from diphenylphosphoric acid autodissociation phenomenon, are observed.

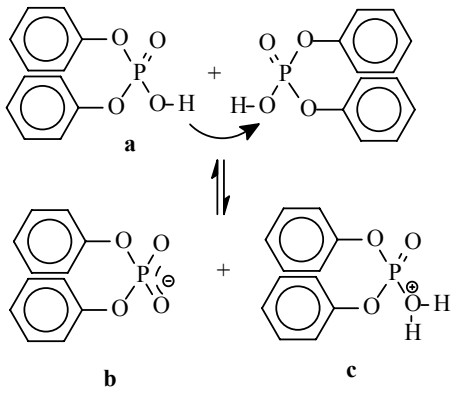

Scheme of diphenyphosphoric acid autodissociation

The diphenylphosphoric acid molecules occur in the form with a localized negative charge on the oxygen atom (**a** and **c**), which results in the presence of an absorption band at $\nu_{P(O)O}$ = 1050 cm^{-1} and in the form with a delocalized negative charge (**b**), bands at $\nu_{P(O)O}$ = 1215, 1237 cm^{-1}.

In the case of Figure III.1.10 recorded for the lithium salt of that acid, the situation is different, since no absorption bands of the phosphate group with a delocalized negative charge are observed. However, bands characteristic of the P–O (Ar) ester bond at 938, 949 and 1102 cm^{-1} are present. The structure of the salt is as follows:

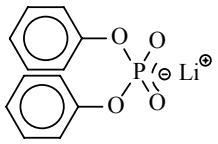

The complexation with triethylaluminum does not eliminate the mesomeric structure characteristic of LiDPhP. This is confirmed by the absorption bands in infrared (Figure III.1.9) of $\nu_{P(O)O}$ = 1208, 1242 cm^{-1}. However, in this spectrum no bands characteristic of the non-dissociated phosphate group appear. Bands characteristic of the P–O(Ar) group vibrations are present in the spectrum at ν = 932 and 1109 cm^{-1}.

On the basis of these data and results of NMR analysis it can be suggested that the LiDPhP complex with $Al(C_2H_5)_3$ has the following structure:

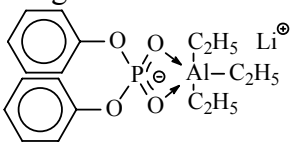

These considerations concern complexes obtained at an equimolar ratio of reagents. ^1H NMR studies indicate that when a several-fold excess of $Al(C_2H_5)_3$ is used in the reaction, also phenyl substituents participate in the complexation. The presence of a signal at 159.0 ppm in the ^{27}Al NMR spectrum, assigned by us to the $(C_2H_5)_4Al^-$ anion, may indicate certain participation of the reaction resulting in the formation of the $[(C_2H_5)_4Al]^-Li^+$ and a neutral product of the structure:

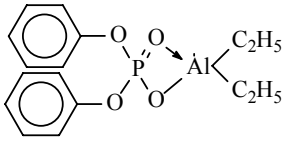

III.1.4.2. Characteristics of electrolytes comprising the lithium diphenylphosphate complex with $Al(C_2H_5)_3$ and poly(AN-co-BuA 2:1)

Electrolytes comprising poly(AN-*co*-BuA 2:1) as a polymeric matrix and LiDPhP complex salt with $Al(C_2H_5)_3$ were prepared. The conductivity of such an electrolyte as a function of inverse temperature is presented in Figure III.1.10. The conductivity values are very low and range within 10^{-10} - 10^{-9} S·cm^{-1}. Moreover, only a slight effect of temperature on its value is observed, which indicates small mobility of ions in the salt studied.

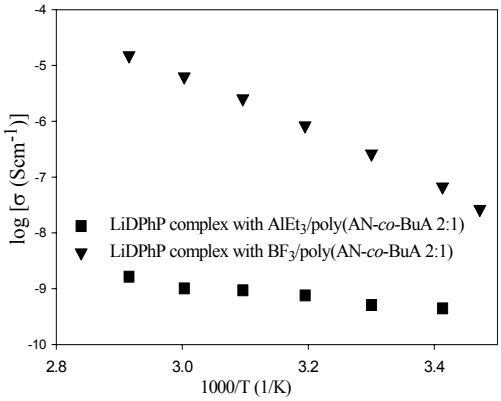

Figure III.1.10. Change of ionic conductivity as a function of inverse temperature of the electrolyte comprising poly(AN-co-BuA 2:1) and LiDPhP complexed with $Al(C_2H_5)_3$ or BF_3.

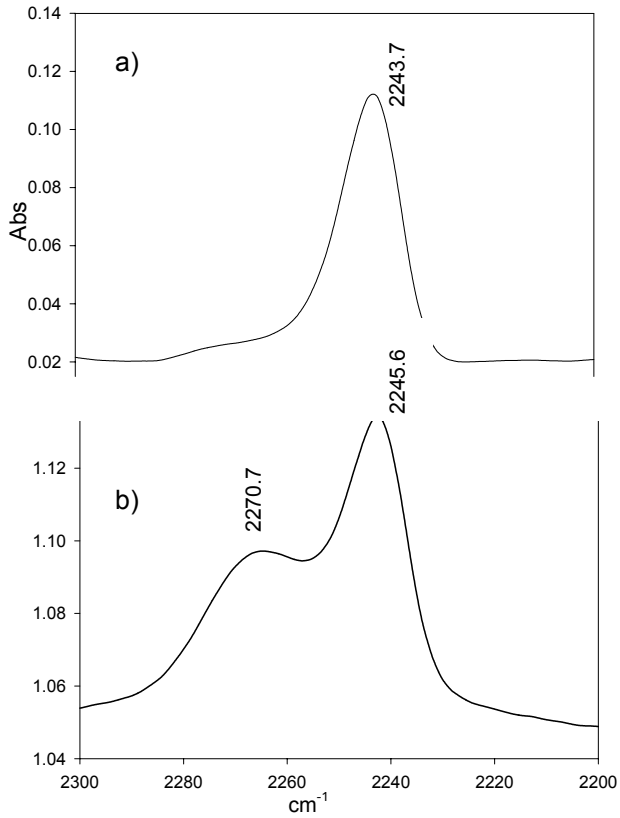

Figure. III.1.11. Polymer matrix C≡N group vibration band in the FTIR spectrum of the LiDPhP + $Al(C_2H_5)_3$/poly(AN-co-BuA 2:1) (a) and LiDPhP + BF_3/poly(AN-co-BuA 2:1) (b) electrolytes.

It results from this that the lithium cation, shifted from the phosphate anion as a result of complexation, still strongly interacts with the counterion. No interaction of the lithium cation

with the nitrile groups of the polymer matrix was observed. Figure III.1.11a shows a fragment of the FTIR spectrum of the electrolyte comprising the LiDPhP complex salt with $Al(C_2H_5)_3$ and poly(AN-*co*-BuA 2:1) as polymer matrix, with the marked CN group absorption band. This band appears at ν_{CN} = 2244 cm^{-1}, characteristic of neat, not complexed acrylonitrile monomeric units. As appears from studies described earlier for systems with inorganic salts, the interaction of the lithium cation with the copolymer matrix causes a shift in the absorption band towards larger wavelength values, about 2260 cm^{-1}. This effect is not seen in the case of the studied complex salt. The preliminary results of studies carried out by us on the application of other Lewis acids for the complexation of LiDPhP show the possibility of achieving an increase in the degree of dissociation of the salt, and thus of the ionic conductivity. Figure III.1.10 shows also the conductivity values for the system containing the LiDPhP complex with BF_3. In this case the conductivity in the polymer-in-salt system is higher by over two orders of magnitude. In the FTIR spectrum (Figure III.1.11b), a band at 2270.7 cm^{-1}, shifted due to the interaction of positively charged salt ions with the polymer matrix, is observed, besides the band of the uncomplexed C≡N group. An increase in conductivity is similarly observed in the classical system based on poly(ethylene oxide), containing 20 mol % of the lithium salt complexed with BF_3. For $P(EO)_{10}$LiDPhP the ambient temperature conductivitiy is 6×10^{-9} $S\cdot cm^{-1}$, and after compexing with BF_3 5.5×10^{-7} $S\cdot cm^{-1}$.

III.1.5. Conclusions

The preliminary results indicate the possibility of synthesis of complex salts of a mesomeric anion structure as a result of complexation of a phosphoric salt with a Lewis acid such as $Al(C_2H_5)_3$. The obtained complex salt of LiDPhP and $Al(C_2H_5)_3$ in a polymer-in-salt system with poly(AN-*co*-BuA 2:1) is characterized by weak conducting properties on the order of 10^{-10}-10^{-9} $S\cdot cm^{-1}$ and practically does not change with temperature. This result indicates a strong interaction of lithium cations with the counterions, which results in a very weak mobility of cations. In the case of this salt no bands assigned to the matrix CN groups interacting with cations are observed. Much better results were obtained in the case of using BF_3 as the Lewis acid, in the complexation of LiDPhP. The conductivity increases by over two orders of magnitude, both in a polymer-in-salt system with poly(AN-*co*-BuA 2:1) as well as at a 10 wt. % of the salt with PEO. The effect of other Lewis acids on the properties of complexing salts will be studied in the next stage of studies.

References

[1] J. R. MacCallum, C. A. Vincent (Eds.), Polymer Electrolyte Review 1&2, Elsevier, London, 1987 & 1989.
[2] B. Scrosati (Eds.), Application of Electroactive Polymers, Chapman & Hall, London, 1993.
[3] J. M. Tarascon, M. Armand, *Nature*, 414, 359 (2001).
[4] P. G. Bruce, M. T. Hardgrave, C. A. Vincent, *Solid State Ionics*, **53-56**, 1087, (1992).
[5] W. Gorecki, M. Jeannin, E. Belorizky, C. Roux, M. Armand, *J. Phys. Condens. Matter*, **7**, 6823 (1995).
[6] F. Croce, G.B. Appetecchi, L. Persi, B. Scrosati, *Nature*, **394**, 456 (1998).
[7] F. Croce, R. Curini, A. Martinelli, L. Persi, F. Ronci, B. Scrosati, R. Caminiti, *J. Phys. Chem. B*, **103**, 10632 (1999).
[8] W. Wieczorek, J. R. Stevens, Z. Florjańczyk, *Solid State Ionics*, **85**, 76 (1996).
[9] W. Wieczorek, P. Lipka, G. Żukowska, H. Wyciślik, *J. Phys. Chem*., **102**, 6968, (1998).
[10] F. Croce, L. Persi, B. Scrosati, F. Serraino-Fiory, E. Plichta, M. A. Hendrickson, *Electrochim. Acta*, **46**, 2457 (2001).
[11] A. S. Best, J. Adebahr, P. Jacobsson, D. R. MacFarlane, M. Forsyth, *Macromolecules*, **34**, 4549 (2001).
[12] H. S. Lee, X. Q. Yang, C. L. Xiang, J. McBreen, L. S. Hoi, J. *Electrochem. Soc*., **145**, 2813 (1998).

[13] X. Sun, H. S. Lee, S. Lee, X. Q. Yang, J. McBreen, Electrochem. *Solid State Lett*., **1**, 39 (1998).
[14] H. S. Lee, X. Q. Yang, X. Sun, J. McBreen, *J. Power Sources*, **97-98**, 566 (2001).
[15] S. S. Zhang, C. A. Angell, *J. Electrochem. Soc*., **143**, 4047 (1996).
[16] M. A. Mehta, T. Fujinami, *Chem. Lett*., **9**, 915 (1997).
[17] M. A. Mehta, T. Fujinami, *Solid State Ionics*, **113-115**, 187 (1998).
[18] M. A. Mehta, T. Fujinami, T. Ionue, *J. Power Sources*, **81-82**, 724 (1999).
[19] T. Fujinami, M. A. Mehta, K. Sugie, K. Mori, *Electrochim. Acta*, **45**, 1181 (2000).
[20] S. Tabata, T. Hirakimoto, M. Nishiura, M. Watanabe, *Electrochim. Acta*, **48**, 2105 (2003).
[21] W. Xu, M. D. Williams, C. A. Angell, *Chem. Mater*., **14**, 401 (2002).
[22] W. Xu, L. Wang, C. A. Angell, *Electrochim. Acta*, **48**, 2037 (2003).
[23] X. Wei, D. F. Shriver, *Solid State Ionics,* **133**, 233 (2000).
[24] J. McBreen, H. S. Lee, X. Q. Yang, X. Sun, *J. Power Sources*, **89**, 163 (2000).
[25] R. Borkowska, A. Reda, A. Zalewska, W. Wieczorek, *Electrochim. Acta*, **46**, 1737 (2001).
[26] P. P. Prosini, B. Banov, *Electrochim. Acta*, **48**, 1899 (2003).
[27] H. Tokuda, M. Watanabe, *Electrochim. Acta*, **48**, 2085 (2003).
[28] S. M. Ivanova, B. G. Nolan, Y. Kobayashi, S. M. Miller, O. P. Anderson, S. H. Strauss, *Chem. Eur. J*., **7**, 503 (2001).
[29] T. Fujinami, A. Tokimune, M. A. Mehta, D. F. Shriver, G. C. Rawsky, *Chem. Mater*., **9**, 2236 (1997).
[30] C. A. Angell, C. Liu, E. Sanchez, *Nature*, **362**, 137 (1993).
[31] J. Fan, J. C. A. Angell, *Electrochim. Acta*, **40**, 2397 (1995).

III.2. Carboxylate Complex Salts

III.2.1. Synthesis and Characteristics of Lithium Salt Carboxylate Complexes with Various Lewis Acids

The expected complexation reaction course is presented below:

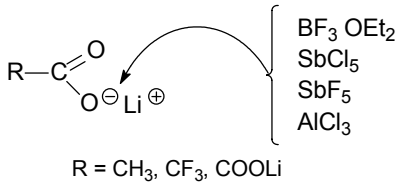

R = CH_3, CF_3, COOLi

The complexation was carried out in the atmosphere of argon in an acetonitrile solution in the case of lithium trifloroacetate or in suspension in the case of the other salts. The Lewis acid was added in an equimolar amount or a five-fold excess of the complexing agent with respect to the carboxylic groups. In case of an exothermic effect the reaction system was cooled with a water/ice mixture. The reaction product was isolated by distillation under reduced pressure of the solvent and excess of the complexing compound. Washing out of the product with a solvent was also employed.

III.2.1.1 Complex of lithium acetate and BF_3

In Figure III.2.1 is presented the FTIR spectrum of lithium acetate. The absorption bands of the carboxylic group ν_{asym} at 1574, 1595 and 1614 cm^{-1} as well as ν_{sym} 1435 cm^{-1} can be observed, which was overlapped by the CH_3 group band.

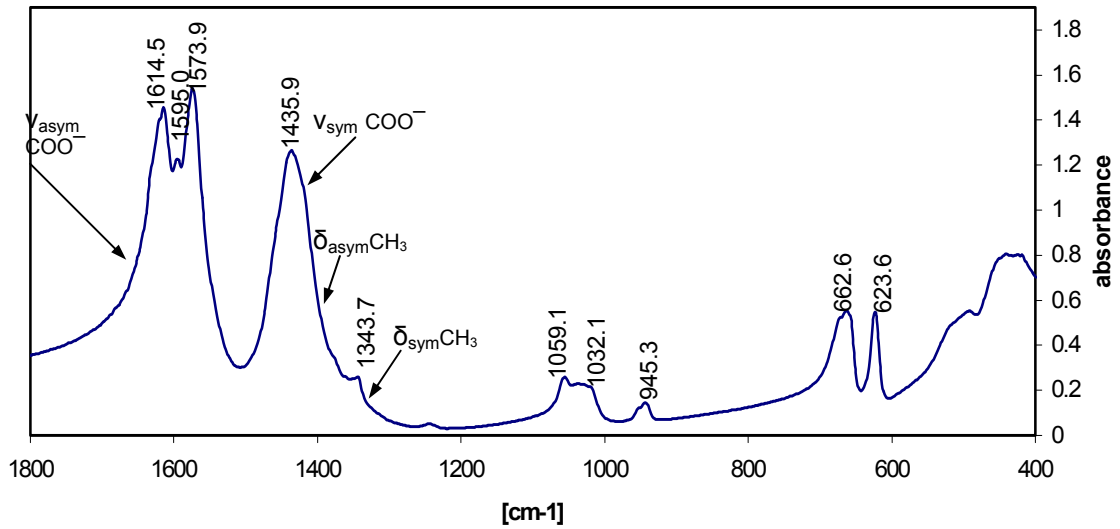

Figure III.2.1. FTIR spectrum of CH_3COOLi.

The FTIR spectrum of the product of the lithium acetate and BF_3 reaction carried out at an equimolar ratio of reactants, measured in KBr pellets, is presented in Figure III.2.2. In this spectrum a strong shift of the carboxylate group at 1709 cm^{-1} is observed. Intense bands originating from the BF bonds are also present in the 1037 – 1090 cm^{-1} region. The very fare shift of the C=O group by about 100 cm^{-1} towards higher wavelengths shows the presence of a strong induction effect in the complex, suggesting a structure with a delocalized negative charge, probably on the boron atom:

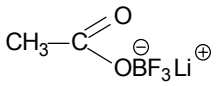

Simultaneously, in the spectrum bands derived from the $LiBF_4$ salt formed during reaction are observed. The formation of this salt can be connected with the fact that lithium acetate is

insoluble in the reaction medium, and during dropping in the BF_3 etherate is in an excess in relation to lithium acetate. The excess BF_3 probably undergoes reaction with the complexed lithium acetate, soluble in the reaction medium, with the formation of a BF_4^- anion, for which the lithium cation is the counterion. Due to the fact that the reactants were used at an equimolar ratio, unreacted lithium acetate remains in the system. The band at 1630 cm^{-1} is attributed to moisture present in this highly hydroscopic system.

In the preliminary reaction step, the formation of the reaction product of complexation with one BF_3 molecule, for which the C=O group absorption band appears at 1709 cm^{-1}, is observed. The following structure has been assigned to this product.

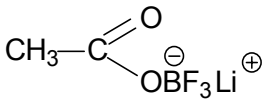

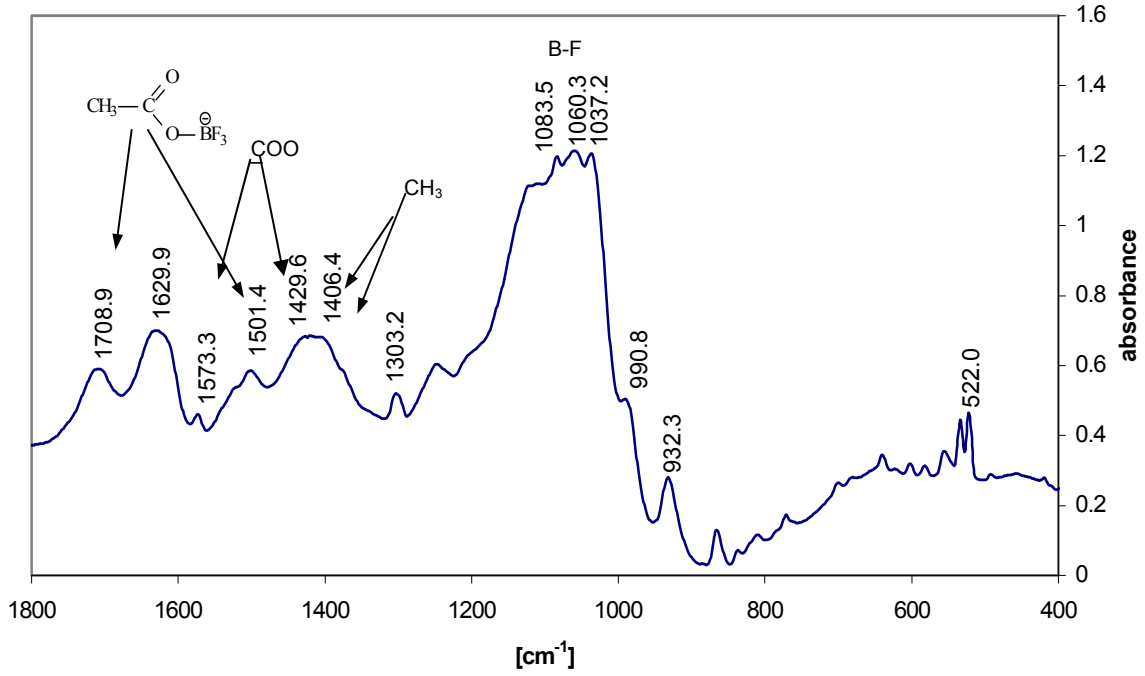

Figure III.2.2. FTIR spectrum of the CH_3COOLi and BF_3 complexation products.

III.2.1.2. Complexes of lithium oxalate and SbF_3

The FTIR spectrum of lithium oxalate is presented in Figure III.2.3.

The bands characteristic of the carboxylic groups occurring at ν_{asym} 1656 cm^{-1} and ν_{sym} 1423 cm^{-1} as well as the band at 1333 cm^{-1} have been assigned to the stretching vibrations of the O=C–C=O bond. The spectrum of the lithium oxalate and BF_3 reaction product is presented in Figure III.2.4.

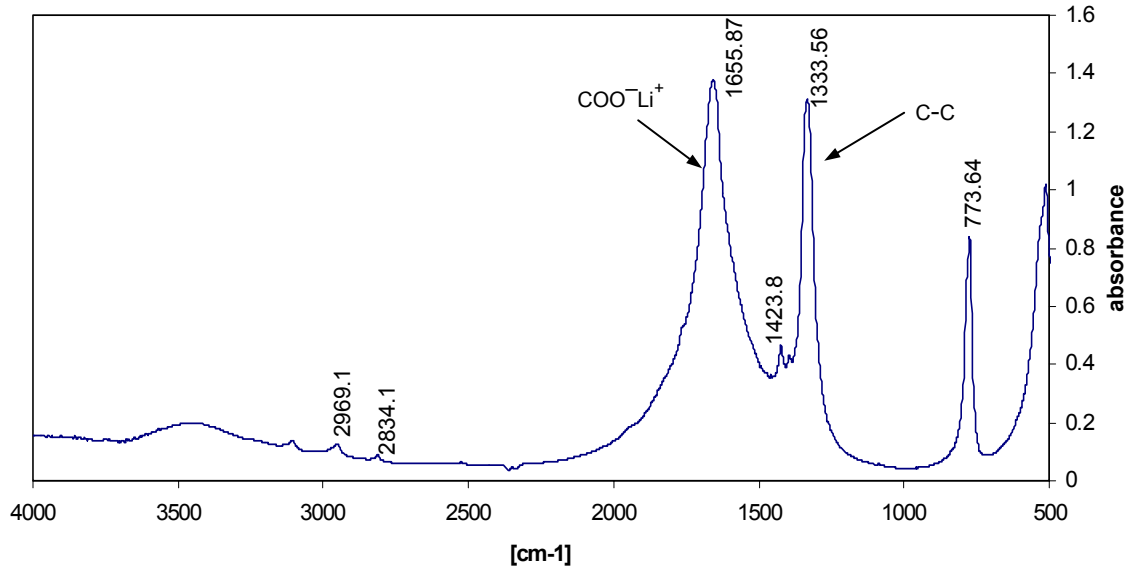

Figure III.2.3. FTIR spectrum of $(CO_2Li)_2$.

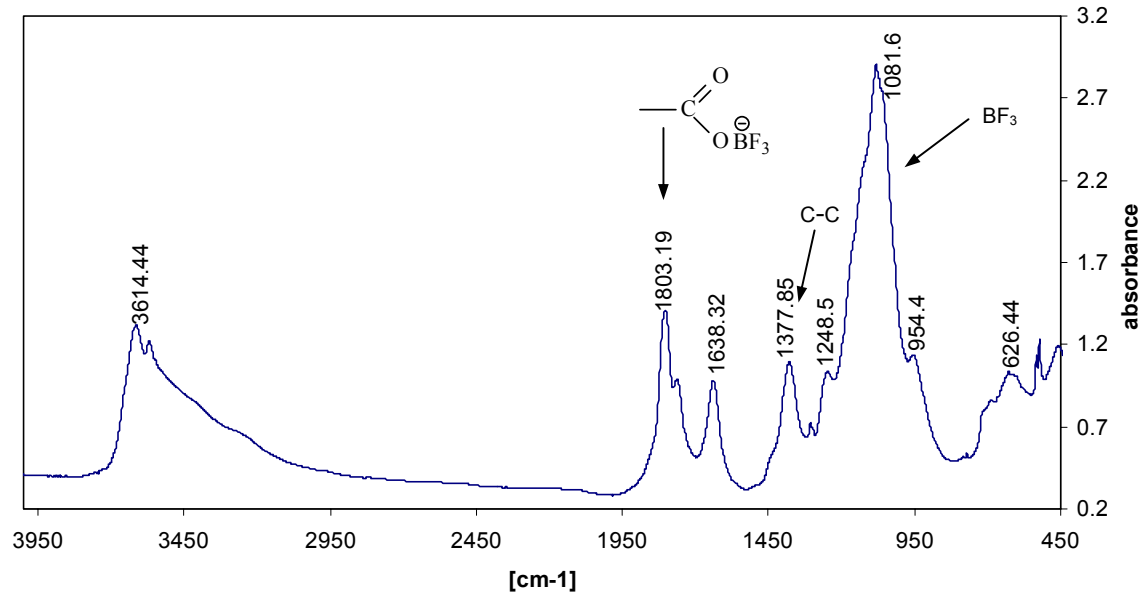

Figure III.2.4. FTIR spectrum of the lithium oxalate and BF_3 etherate reaction product.

As a result of complexation, the carboxylic group band shifts towards the ν_{asym} 1803 and 1763 cm^{-1} values and $\nu_{C\text{-}C}$ occurs at 1378 cm^{-1}. In the spectrum intense B–F bands in the 1039 – 1124 cm^{-1} region are also present. Similarly as in the case of lithium acetate, the far shift of the carboxylate groups absorption bands towards higher wavelengths may be connected with the formation of a complex with a delocalized negative charge on the boron atom:

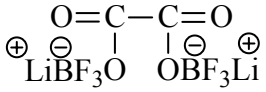

The FTIR spectrum of the lithium oxalate and SbF_5 complexation reaction product is presented in Figure III.2.5.

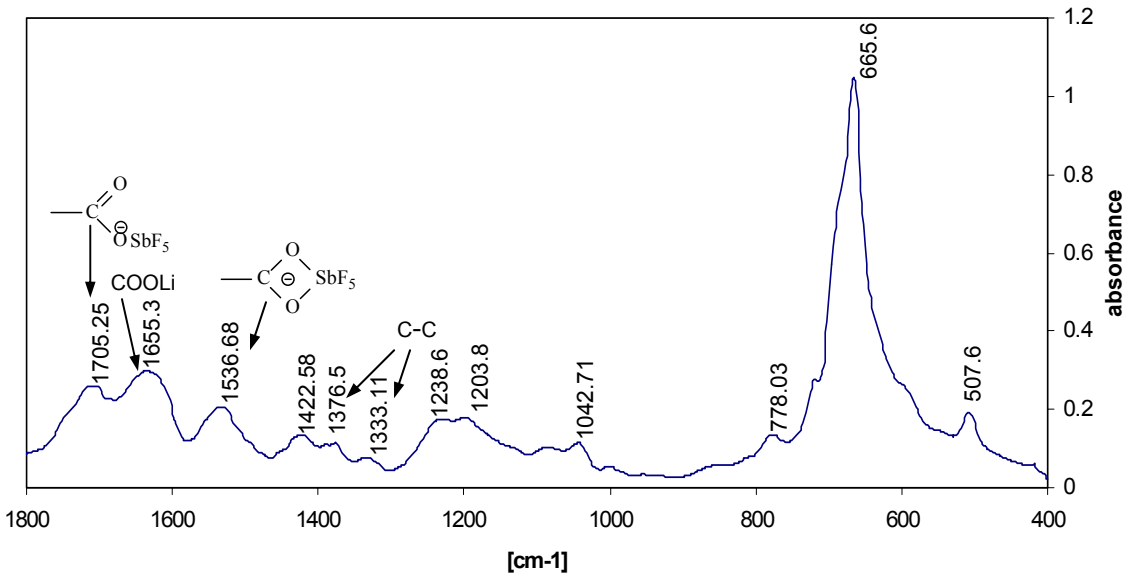

Figure III.2.5. FTIR spectrum of the lithium oxalate and SbF_5 reaction products.

In the spectrum bands assigned to C–C and COO^-Li^+ bonds of the uncomplexed oxalate (ν = 1333 and 1655 cm^{-1}, respectively) as well as new bands originating from the complexed product (1376 cm^{-1}) are observed.

III.2.1.3. Complex salts of lithium trifluoroacetate

Complex with BF_3

In Figure III.2.6 is presented the FTIR spectrum of lithium trifluoroacetate measured in KBr.

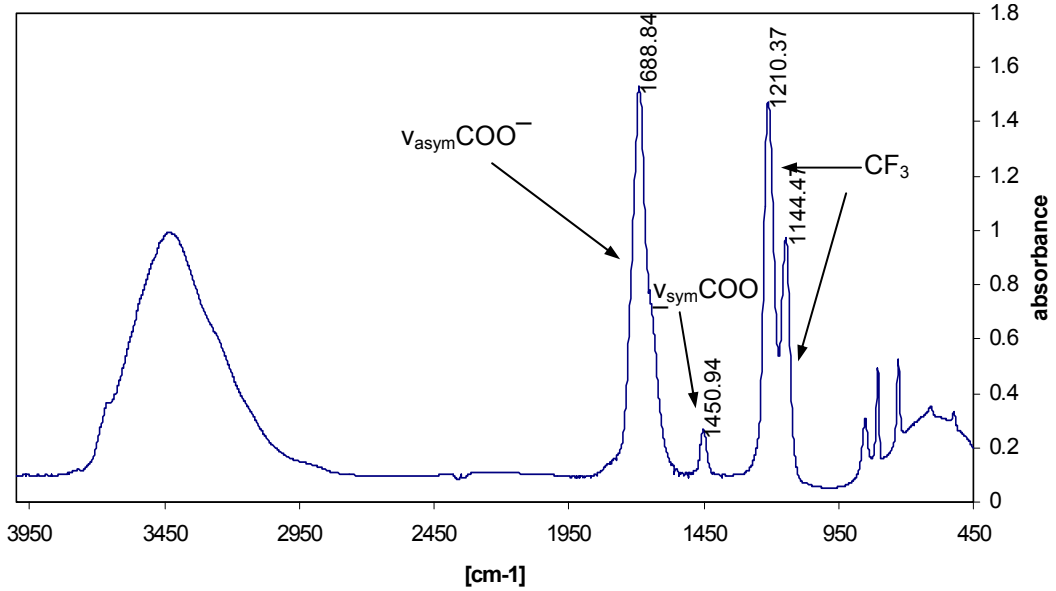

Figure III.2.6. FTIR spectrum of CF_3COOLi.

In the solid state in CF_3COOLi the absorption band of the carboxylate anion occurs at 1668 cm^{-1}. Two absorption bands of the C–F bond in the CF_3 group occur at 1210 and 1145 cm^{-1}. After addition of BF_3 etherate to the salt, gradual precipitation of a solid occurs during solvent

removal. The FTIR spectrum of the isolated solid (Figure III.2.7) and that of commercial $LiBF_4$ (Figure III.2.8) are presented.

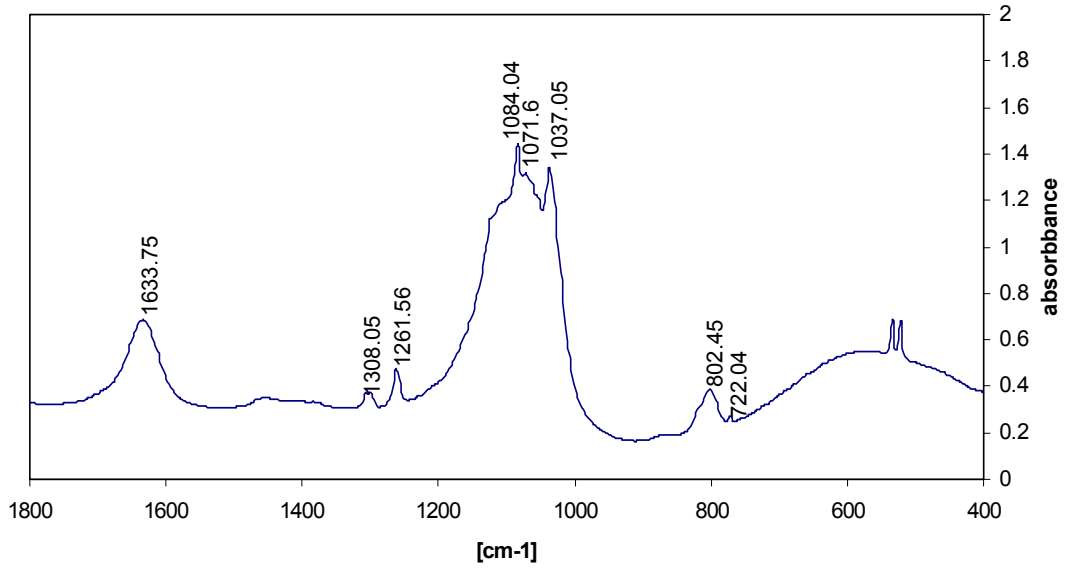

Figure III.2.7. FTIR spectrum of the $CF_3COOLi + BF_3$ reaction precipitate

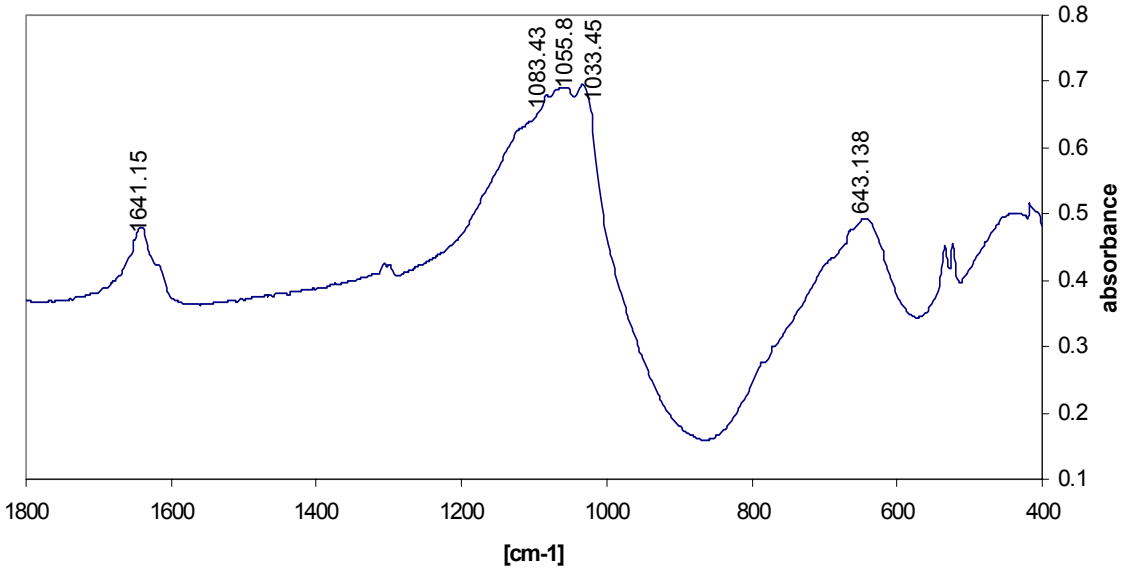

Figure III.2.8. FTIR spectrum of $LiBF_4$.

The FTIR spectrum of the second reaction product, obtained after isolation of the $LiBF_4$ precipitate, measured in Nujol is presented in Figure III.2.9.

In this spectrum bands assigned to the CF_3 group at ν = 1208, 1245 cm^{-1} and to B–F in the 1021 –1091 cm^{-1} range are observed. Three types of carboxylic groups are present: uncomplexed salt at 1683 cm^{-1}, band at 1768 cm^{-1}, to which the band at 1262 cm^{-1} of the C–O bond corresponds, which can be assigned to the $CF_3C(O)OBF_3Li$ complex. A band at 1724 cm^{-1} is also present, which can originate from vibrations of the C=O group in the expected compound CF_3COOBF_2.

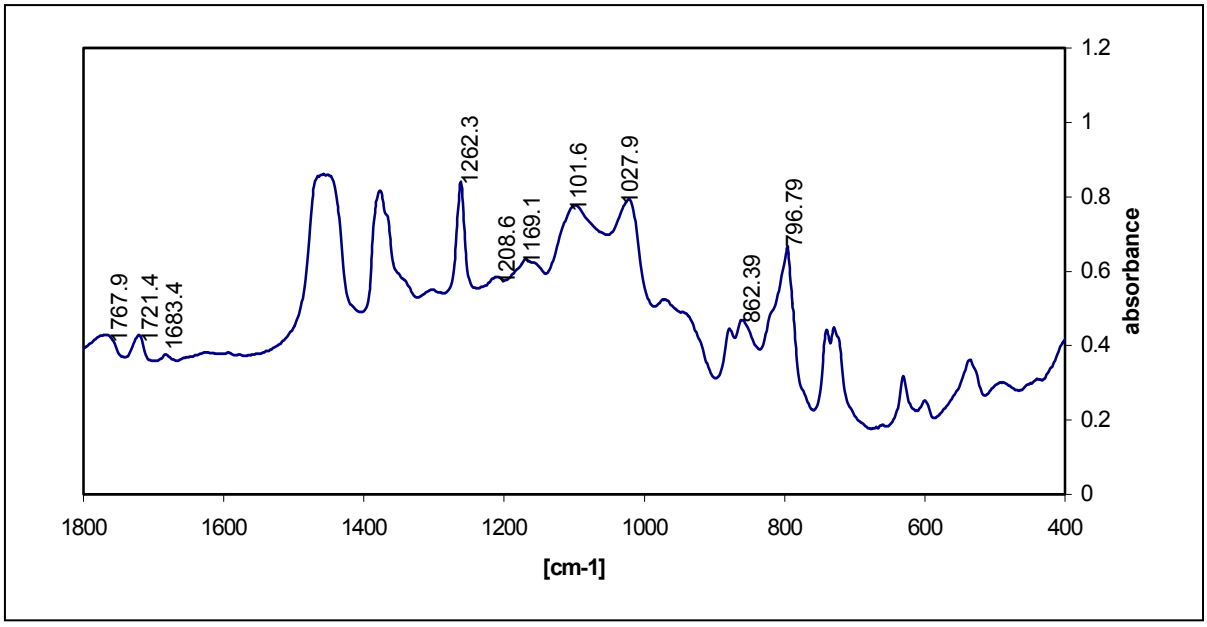

Figure III.2.9. FTIR spectrum of the CF_3COOLi + BF_3 reaction product, after $LiBF_4$ removal.

In order to determine how much the compounds formed are sensitive to moisture, water was added to the complexation product and a FTIR spectrum was measured (Figure III.2.10). Only bands characteristic of carboxylic groups in uncomplexed CF_3COOLi salt and bands characteristic of $LiBF_4$ are present in the spectrum.

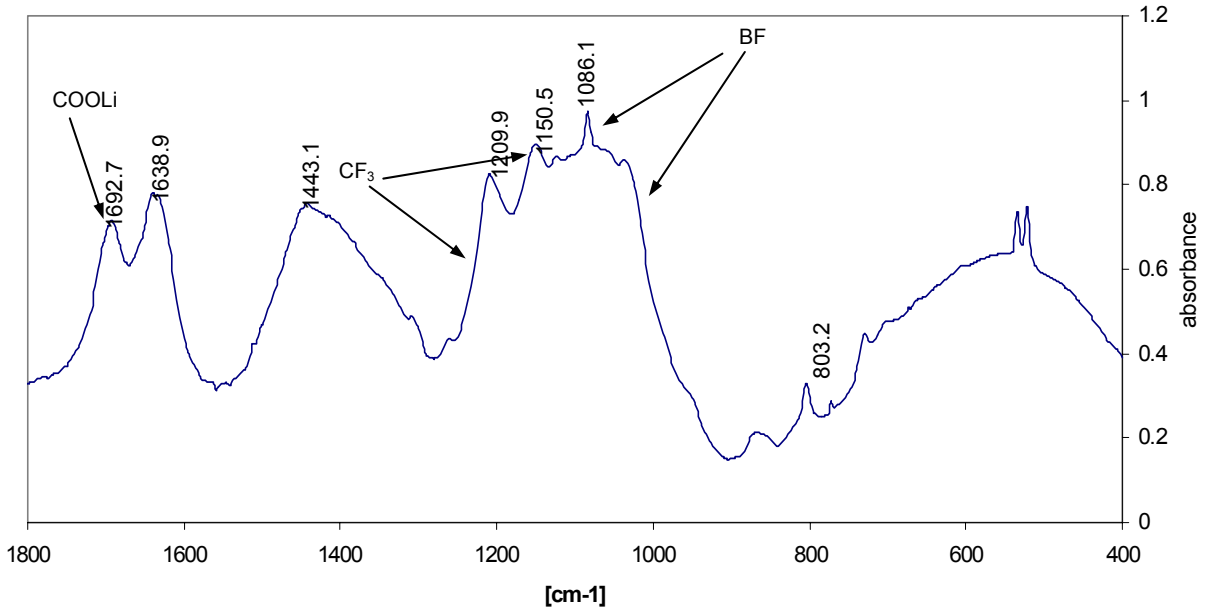

Figure III.2.10. FTIR spectrum of the compound resulting from the addition of water to the CF_3COOLi and BF_3 complex.

Complex with SbF_5

Figure III.2.11 presents a FTIR spectrum of the CF_3COOLi and SbF_5 reaction product.

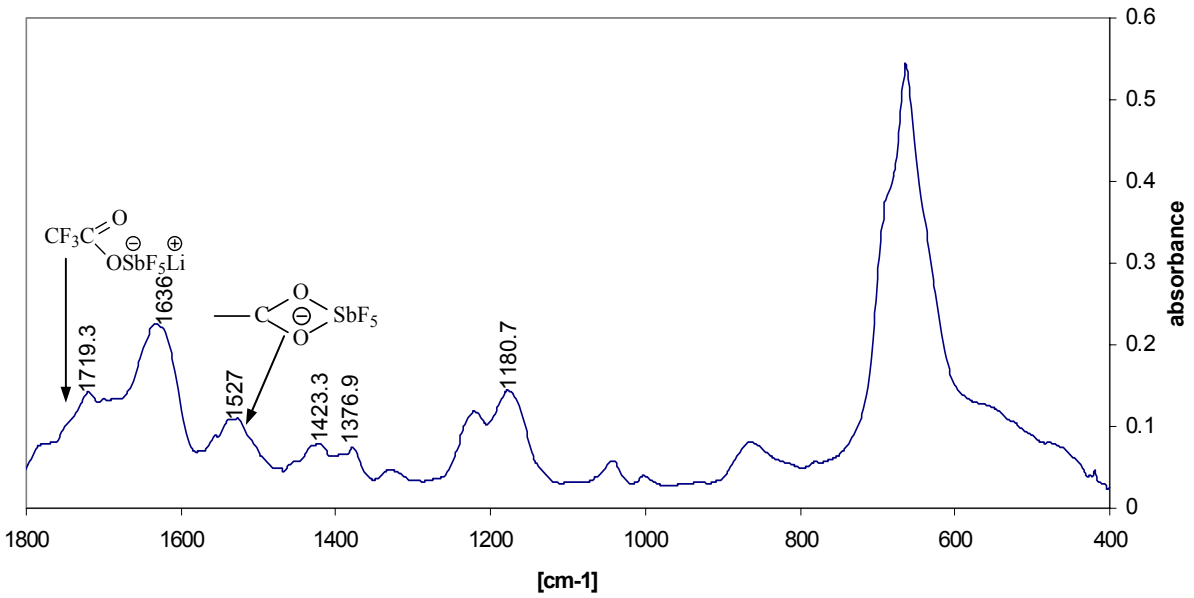

Figure III.2.11. FTIR spectrum of the CF_3COOLi and SbF_5 complexation reaction products.

Similarly as in the case of complexes with BF_3, partial shift of the carboxylate group bands from 1688 to 1719 and 1770 cm^{-1} is observed as well as appearance of a band at 1527 cm^{-1}. On the basis of this spectrum it can be stated that there is a possibility of complex formation of weak interaction with the carboxylic group, of the possible structure:

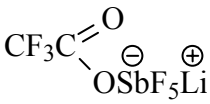

or

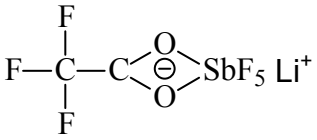

Complexes with $SbCl_5$ and $AlCl_3$

In the case of complexes with $SbCl_5$ and $AlCl_3$, due to their high sensitivity towards moisture, no spectra were obtained which would confirm the interaction of these Lewis acids with CF_3COOLi. Spectra containing bands of the uncomplexed salt were obtained for samples prepared in Nujol and in KBr, as is presented in Figure III.2.12.

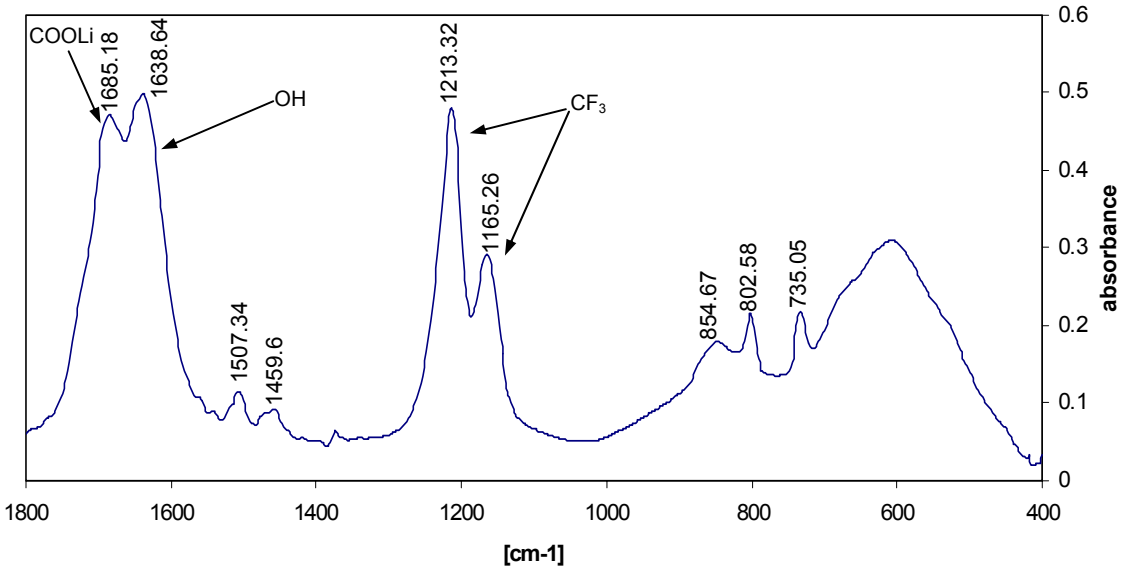

Figure III.2.12. FTIR spectrum of the lithium trifluoroacetate and $AlCl_3$ reaction products.

III.2.2. Polymer-in-Salt Electrolytes Obtained with Carboxylate Complex Salts

The electrolytes were prepared by disolution of lithium trifluoroacetate and the poly(AN-*co*-BuA) polymer matrix in acetonitrile, followed by solvent removal under dynamic vacuum. Drying was continued for about 70 hours after complete distilling off the solvent. The systems obtained were characterized on the basis of DSC and impedance spectroscopy. The mode of interaction of the matrix with the salt was observed in infrared on the basis of analysis of the band characteristic for the CN groups present in poly(AN-*co*-BuA).

III.2.2.1. Electrolytes comprising CF_3COOLi

Electrolytes comprising neat CF_3COOLi

On the thermogram presented in Figure III.2.13 of the electrolyte comprising CF_3COOLi and poly(AN-*co*-BuA) as the matrix a glassy transition at –40.4 °C (IInd heating) can be seen. This means that the introduced salt causes a considerable decrease in the glass transition temperature T_g, which for the neat copolymer is 42.5 °C. A crystalline phase of m.p. 107.6 °C (Ist heating cycle) and 92.5 °C (IInd heating cycle) is also observed in the system.

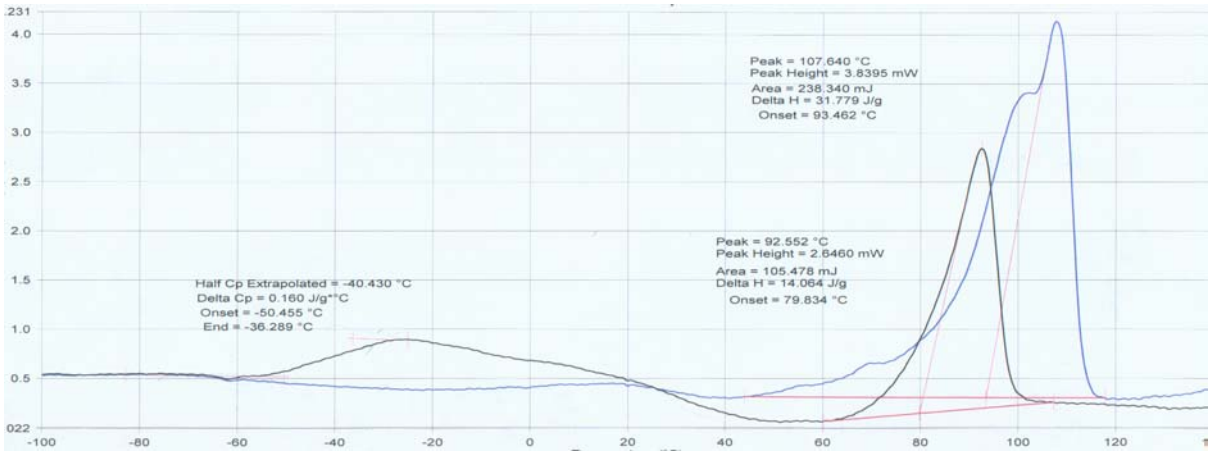

Figure III.2.13. DSC traces of the CF_3COOLi / poly(AN-co-BuA 2:1) [1.2:1] electrolyte.

The conductivity as a function of inverse temperature of the system comprising 55 wt. % of CF_3COOLi (1.2 mol Li per 1 mol of AN monomeric units in copolymer) [1.2:1] is presented in Figure III.2.14 (at room temperature its value is 2.5×10^{-7} S·cm^{-1}).

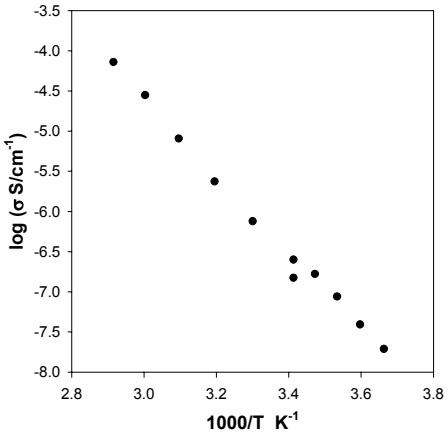

Figure III.2.14. Conductivity of an electrolyte comprising CF_3COOLi and poly(AN-co-BuA 2:1) [1.2:1].

In the IR spectrum a band at 2236 cm^{-1} characteristic of CN groups present in the matrix and a smaller one at 2252 cm^{-1} of the CN groups of the matrix interacting with cations are observed (Figure III.2.15).

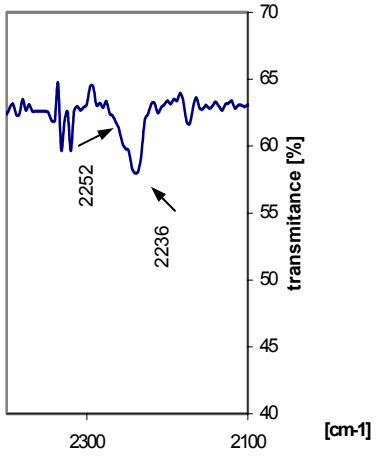

Figure III.2.15. Absorption bands in infrared of the CN group in the CF_3COOLi / poly(AN-co-BuA 2:1) electrolyte.

The system comprising poly(AN-*co*-BuA) and CF_3COOLi complexed with BF_3 shows a lower glass transition temperature than the system with the uncomplexed salt, T_g = –62.5 °C (IInd heating cycle) and a crystalline phase of m.p. 81.4 (Ist heating cycle) (Figure III.2.16).

In the FTIR spectrum (Figure III.2.17) of the (CF_3COOLi+BF_3) / poly(AN-*co*-BuA 2:1) electrolyte a band of the matrix CN groups interacting with the positively charged ions (ν_{CN} = 2254 cm^{-1}) as well as a second less intense band characteristic of the matrix neat CN groups (ν_{CN} = 2240 cm^{-1}) are present.

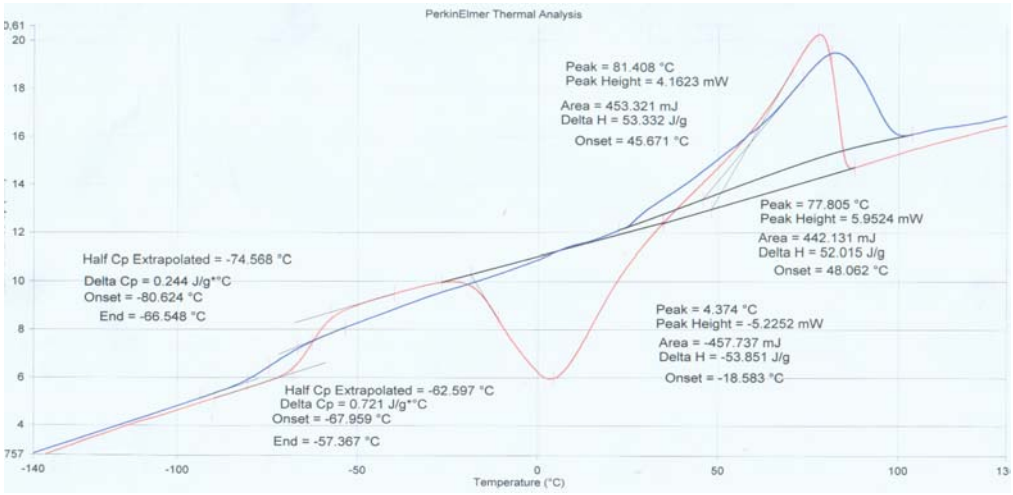

Figure III.2.16. DSC traces of the ($CF_3COOLi+BF_3$) / poly(AN-co-BuA 2:1) [1.2:1] electrolyte

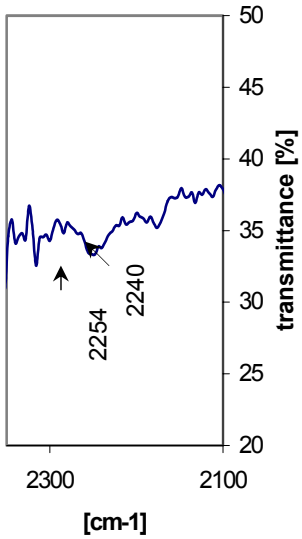

Figure III.2.17. Absorption bands in infrared of the matrix CN groups in the $CF_3COOLi+BF_3$ / poly(AN-co-BuA 2:1)[1.2:1] electrolyte

The results of impedance analysis of the ($CF_3COOLi+BF_3$) / poly(AN-*co*-BuA 2:1) system are presented in Figure III.2.18. The conductivity of the electrolyte comprising lithium trifluoroacetate complexed with BF_3 etherate is over two orders of magnitude higher than that of the system based on the uncomplexed salt and is about 5×10^{-5} S·cm^{-1} at ambient temperature.

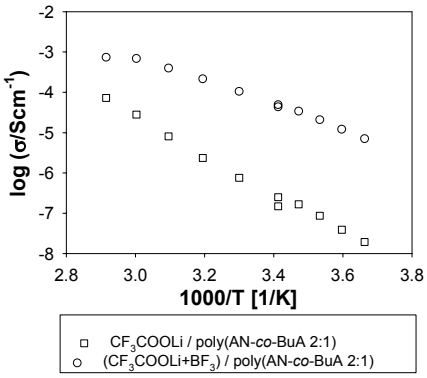

Figure III.2.18. Ionic conductivity of electrolytes comprising CF_3COOLi or CF_3COOLi + BF_3 and poly(AN-co-BuA 2:1)[1.2:1.

Systems comprising CF_3COOLi complexed with $SbCl_5$

The electrolytes comprising poly(AN-*co*-BuA 2:1) and lithium trifluoroacetate complexed with $SbCl_5$ (Li^+ : CN mole ratio = 1.2:1) were characterized by high sensitivity towards moisture. In its presence hydrochloride evolved and the synthesis and all measurements required ideally anhydrous conditions.

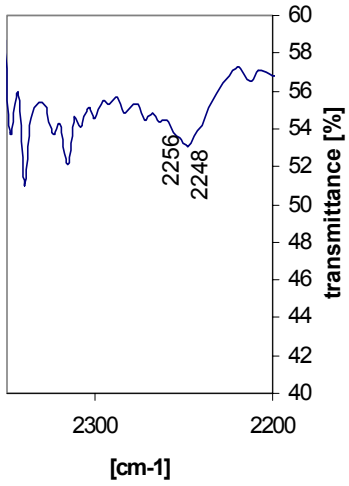

Figure III.2.19. CN groups absorption bands of the electrolyte comprising (CF_3COOLi+$SBCl_5$) / poly(AN-co-BuA 2:1) [1.2:1].

In the IR spectrum of this system bands characteristic of the matrix uncomplexed CN groups (ν_{CN} =2248 cm^{-1}) and of the matrix CN groups interacting with positive ions (ν_{CN} = 2256 cm^{-1}) are observed (Figure III.2.19).

The conductivity of this system is about two orders of magnitude higher than that of the uncomplexed salt and at ambient temperature is of the order of 10^{-6} S·cm^{-1} (Figure III.2.20).

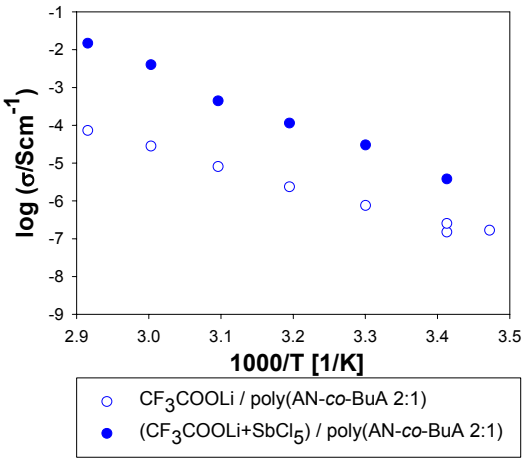

Figure III.2.20. Ionic conductivity of electrolytes comprising CF_3COOLi or CF_3COOLi+$SbCl_5$ and poly(AN-co-BuA 2:1)[1.2:1].

Systems comprising CF_3COOLi complexed with SbF_5

The thermal analysis results of the (CF_3COOLi+SbF_5) / poly(AN-*co*-BuA) electrolyte is presented in Figure III.2.21. In this case the glass transition temperature is higher, but still decreases with respect to that of the neat matrix and is equal to 13.9 °C (II^{nd} heating). The thermogram shows that the system is amorphous.

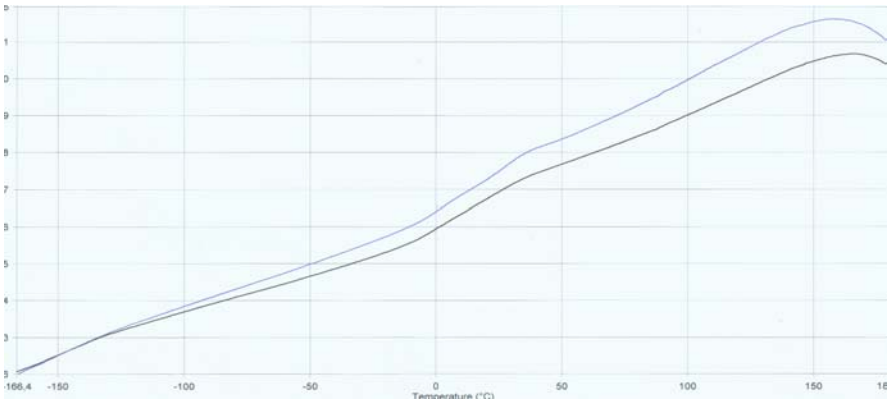

Figure III.2.21. DSC traces of the electrolyte comprising ($CF_3COOLi+SbF_5$ / poly(AN-co-BuA 2:1)[1.2:1].

The analyzed spectrum range of the electrolyte comprising the lithium trifluoroacetate and SbF_5 complex is presented in Figure III.2.22. Bands characteristic of the uncomplexed (2240 cm^{-1}) and complexed (2252 cm^{-1}) CN groups of the matrix are present.

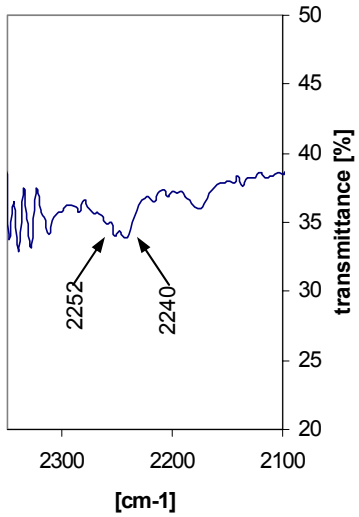

Figure III.2.22. CN groups absorption bands of the electrolyte comprising $CF_3COOLi+SbF_5$ / poly(AN-co-BuA 2:1)[1.2:1].

The results of impedance spectroscopy are presented in Figure III.2.23. The complexing of lithium trifluoroacetate with SbF_5 only to small extent affects the conductivity value.

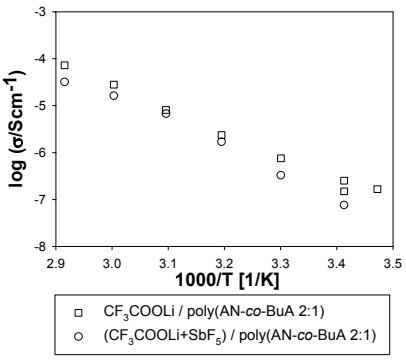

Figure III.2.23. Ionic conductivity of electrolytes comprising CF_3COOLi or $CF_3COOLi+SbF_5$ and poly(AN-co-BuA 2:1)[1.2:1].

Systems comprising CF_3COOLi complexed with $AlCl_3$

The DSC traces of the (CF_3COOLi+ACl_3) / poly(AN-*co*-BuA) system showed two glass transition temperatures: at 9.3 and 44.4 °C (IInd heating) and a melting point peak at 97.5 °C (Ist heating) (Figure III.2.24).

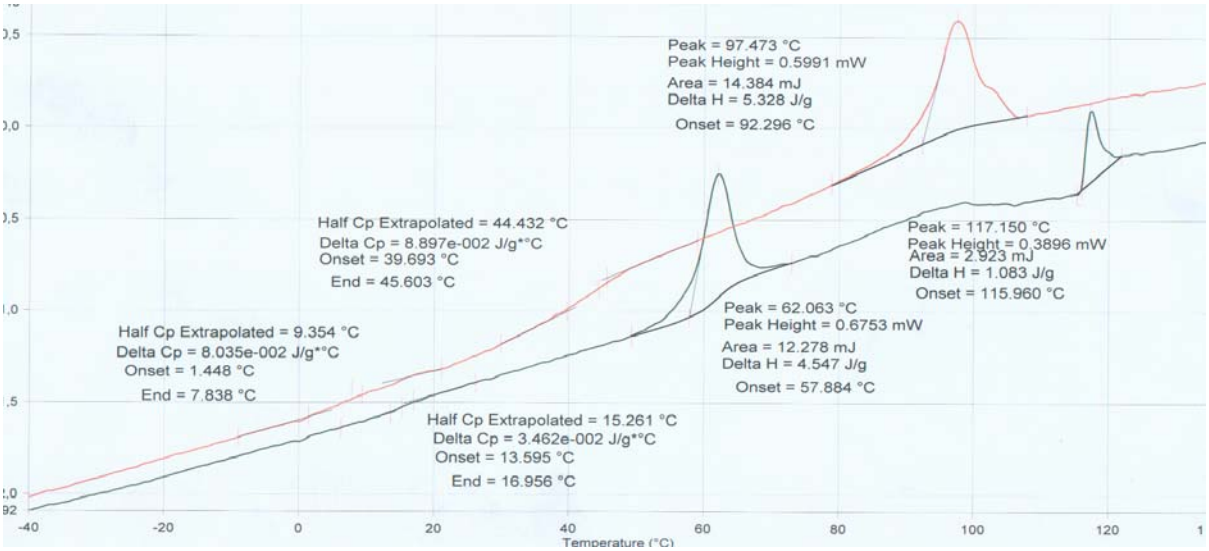

Figure III.2.24. DSC traces of the electrolyte comprising (CF_3COOLi+$AlCl_3$ / poly(AN-co-BuA 2:1)[1.2:1]

No interaction of the salt with the polymer matrix was observed in the infrared spectrum, where only the band corresponding to the matrix CN groups is present (Figure III.2.25).

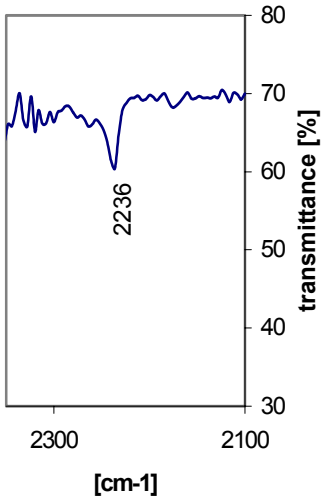

Figure III.2.25. CN groups absorption bands of the electrolyte comprising poly(AN-co-BuA 2:1)[1.2:1] / CF_3COOLi+$AlCl_3$.

The impedance spectra of the studied electrolyte showed a considerable decrease in conductivity in comparison with CF_3COOLi. The ionic conductivity of the (CF_3COOLi+$AlCl_3$) / poly(AN-*co*-BuA 2:1) is of the order of 10^{-10} S·cm^{-1} at 20 °C (Figure III.2.26).

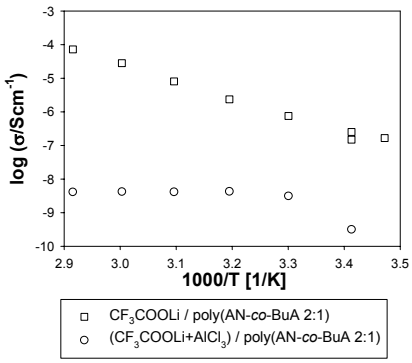

Figure III.2.26. Ionic conductivity of electrolytes comprising CF_3COOLi and $CF_3COOLi+AlCl_3$ / poly(AN-co-BuA 2:1).

III.2.2.2. Electrolytes comprising $(CO_2Li)_2$

Electrolytes comprising neat $(CO_2Li)_2$

Electrolytes with lithium oxalate were obtained using a salt suspension in an acetonitrile solution of the polymer achieving, after solvent removal a stiff heterophase system.

The FTIR spectrum shows the presence of one band, characteristic of uncomplexed matrix CN groups (2236 cm^{-1}) (Figure III.2.27).

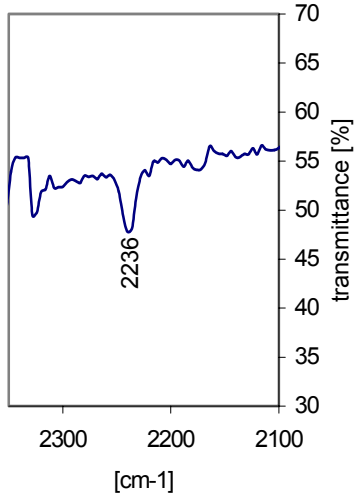

Figure III.2.27. CN groups absorption bands of the electrolyte comprising $(CO_2Li)_2$ and poly(AN-co-BuA 2:1)[1.2:1].

This system shows trace ionic conductivity of the order of 10^{-10} $S \cdot cm^{-1}$ (Figure III.2.28).

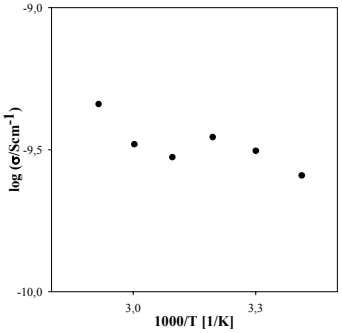

Figure III.2.28. Ionic conductivity of the electrolyte comprising $(CO_2Li)_2$ / poly(AN-co-BuA 2:1[1.2:1].

Electrolytes comprising $(CO_2Li)_2$ complexed with $BF_3 \cdot OEt_2$

The electrolyte was obtained by dissolving in acetonitrile the previously obtained $(CO_2Li)_2$ + BF_3 complex (it dissolves in acetonitrile in this form) and the poly(AN-*co*-BuA) matrix, and then distilling off the solvent under reduced pressure.

In DSC studies this system shows a glass transition temperature equal to −10 °C (IInd heating cycle) and a melting peak at 88.2 °C (Ist heating cycle) (Figure III.2.29).

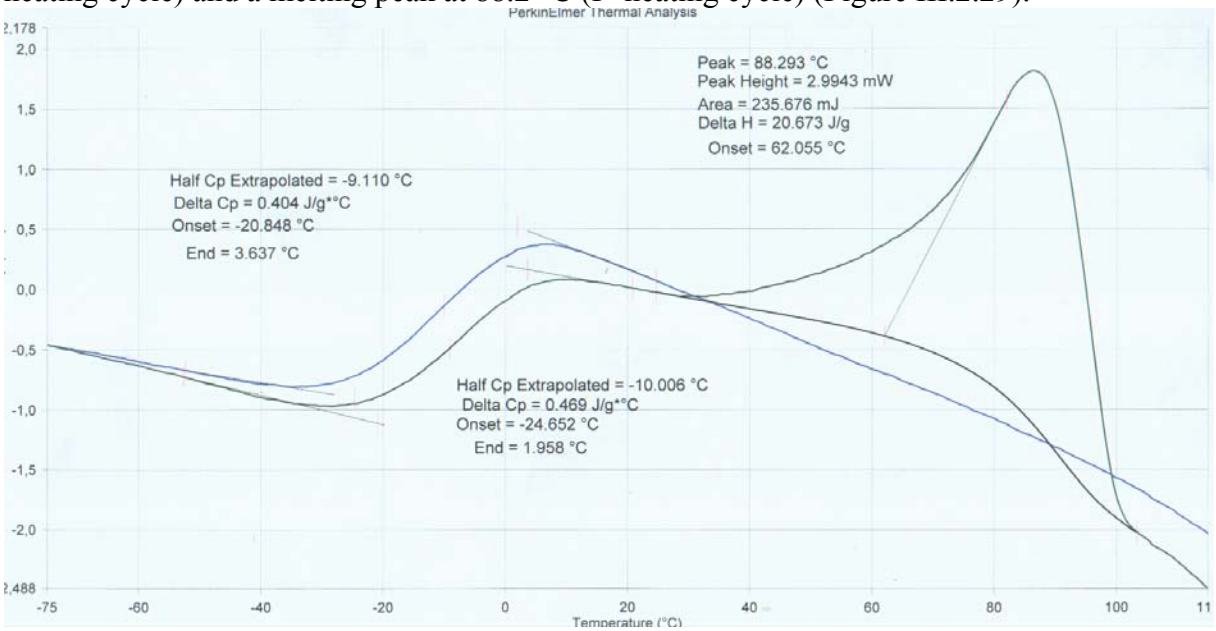

Figure III.2.29. DSC traces of the electrolyte comprising $(CO_2Li)_2$+BF_3 / poly(AN-co-BuA 2:1[1.2:1]).

In the FTIR spectrum (Figure III.2.30) a band corresponding to CN groups interacting with cations (2264 cm^{-1}) and peaks of free CN groups are observed.

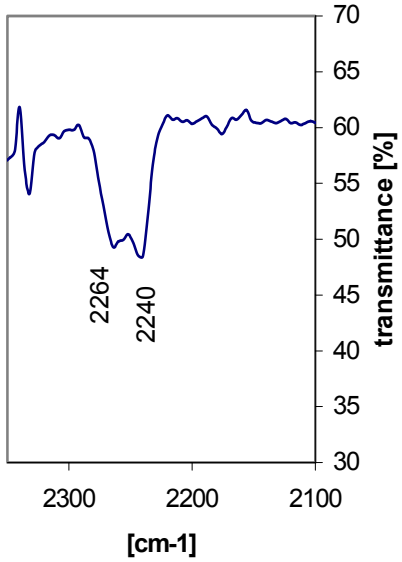

Figure III.2.30. CN groups absorption bands of the electrolyte comprising g$(CO_2Li)_2$+BF_3 and poly(AN-co-BuA 2:1)[1.2:1].

In comparison with the system containing an uncomplexed salt, the $((CO_2Li)_2+BF_3)$ / poly(AN-*co*-BuA 2:1) electrolyte shows conductivity values of four orders of magnitude higher - 10^{-6} S·cm^{-1}) (Figure III.2.31).

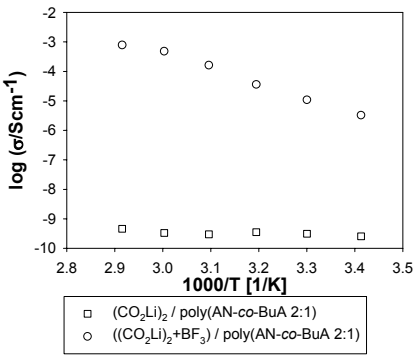

Figure III.2.31. Ionic conductivity of electrolytes comprising $(CO_2Li)_2$ or $(CO_2Li)_2+BF_3$ and poly(AN-co-BuA 2:1[1.2:1].

Electrolytes comprising $(CO_2Li)_2$ complexed with SbF_5

The complexation of lithium oxalate with SbF_5 resulted in a salt soluble in acetonitrile. The electrolytes were obtained as previously by casting from a mutual salt and matrix solution.

In the FTIR spectrum two bands corresponding to CN groups complexed by cations (2260 and 2252 cm^{-1} and a band characteristic of the polymer matrix neat CN groups (2244 cm^{-1}) are present (Figure III.2.32).

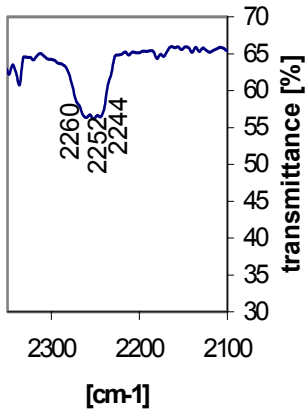

Figure III.2.32. CN groups absorption bands of the electrolyte comprising poly(AN-co-BuA 2:1)[1.2:1] / $(CO_2Li)_2+SbF_5$.

As seen from Figure III.2.33, the complexation of lithium oxalate with SbF_5 causes an increase in the electrolyte conductivity by about two orders of magnitude.

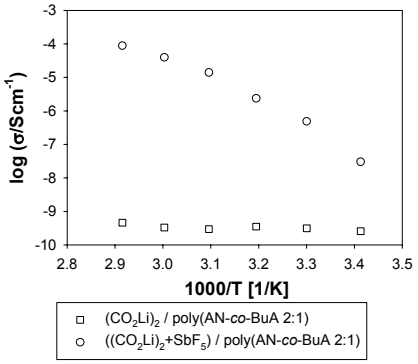

Figure III.2.33. Ionic conductivity of electrolytes comprising $(CO_2Li)_2$ or $(CO_2Li)_2+SbF_5$ and poly(AN-co-BuA 2:1[1.2:1].

III.2.2.3. Electrolytes comprising CH_3COOLi

Electrolytes comprising neat CH_3COOLi

Since CH_3COOLi does not dissolve in acetonitrile, the electrolyte was obtained by distilling off the solvent from a suspension of the salt in the polymer solution. A heterogeneous and rigid film was obtained.

The FTIR spectrum shows the presence of a band characteristic of the matrix uncomplexed CN groups (2240 cm^{-1}) (Figure III.2.34).

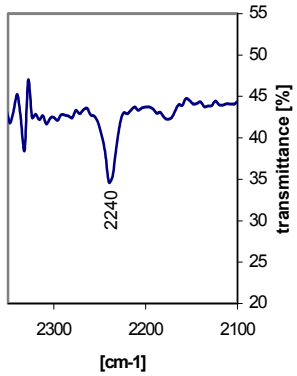

Figure III.2.34. CN groups absorption bands of the electrolyte comprising poly(AN-co-BuA 2:1)[1.2:1] / CH_3COOLi.

The electrolyte obtained is characterized by low ambient temperature ionic conductivity of the order of 10^{-10} $S \cdot cm^{-1}$ (Figure III.2.38).

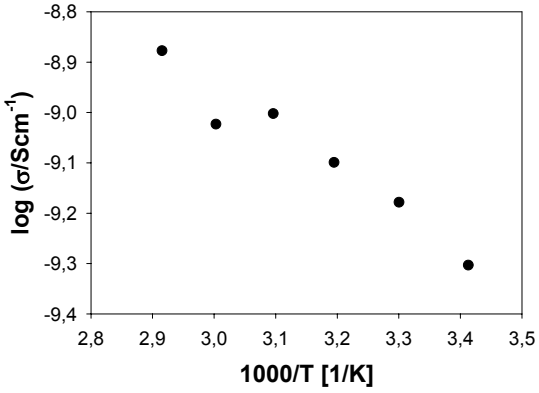

Figure III.2.35. Ionic conductivity of electrolytes comprising poly(AN-co-BuA 2:1[1.2:1] / CH_3COOLi.

Electrolytes comprising CH_3COOLi complexed with $BF_3 \cdot O(C_2H_5)_2$

The lithium acetate complex with BF_3 etherate and poly(AN-*co*-BuA) dissolve in acetonitrile, due to which the electrolyte was obtained in a homogeneous form.

In the FTIR spectrum (Figure III.2.36) a band characteristic of the matrix CN groups interacting with the positively charged ions (2256 cm^{-1}) and a band corresponding to the uncomplexed polymer matrix CN groups (2240 cm^{-1}) are observed.

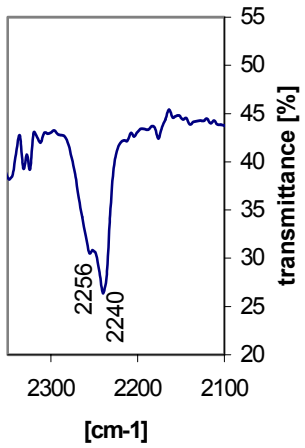

Figure III.2.36. CN groups absorption bands of the electrolyte comprising $CH_3COOLi+BF_3$ and poly(AN-co-BuA 2:1)[1.2:1].

The ambient temperature ionic conductivity of the electrolyte comprising $CH_3COOLi+BF_3$ / poly(AN-*co*-BuA 2:1) is of the order of 10^{-6} $S \cdot cm^{-1}$ (Figure III.2.37), i.e. four orders of magnitude higher than that for systems comprising uncomplexed lithium acetate.

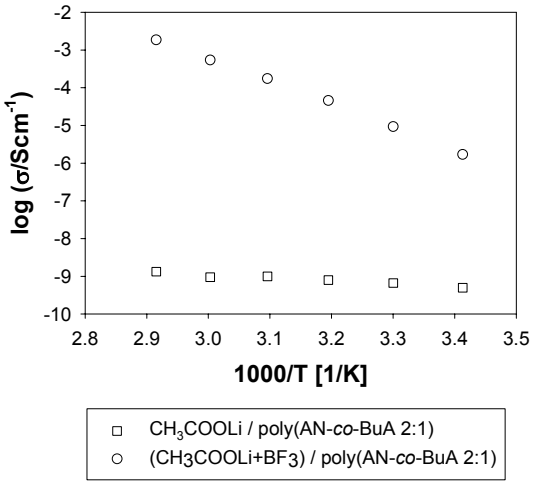

Figure III.2.37. Ionic conductivity of electrolytes comprising poly(AN-co-BuA 2:1[1.2:1] and CH_3COOLi or $CH_3COOLi+BF_3$.

III.2.3. Conclusions

III.2.3.1. Effect of the carboxylic lithium salt on the electrolyte conductivity values

The conductivity of electrolytes comprising various carboxylic lithium salts is presented in Figure III.2.38. The ability to dissociation in the polymer matrix applied has a decisive effect on the conductivity in these systems. Only lithium trifluoroacetate, due to the strong induction effect of the fluorine substituents, is soluble in the polymer matrix and affords homogeneous systems with it. The difference in conductivity with respect to the remaining systems is about 3 orders of magnitude.

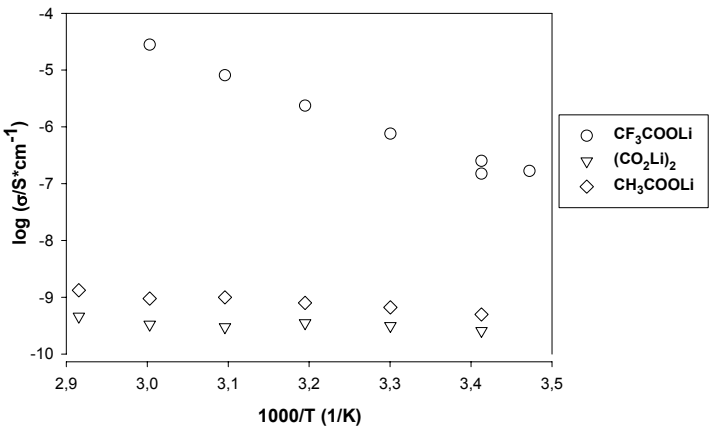

Figure III.2.38. Ionic conductivity of electrolytes comprising various carboxylic lithium salts and poly(AN-co-BuA 2:1)[1.2:1].

III.2.3.2. Effect of complexation with various Lewis acids on the conductivity of electrolytes

Figure III.2.39 shows the conductivity of electrolytes comprising lithium trifluoroacetate and its complexes with various Lewis acids. The best results were obtained for complexes comprising $SbCl_5$ and BF_3. The increase in conductivity, in relation to the system comprising the uncomplexed salt is by about 2 orders of magnitude. The complexation with SbF_5 only slightly affects the conductivity value of the system. $AlCl_3$ used as a complexing agent considerably retards the mobility of ions in the system, which results in a decrease in the electrolyte mobility.

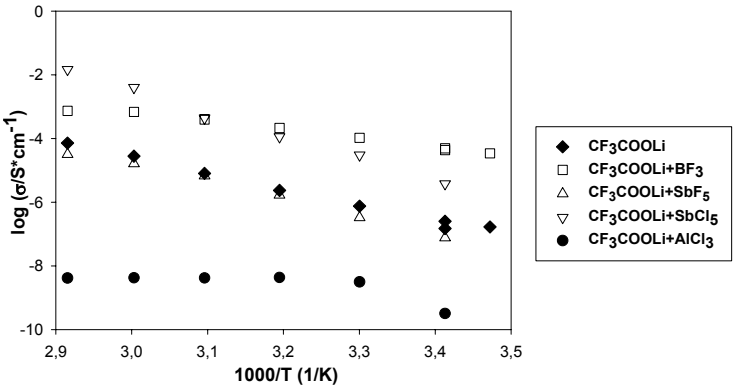

Figure III.2.39. Conductivity of electrolytes comprising poly(AN-co-BuA 2:1) and CF_3CO_2Li [1.2:1] and its complexes with various Lewis acids.

The conductivity of systems comprising lithium oxalate and its complexes with various Lewis acids is presented in Figure III.2.39. The complexation with both BF_3 and SbF_5 causes an increase in the electrolyte conductivity. The system comprising the complex with BF_3 shows conductivity of four orders of magnitude higher with respect to that with the uncomplexed salt, whereas in systems with SbF_5 this value increases by two orders of magnitude.

Similarly as in the case of lithium acetate, complexing with BF_3 favorably affects the ionic conductivity of electrolytes, increasing its value by over four orders of magnitude (Figure III.2.40). Simultaneously, due to dissolution of the complex salt, an improvement of the mechanical properties of the system occurs and the electrolyte achieves the form of a homogeneous and flexible membrane.

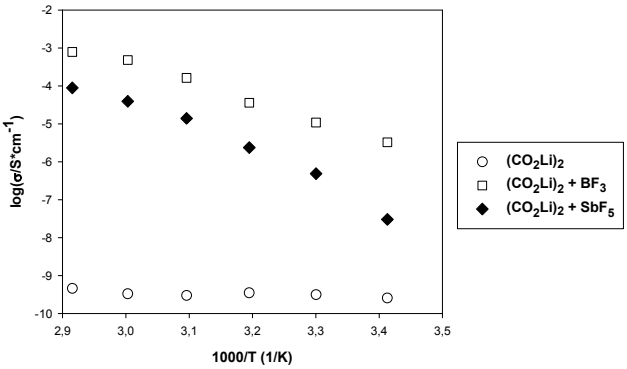

Figure III.2.40. Conductivity of electrolytes comprising poly(AN-co-BuA 2:1) and C_2Li_2O [1.2:1] as well as its complexes with Lewis acids.

III.2.3.3. Effect of complexing carboxylic acid salts with BF_3 on the conductivity of electrolytes

From among the Lewis acids applied for complexing carboxylic acid salts, the best results were obtained for BF_3. The complexation with it caused an increase in the conductivity of each system containing the carboxylic salts studied and positively affected the mechanical properties of electrolytes. Moreover, in the case of CH_3COOLi and $(CO_2Li)_2$ the addition of this Lewis acid improved the solubility of the salt in acetonitrile. Figure III.2.41 shows the effect of BF_3 on the conductivity of electrolytes comprising various lithium salts and the acrylonitrile and butyl acrylate copolymer as the polymer matrix.

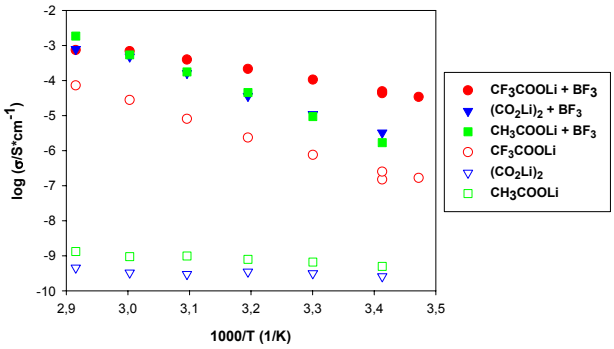

Figure III.2.41. Effect of complexation of $BF_3 \cdot O(C_2H_5)$ on the conductivity of electrolytes comprising lithium carboxylates and poli(AN-co-BuA 2:1).

The studies carried out show considerable possibilities of modification of the lithium salts properties by reacting them with compounds of Lewis acids type. The complexation reactions cause an increase in the salts degree of dissociation, and probably also affect the mobility of anions. The determination of the ability towards immobilization requires further studies (cation transference numbers measurements) for selected, most promising systems. From among the Lewis acids, the best results were obtained for BF_3, both from the conduction and mechanical properties point of view. The hitherto obtained results show the necessity of further characterization of BF_3 complexes in order to determine the complexation reaction mechanism and selectivity.

IV. COMPOSITE ELECTROLYTES WITH SUPRAMOLECULAR ANION RECEPTORS

IV.1. Introduction

Another approach in synthesis and development of new polymer electrolytes with enhanced cation transport, as well as towards understanding its mechanism is by using anion-trapping supramolecular components, namely calix[4]arene R-urea derivatives (with R = phenyl, *t*-butyl, *p*-nitrophenyl; see the Schematic 1), as additives for solid P(EO)-LiX blends (with X = I^- or $CF_3SO_3^-$).

So far, mostly cationic receptors such as crown ethers, cryptands and calixarenes have been used in low molecular weight non-aqueous solutions or in polymer electrolytes. Reviewing the literature, one may note that up to date studies on the use of anion receptors in polymer electrolytes are very limited. To our knowledge, papers dealing with this subject base on either theoretical predictions or studies on the addition of boron family compounds applied into solutions of lithium salts in both aprotic (inert) electrolytes of low molecular weight solvents and gel polyelectrolytes, as well as studies on linear or cyclic aza-ether compounds (with electron-withdrawing groups) incorporated into oligoethers or grafted directly to polymer chain. In this work anion receptors based on calix[4]arene urea derivatives are used as additives in P(EO)-LiI electrolytes.

The aim of the work was to analyze the effect of the type of anion receptor, its concentration, and the concentration of the dopant salt on the conductivity and microstructure of composite polyether-lithium electrolytes containing calixarene additives. To this end three calixarene compounds with various anion complexing ability were synthesized and added to low and high molecular weight polyether electrolytes. In the frame of basic research on ionic transport in polymer electrolytes in the presence of anion receptors, liquid dimethoxy-poly(ethylene-oxide)-lithium iodine (P(EO)DME-LiI) was examined in the first place. This allowed to find out the most important chemical features of the ironically conducting system involving calixarenes on macro- and microscopic levels. Total ionic conductivity and lithium transference numbers t_+ as a function of salts concentrations and fraction of added various calixarene receptors were studied by means of impedance spectroscopy (IS) combined with direct current measurements. The ion-matrix interactions were analyzed using Fourier-Transformed Infrared (FTIR) measurements. Band shifts of infrared modes attributed to C-O-C vibrations were particularly detailed. Additionally, studies on polymer chain flexibility were performed by means of Differential Scanning Calorimetry (DSC) technique. The effect of type of receptor used is shown on the basis of t_+ determination as well as studies of the effect of calixarene on the formation of interfacial electrode-electrolyte layers.

IV.2. Calix[4]arene Derivatives as Additives for Polymer Electrolytes

The interest in calixarenes has grown rapidly because of numerous derivatives that can be created *via* relatively simple synthesis and because of their appealing three-dimensional symmetry. The starting compound **1** (see Scheme 1), a cyclic tetramer composed of phenolic units linked *via* the ortho-positions by methylene bridges, is an important building block in supramolecular chemistry [1]. It has been well established that calix[4]arene could adopt four different conformations [2] (cone, partial cone, 1,2-alternate and 1,3-alternate) rendering different geometries, potentially useful for building blocks. Selective functionalization [3] at the phenolic OH groups (lower rim) and at the para positions of phenol rings (upper rim) has led to development of calix[4]arene host capable of recognizing some neutral molecules [4], cations [5], and anions [6].

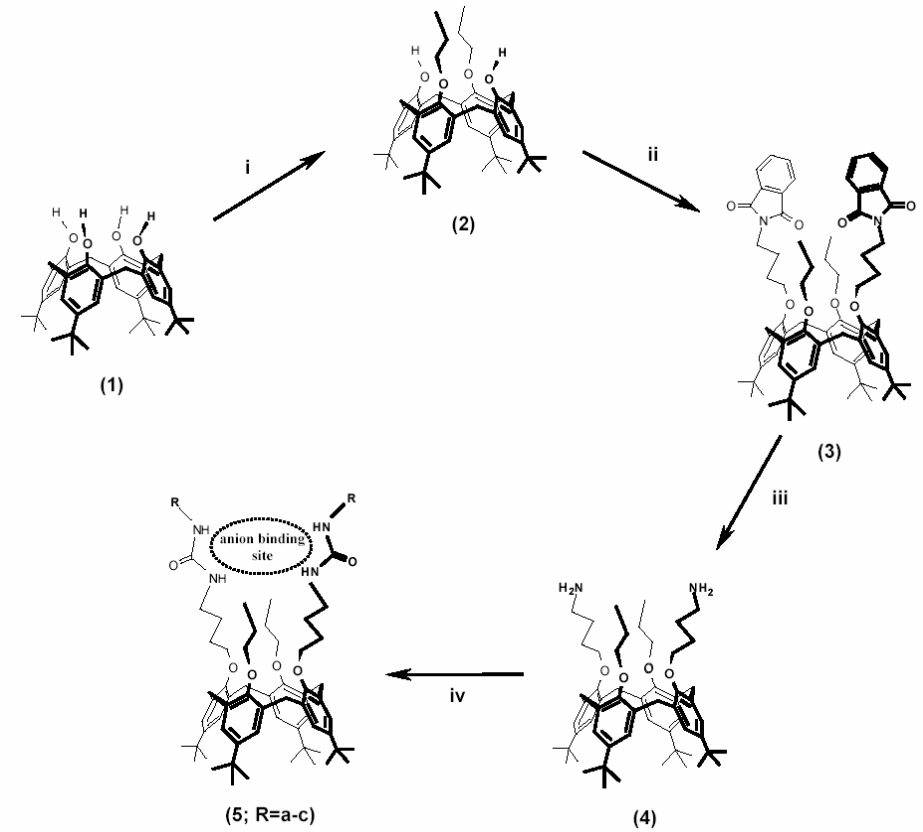

Scheme 1. Synthesis of urea *p-tert*-butylcalix[4]arene derivatives with different substituents (**R**). Note, there is the anion binding site indicated in the resulting macromolecule
Reagents and conditions: **i**, n-C_3H_7I, K_2CO_3, $(CH_3)_2CO$, ΔT; **ii**, $C_{12}H_{12}BrNO_2$, NaH, DMF, 70-75°C; **iii**, $N_2H_4 \cdot H_2O$, EtOH / THF, ΔT; **iv**, $\mathbf{R_{(a-c)}}$-NCO, $CHCl_3$, r.t

In the resulting macromolecule **5** the urea hydrogen atoms form a not preorganized, open arrangement of four dipoles, setting the maximum of positive potential in the center, which could trap a negative charge, such as anions, in the electrolyte. Therefore, the calix[4]arene R-urea derivatives could be applied as additives into a polymer electrolyte in order to relatively enhance cationic transport. Moreover, the approach is supported by the fact that hydrogen atoms binding anions do not reveal high acidity, which in the worst case could affect *e.g.* the lithium anode in the battery.

IV.2.1. Experimental

IV.2.1.1. Synthesis of calix[4]arene derivatives

The synthesis course is illustratively presented in Scheme 1. The starting compounds **1** [7] and **2** [8] were obtained according to procedures previously described in the literature. Compounds **3** and **4** were obtained as described in the preparation procedures given in II.1.1. 1. The synthesis of compound **5a** is explained in II.1.1.2. The procedure differed from that described in literature [9,10]. The main difference was the use of compound **3** as a half product in the synthesis. This resulted in a quadruple increase of the total process yield and enabled obtaining of larger fractions of the end-products. Both final compounds **5b** and **5c** were synthesized for the first time, in a similar way as compound **5a** in these studies.

All reactions, except the synthesis of compounds **1** and **4**, were carried out under the protection of an argon atmosphere. Separation and purification of compounds **3** and **5a-c** were made by flash column chromatography (FCCh) at the pressure of approximately 0.1atm. Silica gel 60 (particle size 0.04-0.063mm, 230-240mesh) was obtained from Merck. The progress of reactions was controlled by thin layer chromatography (TLC) on plastic plates covered with a

0.2mm-thick layer of silica gel 60 F254, manufactured by Merck. To complete the procedure, the organic phase was washed solely with distilled water and, depending on needs, either acidified with a water solution of 1N HCl or alkalized with 1N NH_3 (for compound **4**) and dried over $MgSO_4$.

The typical solvents required in due course of the synthesis, $CHCl_3$ and CH_2Cl_2, were distilled over $CaCl_2$ and stored over molecular sieves type 4A for three days. The solvents together with $C_6H_5CH_3$ (toluene) and other reactants, *t*-$C_4H_9C_6H_4OH$ (*p*-*tert*-butylphenol); HCHO, 37 wt. % *aq*. (formaldehyde); NaOH; C_3H_7I (propyl iodide); K_2CO_3; C_6H_5NCO, *t*-C_4H_9NCO and *p*-C_6H_4NCO (phenyl, *t*-butyl and *p*-nitrophenyl isocyanates), were of reagent-grade and used without further purification. The analytical-grade quality reagents, DMF (*N*,*N*-dimethylformamide) (anhydrous 99.8%); EtOH (ethyl alcohol) (anhydrous 99.9%) and acetone (anhydrous 99.9%), were obtained from Aldrich and NaH, used as 55% suspension in oil, was supplied by Fluka.

For identification, all compounds **1**-**5** were subsequently characterized by melting point, NMR, IR, MS testing measurements, including microanalysis. Before the chemical analysis, they were dried under reduced pressure of ~10^{-5} Torr at 50ºC for 8 hours, except of compound **1** dried at 145ºC for 35 hours.

The melting point of compounds was determined with a capillary melting-point apparatus in vacuum sealed capillary tubes (under 10^{-3} Torr) and in all cases exceed 200ºC. The results for **1** [7], **2** [8a], **4** [9] and **5a** [9] differ from those reported in the literature.

The ^{1}H NMR and ^{13}C NMR spectra of compounds in the form of solutions in $CDCl_3$ were measured using Varian Mercury 400BB (400MHz) and Varian Unityplus 500 (500MHz) spectrometers. The obtained coupling constant values (J) are given in Hz. Chemical shifts (δ) are given in ppm in relation to $(CH_3)_4Si$ as the internal standard. The ^{1}H NMR and ^{13}C NMR spectra of **1** [11,12], **2** [8], **4** [9], and **5a** [9] compounds were identical with those previously described.

FTIR spectra were recorded on a computer-interfaced Perkin-Elmer 2000 FTIR system in the transmittance mode, with the wavenumber resolution of 2 cm^{-1} in the range of 600-4000 cm^{-1} in KBr pellets.

Mass spectra were obtained by both MALDI-ToF (Matrix Assisted Laser Desorption and Ionization Time of Flight) and ESI (Electrospray Ionization) techniques. MALDI-ToF mass spectra were acquired using Kratos Analytical Compact MALDI 4 V5.2.1 mass spectrometer equipped with 337-nm nitrogen laser with a 3-ns pulse duration. The measurements were carried out in linear mode at the acceleration voltage of the instrument set at 20kV. For each sample spectra were averaged out of 200 laser shots. The samples were dissolved in THF (tetrahydrofuran) and $CHCl_3$ using DHB (2,4-dihydroxybenzoic acid) as a matrix. In order to avoid distortions of the signal, the laser power was moderated in the range of 30-65 units characteristic for the type of measurement. ESI mass spectra were acquired with MARINER ESI time-of-flight mass spectrometer (PerSeptive Biosystem) with the resolution of 5000 (FWHM). The needle voltage was 3.5 kV and the inlet capillary temperature was maintained at 140°C. The declustering potential varied from 80 to 140 V, depending on the type of experiment. All the spectra were collected in the positive ion mode. Sample solutions were prepared by mixing the compound with a mixture of solvents: MeOH (methyl alcohol) and CH_2Cl_2. The calculations of molecular mass of compounds were performed using the ACDLabs 5.0/ChemSketch software.

Microanalyses were acquired using Perkin-Elmer PE Serial II CHNS/O.

*IV.2.1.1.1. Preparation procedures of the calix[4]arene derivatives (**3**) and (**4**)*

5, 11, 17, 23-Tetra-*p*-*tert*-butyl-25,27-bis[(*N*-4-phthalimidobutyl)oxy]-26,28-dipropoxycalix[4]arene (**3**)

The sodium salt solution of compound **2** (6.48 g, 8.84 mmol) obtained in a presence of NaH (1.3 g, 29.8 mmol) in DMF (100 ml) was prepared in a separate vessel. The whole solution was

well stirred until complete dissolution at room temperature. Next, the mixture was carefully introduced into a solution of *N*-(4-bromobutyl)phthalimide (11.8 g, 41.82 mmol) (prepared by the Salzberg-Supniewski method [13]) in DMF (55 ml). After about 3 h, the temperature of the reaction mixture was set up to 75°C and the mixture was stirred for 24 h. The reaction course was monitored *in situ* by means of TLC (SiO_2; $CHCl_3$:MeOH = 99:1 or $CHCl_3$). After cooling to room temperature and adding 5 ml H_2O, DMF was evaporated under reduced pressure (~10^{-3} Torr). The residue (ca. 16 g) was dissolved in $CHCl_3$ (250 ml) and subjected to the standard procedure (mentioned above). After drying over $MgSO_4$ the organic solvent was vaporized to dryness. Product **3** was separated from the solid residue *via* FCCh. By using eluents in the following order: CH_2Cl_2:hexane = 1:1, $CHCl_3$ and $CHCl_3$:MeOH = 9:1, FCCh enabled the production of pure **3** as a white powder in 60% reaction yield.

5, 11, 17, 23-Tetra-*p*-*tert*-butyl-25,27-bis[(4-aminobutyl)oxy]-26, 28-dipropoxycalix[4]arene (**4**)

A suspension of compound **3** (6g, 5.28 mmol) in THF (100 ml) and EtOH (400 ml) was refluxed for 5 h after adding hydrazine monohydrate (8 g, 128 mmol, 80%*aq*), and stirred intensively at room temperature for 24 h. The reaction was carried out until the substrate was fully exhausted. The progress of the reaction was monitored by means of TLC (SiO_2; $CHCl_3$:MeOH = 99:1 or $CHCl_3$). Upon cooling of the transparent solution, a white precipitate (phthalide acid hydrazide) was formed. The precipitate was filtered off. The filtrate was concentrated *in vacuo*; $CHCl_3$ (400 ml) was added to the filtrate and the whole mixture was subjected to the standard procedure (as above). After drying over $MgSO_4$ the organic solvent was evaporated. This resulted in a yellowish oil, compound **4**, that was dried (~10^{-3} Torr, 40°C, 3h) subsequently. Compound **4** was obtained as a light yellow powder in 86% reaction yield.

*IV.2.1.1.2. Preparation procedures of the calix[4]arene R-urea derivatives (**5**)*

5, 11, 17, 23-Tetra-*p*-*tert*-butyl-25, 27-bis[[*N*'-phenylureido)butyl]oxy]-26, 28-dipropoxycalix[4]arene (**5a**) with R = phenyl,

5, 11, 17, 23-Tetra-*p*-*tert*-butyl-25, 27-bis[[*N*'-*t*-butylureido)butyl]oxy]-26, 28-dipropoxycalix[4]arene (**5b**) with R = *t*-butyl,

5, 11, 17, 23-Tetra-*p*-*tert*-butyl-25, 27-bis[[*N*'-*p*-nitrophenylureido)butyl]oxy]-26, 28-dipropoxycalix[4]arene (**5c**) with R = *p*-nitrophenyl

In all cases, 10.12 mmol of isocyanate (corresponding to **5a**-**c** in Scheme 1) was added to 4.57 mmol of compound **4** dissolved in $CHCl_3$ (120 ml). The solution was stirred for 24 h at ambient temperature. The reaction was performed until full exhaustion of the substrate. Its progress was monitored by means of TLC (SiO_2; CH_2Cl_2:MeOH = 98:2). Once the process was completed, only H_2O (150 ml) was added. The next step was to separate and dry the organic layer over $MgSO_4$. The organic solvent was evaporated and the crude products were purified as described below.

5a: washed with methanol, purified using FCCh (SiO_2; CH_2Cl_2),

5b: recrystallized from methanol, purified using FCCh (SiO_2; CH_2Cl_2:MeOH 98:2),

5c: washed with methanol, purified using FCCh (SiO_2; CH_2Cl_2:MeOH 98:2).

The corresponding reaction resulted in:

5a (white powder): 85%, **5b** (white powder): 72%, and **5c** (yellow powder): 91%.

IV.2.1.2. Electrolyte preparation

All the procedures of electrolytes preparation have been carried out in an argon-filled dry-box with moisture content lower than 10 ppm. Before electrolyte composing, all ingredients, except anhydrous salts LiI and $LiCF_3SO_3$ (99.999%, Aldrich, reagent grades), were dried separately under reduced pressure (c.a. 10^{-5} Torr) on a vacuum line. Calix[4]arene R-urea derivatives were dried at 50°C for 20 h and P(EO) ($M_w = 5\times10^6$, Aldrich, reagent grade) at 50°C

for 24 h. The liquid P(EO)DME (M_w = 500, Aldrich, reagent grade) was filtered, carefully freeze-dried, using 4 freeze-pump-thaw cycles, before being dried at 45°C for 50h. The solvent used in preparation of the solid electrolytes, CH_3CN (acetonitrile, Lab Scan Ltd, for analysis), was meticulously freeze-dried and double distilled over molecular sieves type 4A.

II.1.1.2.1. P(EO)DME based liquid electrolyte preparation

The chemical compositions of liquid electrolytes were chosen as following: $P(EO)DME_{100}(LiI)_1$(**5a**)$_x$ and $P(EO)DME_{10}(LiI)_1$(**5a**)$_x$ for calixarene molar ratio in respect to salt x = 0 - 0.8. The LiI salt was dissolved in P(EO)DME polymer matrix using a magnetic stirrer. Concentration of the salt with respect to oxirane monomeric units (O:Li ratio) varied from 100:1 to 10:1. All electrolytes were prepared by direct dissolution of the salt in the polymer. Next, appropriate amounts of solution were placed in glass vessels, and the calixarene was carefully added in appropriate proportions. In order to facilitate dissolving, samples with the highest salt and calixarene concentrations were warmed up to 35°C. All electrolyte samples were equilibrated in a dry-box at ambient temperature before being used in any experiment.

II.1.1.2.2. P(EO) based solid electrolyte preparation

The chemical composition was chosen as $P(EO)_y(LiI)_1$ (**5a-c**)$_x$ for calixarene molar ratio in respect to salt x = 0 - 0.8, y = 100, 20, 10, 7. The LiI salt was added into the P(EO) solution in CH_3CN (40 ml) and homogenized by magnetic stirring at ambient temperature in the argon-filled dry-box. Next, the calixarene ingredient was added and the mixture was stirred again until homogenization. In the case of **5a** for x > 0.6 (y = 10) and **5b** for x > 0.3 (y = 7), samples did not reveal complete solubility. The mixture was cast on Teflon® plates. The excessive amount of CH_3CN was evaporated for 24 h under vacuum at ambient temperature. Next, solvent-free films were dried at 45°C for 60h. Before measurements, all the samples were stored in a dry-box at ambient temperature, until they reached intrinsic crystallization in the electrolyte.

IV.2.1.3. Electrolyte samples characterization

IV.1.1.3.1. DSC thermal analysis

Thermal analysis was conducted to measure glass transition temperature (T_g) and melting point (T_m). DSC experiments were performed on a Perkin-Elmer Pyris 1 scanning calorimeter equipped with a low-temperature measuring head and a liquid-nitrogen-cooled heating element. Samples in aluminum pans were loaded into a dry-box under N_2 atmosphere and stabilized by slowly cooling them down to −150°C and then heated at 20°C/min to 70°C. The temperature scale was calibrated with the melting point of indium. In all scans, empty aluminum pans were used as reference. The estimated error in the determination of T_g and T_m was ±2°C.

IV.1.1.3.2. Conductivity measurements

Ionic conductivity at 0-70°C of liquid and 0-90°C of solid electrolytes was determined by means of IS. Liquid electrolytes were placed in a constant-volume cylindrical cell of 1.6 mm thickness with two symmetrical 7.8 mm in diameter electrodes. Solid electrolytes in the form of discs were pressed between stainless-steel blocking electrodes of 8 mm in diameter. Their thickness ranged from 150-330 μm. The measuring cells were evacuated (~10^{-5} Torr) for 2h prior to the experiments. The measurements were carried out on a PC-controlled Solartron-Schlumberger 1255 Impedance Analyzer over the frequency range of 1 Hz – 100 kHz. The experimental data were analyzed using the complex nonlinear least square fitting (CNLS) procedure, developed by Boukamp [14]. The reproducibility of the IS results was checked in multiple experiments, performed over the whole temperature range. The samples before measurements were thermostated for 0.5h. Due to the temperature gradient between thermocouple and the sample, its temperature could not be determined with a better accuracy than ±2°C.

IV.2.1.3.3. Determination of the lithium ion transference number

The lithium ion transference number (t_+) of the membrane samples were measured between 50°C and 90°C for various contents of calixarene and salt in the polymer electrolyte system. The steady state technique, which involves a combination of ac- and dc-measurements, was applied. The impedance response of the Li//solid-electrolyte//Li cell was measured prior to the dc-polarization run, in which a small voltage pulse (ΔV) was applied to the cell until the polarization current reached the steady-state I_{ss} (after 2 or 3h at 90 or 50°C respectively). Various voltage pulses (3-30 mV) were applied in order to test the experimental error, which did not exceed 10% in determination of transference numbers t_+. Finally, the impedance response of the cell was measured again. The double ac test is required to determine electrolyte resistance (R_e), as well as the solid electrolyte interface (SEI) resistance before (R_0) and after (R_{ss}) dc-polarization. That allowed evaluation of the initial current (I_0) arising immediately (~10μs at 50°C) after appliance of the voltage, since, along with the Ohm's low, $I_0 = \Delta V/(R_e + R_0)$.

According to this method [15], the transference number t_+ of lithium ions, as the carriers of charge flowing through the Li//solid-electrolyte//Li cell, could be calculated with the following equation:

$$t_+ = \frac{I_{ss}(\Delta V - I_0 R_0)}{I_0(\Delta V - I_{ss} R_{ss})} = \frac{R_e}{\frac{\Delta V}{I_{ss}} - R_{ss}} \qquad (1)$$

where:

R_0 – initial SEI resistance of passive layers formed at both lithium electrodes;

R_{ss} – secondary passive layer resistance (as the steady state polarization current is reached).

All the t_+ values obtained from equation (1) are collected in Table IV.2.5.

IV.2.1.3.4. FTIR spectroscopy

Infrared transmittance spectra were recorded on a PC-interfaced Perkin-Elmer 2000 FTIR spectrophotometer with the wavenumber resolution of 2 cm^{-1}. FTIR studies were performed at 25°C. Electrolytes were sandwiched between two NaCl plates in a drybox under N_2 atmosphere and were transferred into the FTIR chamber with controlled temperature. The accuracy of the sample's temperature measurement was ±1°C. A Galactic Grams 386 software package was used to analyze the FTIR data.

IV.2.2. Results

IV.2.2.1. IS, DSC and FTIR characteristics of the composite polymer electrolytes

Figure IV.2.1 presents the conductivity isotherms obtained at 15, 40 and 70°C for P(EO)DME based electrolytes as a function of calixarene **5a** concentration for samples containing various amounts of LiI (expressed as O:Li ratios). Generally, the addition of calixarene (at O:Li constant) results in a decrease in the total ionic conductivity (even below 10^{-5} Scm^{-1}), reflecting the complexing phenomenon. An increase in salt concentration (at x constant) gives rise to a local maximum (well above 10^{-3} Scm^{-1} at 70°C, x = 0). Adding a calixarene receptor, the maximum shifts toward lower salt concentrations (see dashed lines in Fig. IV.2.1a and b) except at the highest temperature (70°C), where the tendency is opposite (Fig. IV.2.1c). From a macroscopic point of view, the occurrence of the total conductivity local maxima versus salt concentration reflects a natural limit of its chemical solubility and dissociation in polymer matrix. Microscopically, it is related to unavoidable ionic association developing with an increase in concentration. Basing on Fuoss-Kraus calculations, one may conclude that in the range where conductivity increases, the contribution of free ions decreases while a population of positively charged triplets develops [16]. The trend breaks most probably when triplets aggregate into more complex multiplets and macroscopic viscosity effect is predominant.

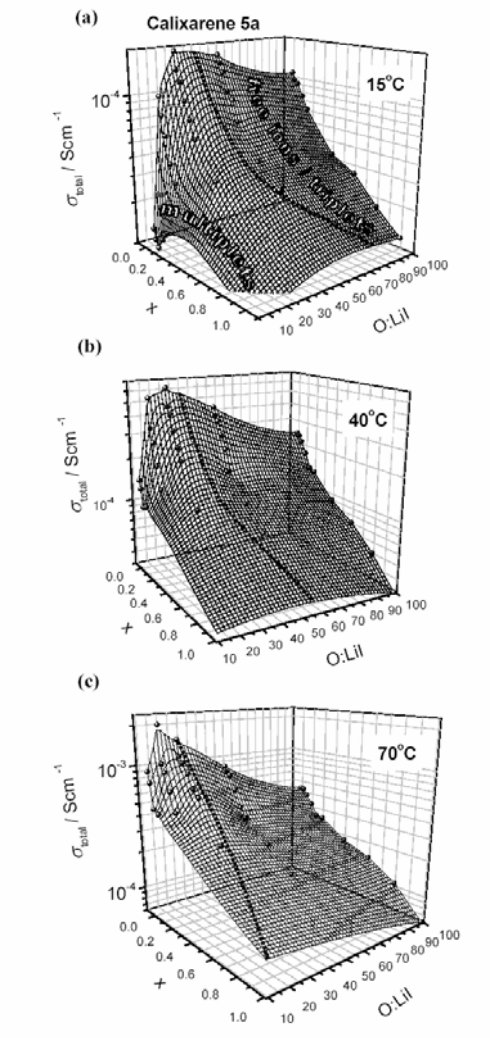

Figure IV.2.1. Conductivity isotherms (a),(b),(c) of the system P(EO)DME$_y$ (LiI)$_1$(Calixarene)$_x$ as a function of calixarene content and amount of salt expressed by O:Li ratio at various temperatures. The apparent conductivity changes are hypothetically assigned to changes of the charge carriers type in the system (from free ions and triplets toward multiplets).

It is worthy to note that at highest salt concentration (O:Li < 20) and lower temperature range, calixarene causes an increase in conductivity of the electrolyte, evidenced as a local maximum (Fig. IV.2.1a). The position of this maximum shifts to the higher salt concentration range with an increase in temperature. That is one of the important evidences for positive acting and usefulness of this agent in the electrolyte, since, when iodine anion is being complexed, two free cations might be released from a positively charged triplet or even more from a multiplet. The same phenomenon occurs in solid state polymer electrolytes (see Fig. IV.2.4b).

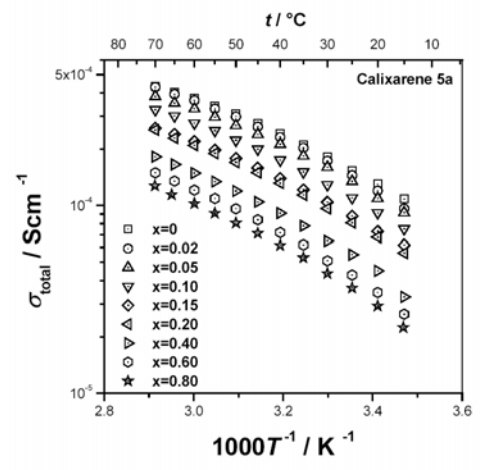

Figure IV.2.2. Temperature dependence of conductivity for the $P(EO)DME_{100}(LiI)_1(Calixarene)_x$ electrolyte.

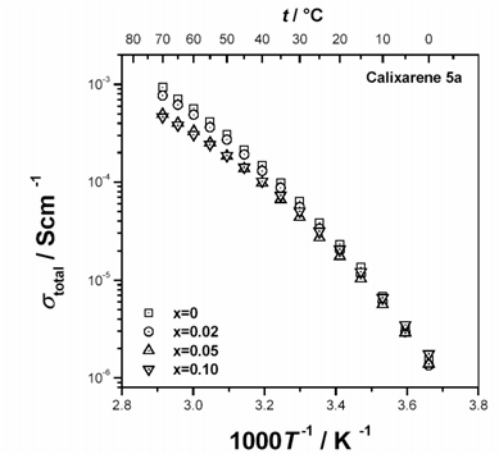

Figure IV.2.3. Temperature dependence of conductivity for the $P(EO)DME_{10}(LiI)_1(Calixarene)_x$ electrolyte.

Changes in the conductivity as a function of reciprocal temperature for P(EO)DME based electrolytes with O:Li ratio 100:1 and 10:1, containing various amounts of calixarene are shown in Figures IV.2.2 and IV.2.3, respectively. For 100:1 electrolytes, the conductivity decreases with an increase in the calixarene concentration over the entire temperature range. For 10:1 electrolytes, at below 30°C, the conductivity increases with increasing calixarene concentration. At higher temperatures, trends similar to those of the 100:1 electrolytes are evidenced in Figure IV.2.3. Figure IV.2.4a presents changes in the ionic conductivity as a function of reciprocal temperature for $P(EO)_{10}LiI$ solid electrolytes with various content of calixarene. At below 30°C conductivities obtained for electrolytes with x = 0.05, 0.10 and 0.20 are higher than for the pristine $P(EO)_{10}LiI$ electrolyte. At temperatures above the melting point of the crystalline phase, conductivity of the $P(EO)_{10}LiI$ electrolyte is the highest. On each curve one may distinguish two intervals, in which the dependence of conductivity on temperature can be fitted with the Arrhenius type equation:

$$\sigma = \sigma_0 \exp(-\frac{E_a}{k_B T}) \qquad (2)$$

where, E_a is the activation energy for effective ionic conduction in electrolyte, σ_0 is the pre-exponential factor including information about concentration of mobile ions and the entropy of ionic migration, and k_B denotes Boltzmann's constant. The point of inflection on each curve corresponds approximately to the melting temperature of the eutectic or crystalline P(EO) phase. The temperature dependencies of ionic conductivity have been fitted separately using equation (2) for the two intervals mentioned above. The values of activation energy calculated according to this procedure are included in Table IV.2.1. Generally, the activation energy at the lower regime is higher than at temperatures above the melting point. The addition of calixarene significantly lowers the activation energy at the low temperature region, whereas above the melting point of the crystalline phase, the activation energy for $P(EO)_{10}LiI$ electrolyte is ca. 0.1 eV lower than that of electrolytes with calixarene additives.

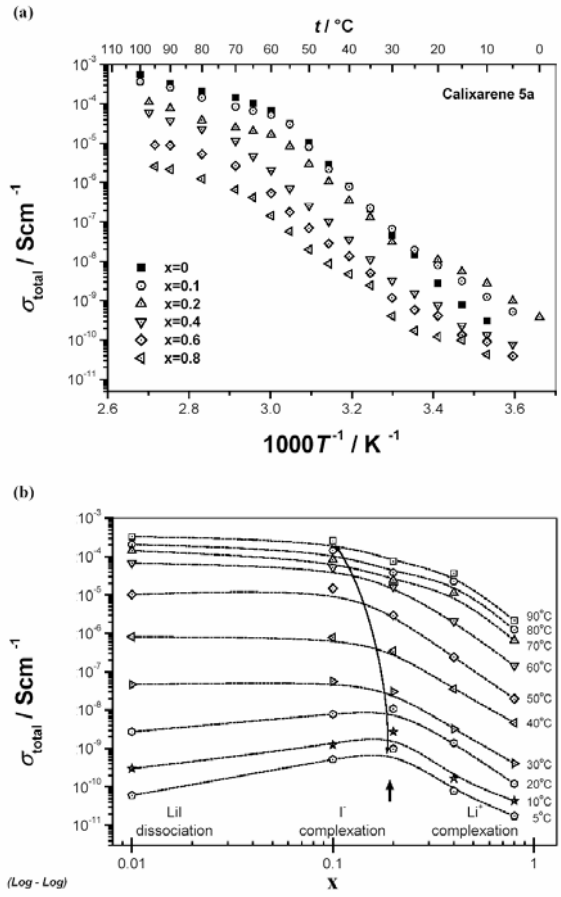

Figure IV.2.4. a) Temperature dependence of conductivity for the $P(EO)_{10}(LiI)_1(Calixarene)_x$ solid electrolyte and b) conductivity isotherms in the log-log representation. Particular ranges are hypothetically associated to calixarene induced salt dissociation, anionic and also cationic complexation

Table IV.2.1. Values of activation energy for ionic conduction calculated from the Arrhenius type equation (3) for the homogeneous $P(EO)_{10}(LiI)_1(Calixarene)_x$ solid electrolytes

X ratio[a]	E_{a1} / eV	E_{a2} / eV	E_m / eV	E_c / eV
0	2.19	0.51	0.51	1.68
0.05	1.14	0.59	0.59	0.55
0.10	1.30	0.60	0.60	0.60
0.20	1.11	0.63	0.63	0.63
0.40	1.10	0.62	0.62	0.62

[a] Calixarene **5a** in respect to LiI salt molar concentration

E_{a1} – activation energy for the conduction below melting point of the crystalline phase
E_{a1} – activation energy for the conduction above melting point of the crystalline phase
E_{a1} – activation energy for migration, assumed to be equal to E_{a2}
E_c – activation energy for the charge carrier creation calculated as $E_c = E_{a1} - E_{a2}$

Assuming that the activation energy consists of both the ion creation and migration terms [17], and taking into consideration that above the melting point the migration is predominant [19], it can be concluded that the addition of calixarene results in a decrease in the activation energy for creation of charge carriers and an increase in the activation energy for ionic migration.

As evidenced from Figure IV.2.4b, in solid polymer electrolytes, at temperatures below 40°C, the addition of calixarenes up to x = 0.2 results in an increase in the total conductivity, which is particularly advantageous for samples with high LiI content of O:Li ratio 10:1. This could be attributed to an improvement in ionic dissociation related to the calixarene complexation. Above x = 0.2, conductivity generally decreases. At above 40°C, the decrease in conductivity is observed over the entire x range, which is due to a "removal" of mobile charge carriers ("preferably anions") from the well dissolved salt by calixarene.

Table IV.2.2. T_g values for solid Polyether-LiI-Calixarene electrolytes

Polyether	O:Li ratio[a]	x ratio[b]	T_g / K
P(EO)DME	no salt	no additive	187
P(EO)DME	100	no additive	199
P(EO)DME	100	0.02	203
P(EO)DME	100	0.05	209
P(EO)DME	100	0.20	211
P(EO)DME	10	no additive	230
P(EO)DME	10	0.02	229
P(EO)DME	10	0.05	225
P(EO)DME	10	0.10	219
P(EO)	no salt	no additive	214
P(EO)	10	no additive	251
P(EO)	10	0.05	240
P(EO)	10	0.10	239
P(EO)	10	0.20	238

[a] oxirane monomeric units in respect to salt molar concentration

Table IV.2.2 shows the values of glass transition temperature T_g based on DSC experiments as a function of calixarene concentration for P(EO)DME electrolytes with O:Li ratio 100:1 and 10:1. For comparison, the T_g values obtained for $P(EO)_{10}$-LiI-calixarene solid electrolytes are also shown in Table IV.2.2. For the 100:1 electrolytes, T_g increases with the calixarene concentration. This is in contrast to both 10:1 electrolytes (based on low and high molecular weight polyethers), in which T_g decreases as the calixarene concentration increases. Figure IV.2.5 shows T_g values and degree of crystallinity (X_c) for P(EO) based polymer electrolytes with various content of calixarene additives. The X_c is calculated from the ratio of the latent melting heat (Q_m) for the polyether used to the latent melting heat found for the crystalline P(EO) phase:

$$X_c = \frac{Q_m}{Q_{mPEO}} \qquad (4)$$

where Q_{mPEO} = 213.7J/g [19,20]. As one may see in Figure IV.2.5, X_c decreases as the calixarene concentration increases. For comparison, DSC data for the P(EO)-calixarene system not containing LiI are shown in Table IV.2.3. For the LiI free system, T_g increases with calixarene concentration, whilst X_c decreases. The X_c values calculated for the doped and undoped system were normalized with respect to pure P(EO) content for the studied samples. The apparently opposite trends in T_g dependence on calixarene content in the case of highly doped (Table IV.2.2) compared to undoped (Table IV.2.3) systems suggest an interaction between calixarene and salt. This may also indicate asteric hindrance caused by calixarene, which leads to a lower degree of polymer crystallinity.

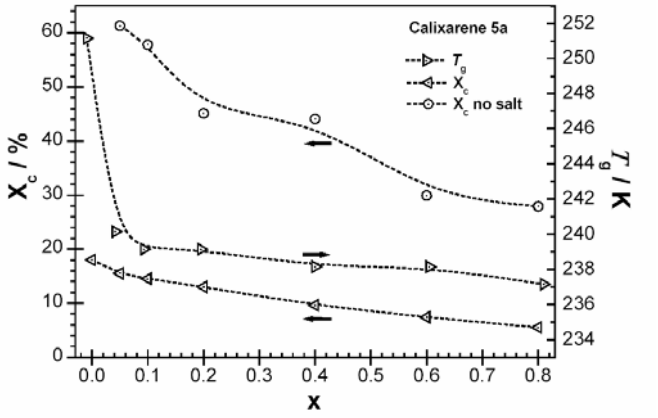

Figure IV.2.5. The effect of calixarene content on T_g and X_c of the solid system $P(EO)_{10}(LiI)_1(Calixarene)_x$. Dashed lines are guiding eyes

Table IV.2.3. DSC data for solid Polyether-Calixarene system without salt

Polyether	x ratio[a]	T_g / K	T_{mc} / K	Q_m / Jg^{-1}	X_c (%)
P(EO)	0	214	343.15	137	64
P(EO)	0.05	215	339.25	131.1	61.3
P(EO)	0.10	216	338.55	123.6	57.8
P(EO)	0.20	217	338.25	96.3	45.1
P(EO)	0.40	218	339.25	94.3	44.1
P(EO)	0.60	219	338.55	63.9	29.9
P(EO)	0.80	219	337.85	59.6	27.9

[a] Calixarene **5a** in respect to LiI salt molar concentration

Table IV.2.4 contains FTIR data for P(EO)DME_{100}LiI and P(EO)DME_{10}LiI electrolytes containing various amounts of calixarene. The position of the maximum of the C–O–C mode initially downshifts in the case of samples with low calixarene content and then slightly upshifts as the calixarene concentration in P(EO)$DME_{100}LiI_1$-calixarene electrolytes increases. The increase is more pronounced for the systems with higher salt concentration. Such a trend suggests weakening of the polymer-salt and strengthening of the ion-ion interactions, which leads to a decrease in the transient crosslink density. FTIR data the confirmed DSC observations

of the decrease in the glass transition temperature for samples with various amounts of calixarene.

Table IV.2.4. FTIR data for liquid and solid Polyether-LiI-Calixarene electrolytes

Polyether	O:Li ratio[a]	x ratio[b]	C-O-C max / cm^{-1}
P(EO)DME	no salt	no additive	1112
P(EO)DME	100	no additive	1107
P(EO)DME	100	0.02	1108
P(EO)DME	100	0.05	1108
P(EO)DME	100	0.20	1109
P(EO)DME	10	no additive	1093
P(EO)DME	10	0.02	1094
P(EO)DME	10	0.05	1095
P(EO)DME	10	0.10	1096

[a] oxirane monomeric units in respect to salt molar concentration

[b] Calixarene **5a** in respect to LiI salt molar concentration

IV.2.2.2. Interfacial stability

The stability of the solid electrolyte interface (SEI), i.e. lithium metal electrode/polymer electrolyte membrane, has been measured by means of IS. Figure IV.2.6 presents typical time dependence of the SEI resistance on the example of electrolytes containing low (x = 0.3) and high (x = 1) concentration of calixarenes **5a** (Figure IV.2.6a) and **5c** (Figure IV.2.6b).

The initial primary interfacial resistance may originate from chemical impurities in sample surface and apparently depends on the type of calixarene used increasing with its concentration increase. This resistance is usually slightly higher than the primary interfacial resistance (~10^2 Ω) for the pristine $(PEO)_{20}$ LiI electrolyte. On the other hand, the interfacial resistance R_{SEI} was found to be stable up to 250 h at 50°C independently on the type of calixarene used and its concentration. This result suggests that there is no significant growth of the passive layer at the lithium metal surface when in contact with the calixarene-based electrolyte membranes.

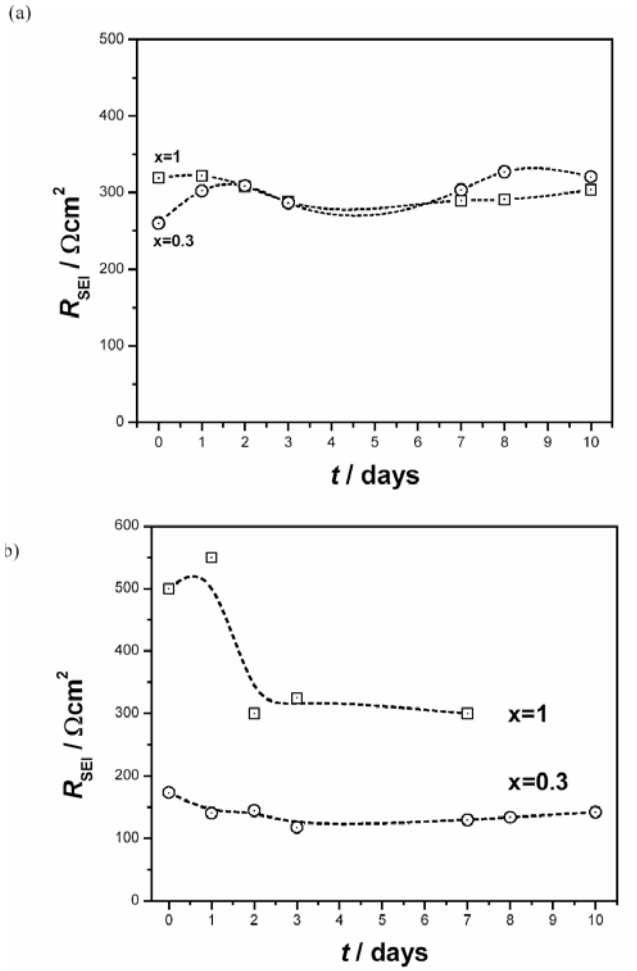

*Figure IV.2.6. Time evolution of passivating resistance R_{SEI} at 50°C in the $Li//P(EO)_{20}:(LiI)_1:(Calixarene)_x//Li$ cell for a) **5a** and **b) 5c** at x=0.3 and 1 (data determined in the Tel Aviv lab of Professor Emanuel Peled and Professor Diana Golodnitsky).*

IV.2.2.3. Lithium ion transference number

Table IV.2.5 lists the results of the Li^+ transference numbers t_+ determination, performed according to the procedure described in the experimental section.

As can be seen for O:Li = 100:1 samples, t_+ remains almost unchanged regardless of the calixarene **5a** addition, whilst for 20:1 samples a considerable increase from 0.35 up to 0.59 in the case of electrolyte with calixarene concentration x = 0.3 is followed by a decrease down to again nearly 0.35 at x = 1. That would suggest a possibility to complex also cations, besides anions, by calixarene **5a**.

Further in Table IV.2.5, there are t_+ presented for concentrated electrolytes (O:Li = 20:1 or 7:1) as a function of calixarene **5c** content and the type of anion used. The addition of calixarene **5c** (or **5b**) into the $(PEO)_7LiI$ electrolyte results in an increase in t_+ even above 0.7 for x = 0.3 (it should be stressed that in this case we were unable to synthesize homogeneous electrolytes with calixarene to salt ratio higher than 0.3). For comparison, data obtained for the $(PEO)_{20}LiCF_3SO_3$ electrolyte with and without calixarene additive are also shown to point up both a possibility to complex various anions by the same receptor and the significant increase in t_+ up to 0.9, following the addition of calixarene **5c**.

Table IV.2.5. Lithium ion transference number t_+ for solid $P(EO)_y(LiI)_1(Calixarene)_x$ and $P(EO)_y(LiCF_3SO_3)_1(Calixarene)_x$ polymer electrolytes as a function of temperature or salt and calixarene content *(some data determined in the labs of Professors Emanuel Peled and Diana Golodnistrky in Tel Aviv and of Professor Bruno Scrosati in Rome)*

Additive in electrolyte	Salt in electrolyte	t / °C	O:Li ratio[a]	x ratio[b]	t_+
Calixarene **5a**	LiI	90	100	0	0.14
		90	100	0.25	0.15
		90	100	0.50	0.18
		50	20	0	0.35
		50	20	0.30	0.59
		50	20	1.00	0.36
Calixarene **5b**	LiI	75	7	0	0.56
		75	7	0.30	0.70
Calixarene **5c**	$LiCF_3SO_3$	60	20	0	0.26
		60	20	1.00	0.90
	LiI	90	7	0.30	0.69
		75	7	0.30	0.74
		55	20	0.30	0.51
		90	20	1.00	0.80
		75	20	1.00	0.93
		50	20	1.00	1.00

[a] oxirane monomeric units in respect to salt molar concentration

[b] Calixarene content in respect to LiI salt molar concentration

In the case of electrolytes with the I^- anion, the effects of salt concentration and temperature on t_+ may also be derived from the data. Commonly, the higher salt content with respect to polymer matrix, the higher t_+, apparently reflecting the complexation phenomenon dependence on ion-ion and ion-matrix interactions, competing with anion binding by receptors. It can be noticed that generally t_+ decreases with an increase in temperature. For the electrolytes including calixarene **5c** with the additive to salt molar ratio 1:1 at 50°C, the highest Li^+ transference number equal to unity is achieved.

IV.2.3. Discussion

The design of new ligands for the selective complexation of anionic guests is a new area of coordination chemistry of significant relevance to improved transportation of cations, *e.g.* lithium-ions across polymer electrolytes. We have studied receptor systems such as *p-tert*-butylcalix[4]arene containing neutral urea moieties, which are capable of coordinating and sensing the group of halogen anions (Cl^-, Br^-, I^-) by formation hydrogen bonds, as discovered by Reinhoudt's group [9]. Since neither chloride nor bromide anion containing salts can be

dissolved in the polyether matrix, in the studied salt concentration range, the entire data set acquired in our experiments concerned mostly the iodide anion electrolytes.

The usage of the calixarene macromolecules in liquid and solid polymer electrolytes led us to the following conclusions. Firstly, in these compounds some of the strongest hydrogen anion-receptor bonds can be formed. Secondly, the receptors meet the requirement of low protonic acidity [21], which (if too high) could contribute to passivation of the lithium electrode. The addition of calixarene may then simultaneously do both, "purify" the electrolyte from mobile anions as well as suppress the formation and growth of SEI layers, as evident from Figure IV.2.6. The above conclusions are confirmed by the electrochemical studies performed in the symmetrical Li//solid-polymer-electrolyte//Li cells.

Usually, in nature one may find receptors recognizing (sensing) individual substrates due to agreement in geometries *via* fitting the appropriate site to a molecule. The better agreement the higher selectivity. Once the molecule was charged as in the case of a cation or anion in an electrolyte, complexation would be also determined by electrostatic interactions. In the case of calixarene receptors (compounds **5a-c**) applied in the polymer electrolyte, we could observe complexation of anions of extremely different geometries by the same receptor (see results for **5c** in Table IV.2.5). Despite small differences in the effectiveness of complexation due to the geometry mismatch, we may then consider the phenomenon of anionic complexation by calixarene receptors as depending mostly on its ability to create hydrogen bonds with anions, and thus, we may consider the anionic site as universal. Unlike in the case of other receptors, such as e.g. calixpyrrole, the calixarene "anion binding site" (see Schematic 1) prefers to host only one anion per one supramolecule, leading to formation 1:1 complexes in polymeric electrolyte [9]. The latter calixarene feature enables the estimation of changes of the mobile charge carriers fraction due to the complexation of anions in the mixed ionic polymer conductor. However, one has to take into account that the ability to bind an anion might compete with effective polarizability of a solvent in the electrolyte [9]. Moreover, N. McDonald et al. in the Monte Carlo molecular dynamics studies interestingly show that solvatation by water molecules might even block off the F^- complexation [22].

In our case, as shown in Figure IV.2.1, the addition of calixarene (at O:Li constant) resulted in a general decrease in the total ionic conductivity. In view of DSC data (Table IV.2.2), such a trend can be taken as evidence for the ion complexing phenomenon rather than *e.g.* decrease in fluidity or increase in electrolyte viscosity, which indeed decreases with calixarene content increase (regardless of its macromolecular dimensions).

Based on the conductivity, DSC and FTIR spectroscopy results, the following mechanism of polyether electrolyte-calixarene interaction could be concluded. The calixarene interacts preferably with the iodide anions rather than lithium cations, which has a different effect on the ionic conductivity of electrolytes, either with low or high salt content. For low salt concentration (see data for the 100:1 electrolyte) intramolecular crosslinks formation dominates. This is associated with the trapping of cations inside cages formed by polyether oxygen atoms. In these electrolytes, any addition of calixarene results in the immobilization of associated iodide anions which in turn lowers the electrolyte conductivity (see Figure IV.2.2). The presence of a bulky supramolecular additive acts as a steric hindrance for segmental motions of polyether chains. This increases the T_g values for this set of electrolytes and hinders the electrolyte crystallinity (see Table IV.2.2, IV.2.3 and Figure IV.2.5). In these electrolytes the addition of calixarene has no effect on the cation transport number (see Table IV.2.5). In the case of high LiI concentration (see data for the 10:1 samples), intermolecular crosslinks *via* positively charged triplets linking the polyether chains dominate. Moreover, the addition of calixarene results in breaking of the triplet links by taking out the iodide anion. That in turn frees some mobile cations and as well decreases the T_g values of the electrolyte. Both effects result in the conductivity and cation transference number enhancement (see Figure IV.2.3, IV.2.4 and Table IV.2.5). The results do

not depend on the molecular weight of the polyether used. The above assumptions were confirmed by studies on Li^+ conduction which revealed an increase in lithium transference number in the case of O:Li = 20:1 electrolytes containing x = 0.3 of calixarene **5a**. Interestingly, for higher calixarene concentrations the lithium transference number decreases. Likewise, this might be connected to the subsequent cation complexation.

The main goal of this study was to analyze the effect of various functional groups in urea calixarenes (**5a-c**) on complexation of different anions, toward chemical programming of the desired transport properties of polymeric electrolytes (see Table IV.2.5). Assuming that anion complexation occurs in the cage placed between active urea protons, an increase in protonic acidity should provide an increase in the complexation constant. Therefore, the use of electron-accepting functional groups such as *p*-nitrophenyl was expected to cause better complexation of iodide anions. And indeed, the stronger electron withdrawing nature of the *p*-nitrophenyl compared to phenyl substituent makes the chemical shift of urea hydrogens in presence of the anion-free solution more downfield (see ^{1}H NMR data). This effect is clearly expressed in terms of data shown in Table IV.2.5, where t_+ approaches unity in the final case of $(PEO)_{20}$LiI-calixarene **5c** electrolyte. On the other hand, the application of electron-donating bulky *t*-butyl groups might result in a steric hindrance and some enlargement of the molecular cage of the receptor, which also could improve its complexation ability towards anions.

IV.2.4. Summary

New supramolecular compounds calix[4]arene R-urea derivatives (R = phenyl, *t*-butyl, *p*-nitrophenyl) have been synthesized and used as anion bonding receptors in polyether based polymeric electrolytes.

It was established that most properties of the system studied do not depend on molecular weight of the polymer matrix used but are rather sensitive to structure and concentration of the additive.

Two breakthrough results were obtained. Firstly, addition of the supramolecular compounds has been found to suppress the formation and growth of secondary passive layers at the lithium electrodes. Secondly, changes in the electrolyte conductivity were associated to complexation by anion preferring calixarene receptors, causing considerable modification of the ion transport mechanism from almost anionic through mixed to purely cationic.

From the results obtained in this work, it was concluded that further research is required with the focus on supramolecular compounds binding anions, of which little is known as far as application in polymer electrolytes is concerned.

References

1. Vinces, J.; Böhmer, V. *Calixarenes, a Versatile Class of Macrocyclic Compounds* Kluwer Academic Press: Dordrecht, 1991; Vol. 3.
2. Gutsche, C.D.; Bauer, L.J. *J. Am. Chem. Soc.* **1985**, *107*, 6052.
3. a) van Loon, J.D.; Verboom, W.; Reinhoudt, D.N. *Org. Prep. Proc. Int.* **1992**, *24*, 437;
   b) van Dienst, E.; Bakkeer, W.I.; Engbersen, J.F.J.; Verboom, W.; Reinhoudt, D.N. *Pure & Appl. Chem.* **1993**, *65*, 387.
4. a) Gutsche, C.D.; See, K.A. *J. Org. Chem.* **1992**, *57*, 4527.
   b) van Loon, J.D.; Janssen, R.G.; Verboom, W.; Reinhoudt, D.N. *Tetrahedron Lett.* **1992**, *33*, 5125.
   c) Murakami, H.; Shinkai, S. *J. Chem. Soc., Chem. Commun.* **1993**, 1533.

5. a) Shinkai, S.; Fujimoto, K.; Otsuka, T.; Herman, H.L. J. *Org. Chem.* **1992**, *57*, 1516; b) Arnaud-Neu, F.; Barrett, G.; Harris, S.J.; Owens, M.; McKervey, M.A.; Schwing-Weill, M.J.; Schwinte, P. *Inorg. Chem.* **1993**, *32*, 2644.
6. a) Beer, P.D.; Dickson, C.A.P.; Fletcher, N.; Goulden, A.J.; Grieve, A.; Hodacova, J.; Wear, T. *J. Chem. Soc., Chem. Commun.* **1993**, 828;
   b) Morzherin, Y.; Rudkevich, D.M.; Verboom, W.; Reinhoudt, D.N. *J. Org. Chem.* 1993, 58, 7602;
   c) Beer, P.D.; Chen, Z.; Goulden, A.J.; Stokes, S. E.; Wear, T. *J. Chem. Soc., Chem. Commun.* 1993, 1834.
7. a) Gutsche, C.D.; Iqbal, M.; Stewart, D. *J. Org. Chem.* **1986**, *51*, 742;
   b) Gutsche, C.D.; Iqbal, M. *Org. Synt. Coll*. Vol. VIII, 75;
   c) Gutsche, C.D.; Dhawan, B.D. *J. Am. Chem. Soc.* **1981**, *103*, 3782.
8. a) Iwamoto, K.; Yanagi, A.; Araki, K.; Shinkai, S. *Chem. Lett.* **1991**, 473;
   b) Iwamoto, K.; Araki, K.; Shinkai, S. *Tetrahedron.* **1991**, *47*, 4325;
   c) Iwamoto, K.; Fujimoto, K.; Shinkai, S. *Tetrahedron. Lett.* **1990**, *31*, 7169.
9. Scheerder, J.; Fochi, M.; Engbersen, J.F.J.; Reinhoudt, D.N. *J. Org. Chem.* **1994**, *59*, 7815.
10. Kenis, P.J.A.; Noordman, O.F.J.; van Hulst, N.F.; Engbersen, J.F.J.; Reinhoudt, D.N. *Chem. Mater.* **1997**, *9*, 596.
11. Kammerer, H.; Happel, G.; Caesar, F. *Makromol. Chem.* **1972**, *162*, 179.
12. Gutsche, C.D. *Calixarenes*; Ed. Stoddart, J.F.; The Royal Society of Chemistry: Cambridge, UK, 1998.
13. a) Salzberg, P.L.; Supniewski, J. V. *Org. Synt. Coll.* Vol. 1, 2nd edition, John Wiley and Sons, Inc., 1941, NY, 119;
   b) Mizzoni, R.H.; Hennessey, M.A.; Scholz, C.R. *J. Am. Chem. Soc.* **1954**, *76*, 2414;
   c) Cope, A.C.; Nace, H.R.; Hatchard, W.R.; Jones, W.H.; Stahmann, M.A.; Turner, R.B. *J. Am. Soc.* **1949**, *71*, 554.
14. Boukamp, B.A. *Solid State Ionics* **1986**, *18-19*, 136.
15. Bruce, P.G.; Vincent, C.A. *J. Electroanal. Chem. Interfacial Electrochem.* **1987**, *225*, 1.
16. Zalewska, A.; Stygar, J.; Ciszewska, E.; Wiktorko, M.; Wieczorek, W. *J. Phys. Chem. B* **2001**, *105*, 5847
17. Siekierski, M.; Wieczorek, W. *Solid State Ionics* **1993**, *60*, 67.
18. Wieczorek, W. *Solid State Ionics* **1992**, *53-56*, 1064.
19. Li, X.; Hsu, S.L. *J. Polym. Sci.*, *Polym. Phys. Ed.*, **1984**, *22*, 1331.
20. Przyłuski, J.; Wieczorek, W. *J. of Thermal Analysis* **1992**, *38*, 2229.
21. Bordwell, E.; Algrim, D.J.; Harrelson, J.A. *J. Am. Chem. Soc.* **1988**, *110*, 5903.
22. McDonald, N.A.; Duffy, E.M.; Jorgensen, W.L. *J. Am. Chem. Soc.* **1988**, *120*, 5104.

IV.3. Calix-6-pyrrole derivatives as new anion receptors for polyether electrolytes

In the next step of the work we decided to try another type of anion receptors: calix-6-pyrrole. In the first part of the studies we concentrated on the development of a new method of transference number determination using composite systems with calix-6-pyrrole.

IV.3.1. Introduction to the determination of lithium transference numbers.

In a polymer electrolyte the salt is dissolved but not fully dissociated, which is a consequence of the low solvent dielectric constant as well as relatively high salt concentration. This leads to the presence of ion-pairs, triplets and other higher associates, besides separate cations and anions. All of them may be mobile in an electrolyte and affect the total charge transport. Two important material parameters of the system studied are affected by the above mentioned effect: ionic conductivity and transference numbers. The overall conductivity is a simple sum of all the present charge carriage species contributions. Thus, the formation of undissociated salt clusters and ion pars (which are formally uncharged) decreases the conductivity value.

The determination of the total ionic conductivity is simple with the aid of impedance spectroscopy. The relation between conductivity and salt concentration is well defined in the literature. The determination of transference numbers is much more complicated, mainly due to the above mentioned exemptions of the system studied from the theory of ideal and dilute electrolytes.

So far several methods have been employed for the measurements of the transference number. These are: Hittorf/Tubandt ac impedance, dc polarization, NMR and Radio Tracers. The idea of the Newnan's method applied by us is to measure a complete set of transport properties like conductivity, salt diffusion coefficient and cation transference number. The advantage of the chosen method is that it does not require the solution to be dilute or ideal.

Because of the solution non-ideality, in order to describe completely the transport processes it is necessary to have n(n-l)/2 concentration-dependent transport properties, where n is the number of independent species in the solution. To describe the PEO-DME-LiI system, three independent species were chosen: Li^+, I^- and PEO-DME matrix, without regard for microscopic speciation. To determine individual transport properties the following measurements were performed:

- Conductivity - standard impedance measurement.
- Salt diffusion coefficient - restricted diffusion measurement.
- Cation transference number concentration cell OCV measurements and symmetric cell polarization.

The addition of supramolecular compounds which selectively complex anions should lead to stabilization of the separate ion species and therefore should favor the cationic charge transport. If this assumption is true, one should observe an increase in the cation transference number in samples with supramolecular additives comparing to the reference sample without such a compound. 1,1,3,3,5,5-*mezo*-Hexaphenyl-2,2,4,4,6,6-*mezo*-hexamethylcalix[6]pyrrole was chosen as an additive.

IV.3.2. Synthesis

All substrates were dried under high vacuum of 10^{-5} Torr for 72 h and then transferred to an argon-filled dry-box (moisture content lower than 2 ppm), where the synthesis and measurements were performed. Samples compositions are collected in Table IV.3.1. Samples of the salt concentration from 1.5 mol·kg^{-1} down to 0.5 mol·kg^{-1} were prepared by direct dissolution of the salt in a polymer. Samples of lower salt concentration were prepared by the successive dilution of a batch containing the electrolyte with 0.5 mol·kg^{-1} LiI. Finally,

supramolecular additive (calix[6]pyrrole derivate) was added (molar ratio C[6]P:LiI was constant in all samples).

All samples were equilibrated at ambient temperature for 3 weeks before undertaking any further experiments.

IV.3.3. Measurements

Ionic conductivity was determined using the complex impedance method at room temperature (20°C) controlled by HAAKE DC 50 cryostat. The samples were sandwiched between titanium blocking electrodes. The impedance measurements were carried out on a computer interfaced Atlas HJ98 impedance analyzer over the frequency range 1 Hz - 100 kHz (Figure IV.3.1).

The polarization cell and restricted diffusion experiments were performed in a symmetric cell. The electrolyte was placed between two lithium electrodes with 1cm^2 area each. Fixed distance between the electrodes was achieved by using a Teflon spacer. A scheme of the used cell is shown in Figure IV.3.2c and Figure IV.3.2d. For dc polarization results recording, an EG&G PAR 263 galvanostat/potentiostat was used.

In order to perform concentration cell experiments a special cell was designed (shown in Figure IV.3.2a). The cell consists of two half-cells made of polyethylene as shown in the picture. The lithium electrode is placed in a special polypropylene "holder" (Figure IV.3.2b). Electric contact is provided by copper wiring. After electrode assembly the electrolyte is deposited/spread, the halves are connected and the OCV is measured. To perform OCV measurements a Brymen BM5155X multimeter was used.

Salt diffusion coefficient determination is based on the polarization of the symmetrical cell using direct current until the concentration gradient is generated. Consequently, the potential of the return to the equilibrium state is registered as a time function (|ln(Φ)| = f(c). If the relationship is linear the diffusion coefficient can be determined from:

$$D = \frac{\pi^2 A}{L^2}$$

where: A is the slope of a straight line, L - thickness of the electrolyte layer.

A typical plot is shown in Figure IV.3.3. To keep identical calculation assumptions, always the same number of points was taken for slope of straight line calculations.

Cation transference number measurements were performed in two stages. In the first one the potential of a concentration cell M|PEG-DME$_x$MX|PEG-DME$_y$MX|M, (where *x* is constant and *y* varies) was measured. The plot U = f(ln[c]) was drawn from gathered data.

If the investigated system were ideal the plot would be linear. The concentration cell potential could be described by the equation:

$$d\Phi = \frac{2RT}{F}\left(1 + \frac{d\ln(f_{\pm})}{d\ln(c)}\right) t_{-}^{0} d\ln(c)$$

where:

Φ - concentration cell potential

$1 + \frac{d\ln(f_{\pm})}{d\ln(c)}$ - thermodynamic factor

t_{-}^{0} - anion transference number

c - concentration ratio

The second experiment consisted in applying a short current pulse to the symmetric cell (M|MX|M) and measurement of the generated concentration cell potential. If the condition: $L >> (Dt_i)^{1/2}$ (where L is the distance between electrodes, D is salt diffusion coefficient and t_i is

time) is fulfilled, the investigated cell can be considered as the concentration cell $M|MX_1|MX_0|M$ and the concentration change close to the electrode region is given by the equation:

$$\Delta c = \pm \frac{2t_-^0}{F(\pi * D)^{1/2}} (It_i^{1/2})$$

assuming that $x \approx ln(x + 1)$, the generated concentration potential is equal to:

$$\Phi = 2 * \frac{2t_-^0}{c_0 F(\pi * D)^{1/2}} \left(\frac{d \ln(c)}{dU} \right) \left(It^{1/2} \right)$$

For all salt concentrations the plot of the function

$$\Phi(\tau_0) = f(It^{1/2})$$

where: τ_0 - time of pulse interruption; I - current intensity; t - pulse time
is registered and thus the cation transference number can be calculated according to the equation:

$$t_+^0 = 1 - \frac{mcF(\pi * D)^{1/2}}{4} \left(\frac{d \ln(c)}{dU} \right)$$

where m is the slope of a straight line taken from the polarization experiment, and inverse of the slope of a straight line from the concentration cell experiment.

IV.3.3. Results

Table IV.3.1.. Results for samples with calix[6]pyrrole additive (1:3 C[6]P:LiI molar ratio)

Sample No.	n [mol/kg]	**D**	Coeff. m from OCV vs. It^0.5	dlnc/dlnU	t+	σ [S/cm]
1	1.5	1.46936×10^{-7}	9.354746136	0.04923373	-10.3194104	4.13×10^{-5}
2	1.0	1.30374×10^{-7}	6.875023889	0.039397713	-3.180364357	1.09×10^{-4}
3	0.75	5.16522×10^{-8}	2.875651466	0.036417663	0.236994823	1.33×10^{-4}
4	0.5	9.3297×10^{-8}	2.789855666	0.062327425	-0.135111035	1.34×10^{-4}
5	0.25	1.03539×10^{-7}	7.517114441	0.074369903	-0.922272891	8.74×10^{-5}
6	0.1	1.21081×10^{-6}	6.659501101	0.08845186	-1.770508234	3.99×10^{-5}
7	0.05	1.60899×10^{-7}	16.19281243	0.086471114	-0.200364091	2.06×10^{-5}
8	0.01	1.26227×10^{-7}	175.0527311	0.156682869	-3.165243109	3.51×10^{-6}
9	0.001	1.78428×10^{-7}	4080.453454	0.09881449	-6.280050868	2.39×10^{-6}

Table IV.3.2.. Results for reference samples PEG-DME-LiI without a supramolecular additive

Sample No.	n [mol/kg]	**D**	Coeff. m from OCV vs. It^0.5	dlnc/dlnU	t+	σ [S/cm]
1	1.5	1.73×10^{-7}	6.739811804	0.059477942	-9.689340396	9.67×10^{-5}
2	1.0	5.41×10^{-7}	3.895946889	0.036213096	-3.437240746	9.76×10^{-4}
3	0.75	9.60×10^{-7}	3.229045872	0.066761181	-5.77264382	5.56×10^{-4}
4	0.5	2.00×10^{-7}	3.063008783	0.075066355	-1.196019483	2.55×10^{-4}
5	0.25	1.48×10^{-6}	3.959233769	0.077757132	-3.007152517	1.40×10^{-4}
6	0.1	1.94×10^{-7}	14.68340939	0.084920078	-1.347739091	4.60×10^{-5}
7	0.05	1.08×10^{-6}	17.34999152	0.085557131	-2.296482053	2.35×10^{-5}
8	0.01	1.46×10^{-6}	28.95329684	0.147932544	-1.212842716	3.86×10^{-6}
9	0.005	1.96×10^{-7}	379.8983628	0.123941492	-3.452068894	2.37×10^{-6}

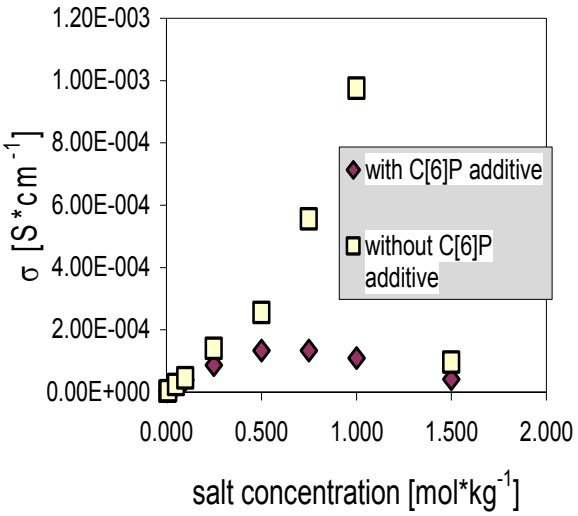

Figure IV.3.1. Ionic conductivity at 20 °C depending on salt concentration.

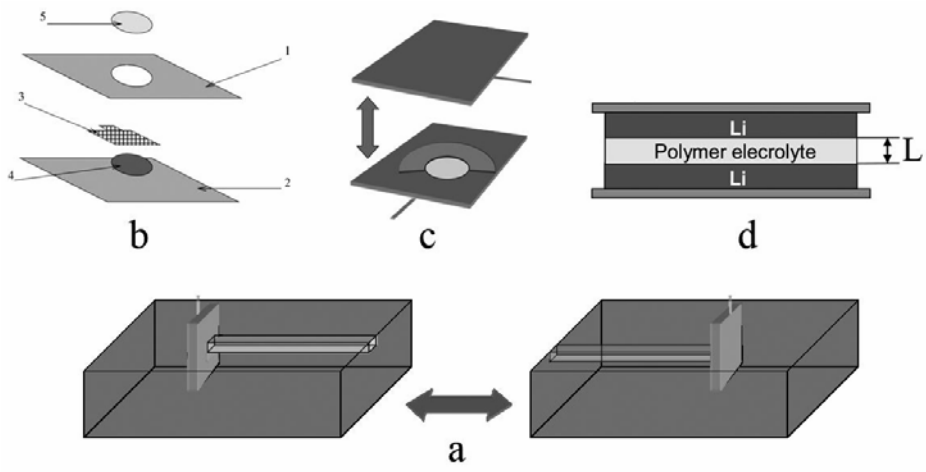

Figure IV.3.2. Measurement cell.

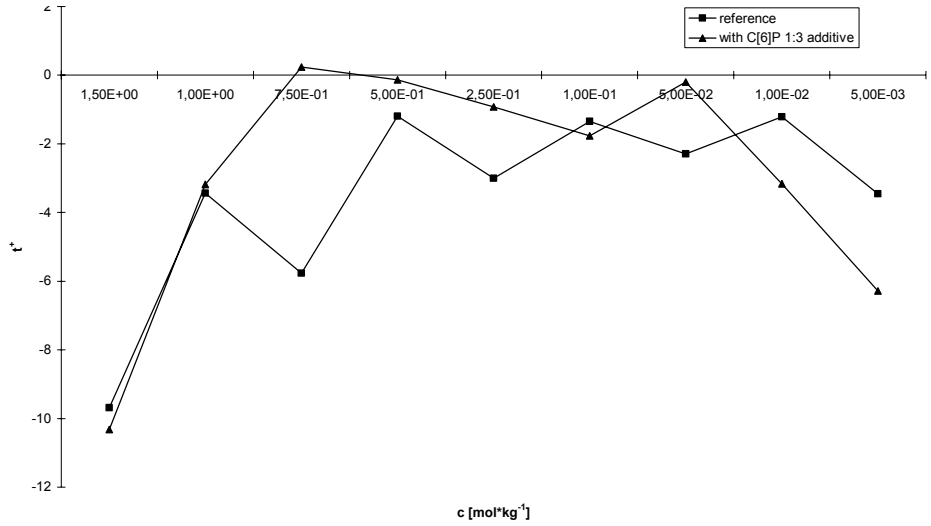

Figure IV.3.3. Li^+ cation transference numbers.

It is clear that the addition of a calix[6]pyrrole derivate leads to an overall conductivity decrease (by about one order of magnitude). On the other hand, the transference numbers are generally higher in samples with an additive (especially in samples with the highest conductivity). This can be treated as partial proof that a supramolecular additive works as we assume.

It is worth mentioning that not all of the additive dissolves in the samples (especially in samples with higher salt concentration).

Further studies of calix-6-pyrrole derivatives as anion receptors for polyether electrolytes are planned.

V. LIST OF PUBLICATIONS RESULTING FROM WORK CARRIED OUT WITHIN THE PROJECT:

1. Z. Florjańczyk, E. Zygadło-Monikowska, W. Wieczorek, A. Ryszawy, A. Tomaszewska, K. Fredman, D. Golodnitsky, E. Peled, B. Scrosati *J. Phys. Chem. B* **2004**, *108*, 14907-14914.
2. A. Zalewska, I. Pruszczyk, E. Sułek, W. Wieczorek *Solid State Ionics* **2003**, *157*, 233-239.
3. E. Zgadło-Monikowska, Z. Florjańczyk, A. Ryszawy, A. Tomaszewska „Synthesis and Characterization of Lithium Diphenylphosphate Complexes with Triethylaluminum and Their Application as Conducting Salts" *Journal of New Materials for Electrochemical Dewices*, submitted for publication.
4. A. Błażejczyk, W. Wieczorek, R. Kovarsky, D. Golodnitsky, E. Peled, L.G. Scanlon, G.B. Appetecchi and B. Scrosati *J. Electrochem. Soc.* **2004**, *15(10)*, A1762.
5. A. Błażejczyk, M. Szczupak, P. Cmoch, W. Wieczorek, R. Kovarsky, D. Golodnitsky, E. Peled, L.G. Scanlon, G.B. Appetecchi and B. Scrosati *Chem. Mater*., accepted for publication.